EUCLIDEAN-MONTE-CARLO INFORMED GROUND-STATE PREPARATION FOR SCALAR FIELD THEORY

Navya Gupta

(University of Maryland, College Park)

Work done in collaboration with Prof. Zohreh Davoudi and Dr. Christopher White

arXiv.2506.02313

QuantHEP (LBNL), Sep 2025

Understanding the strong force

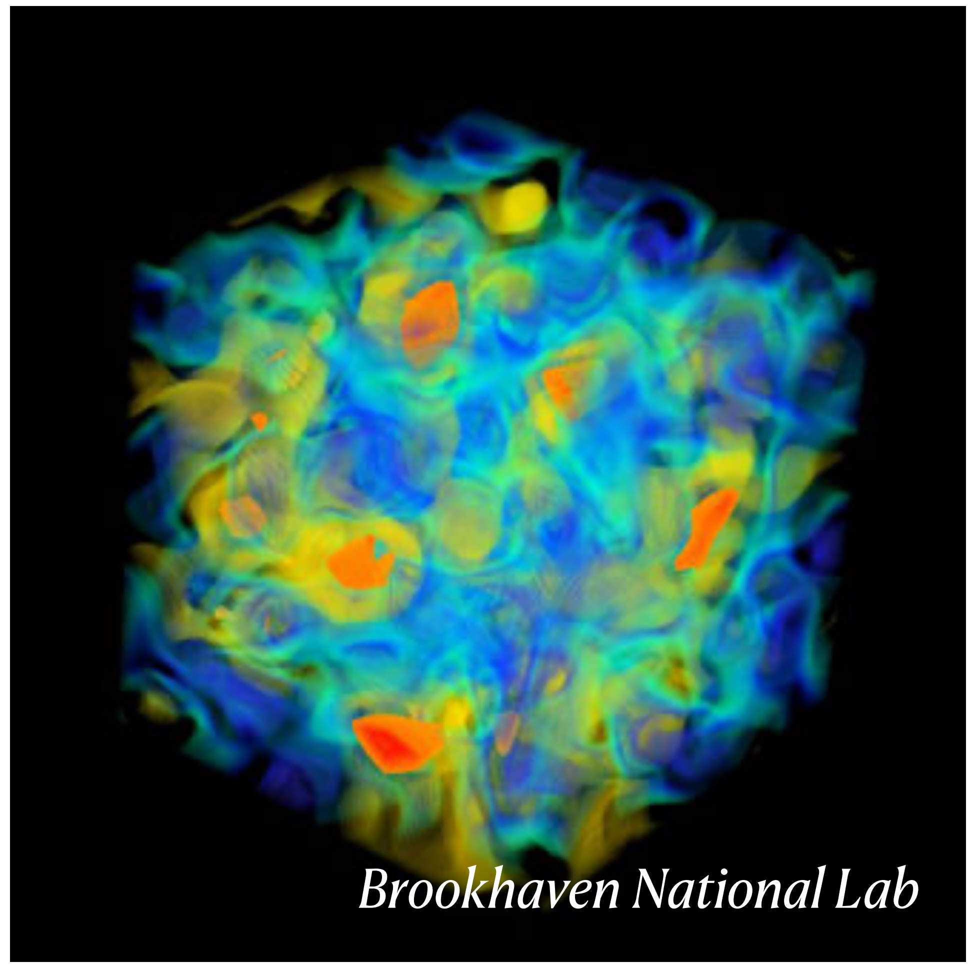
Brookhaven National Lab

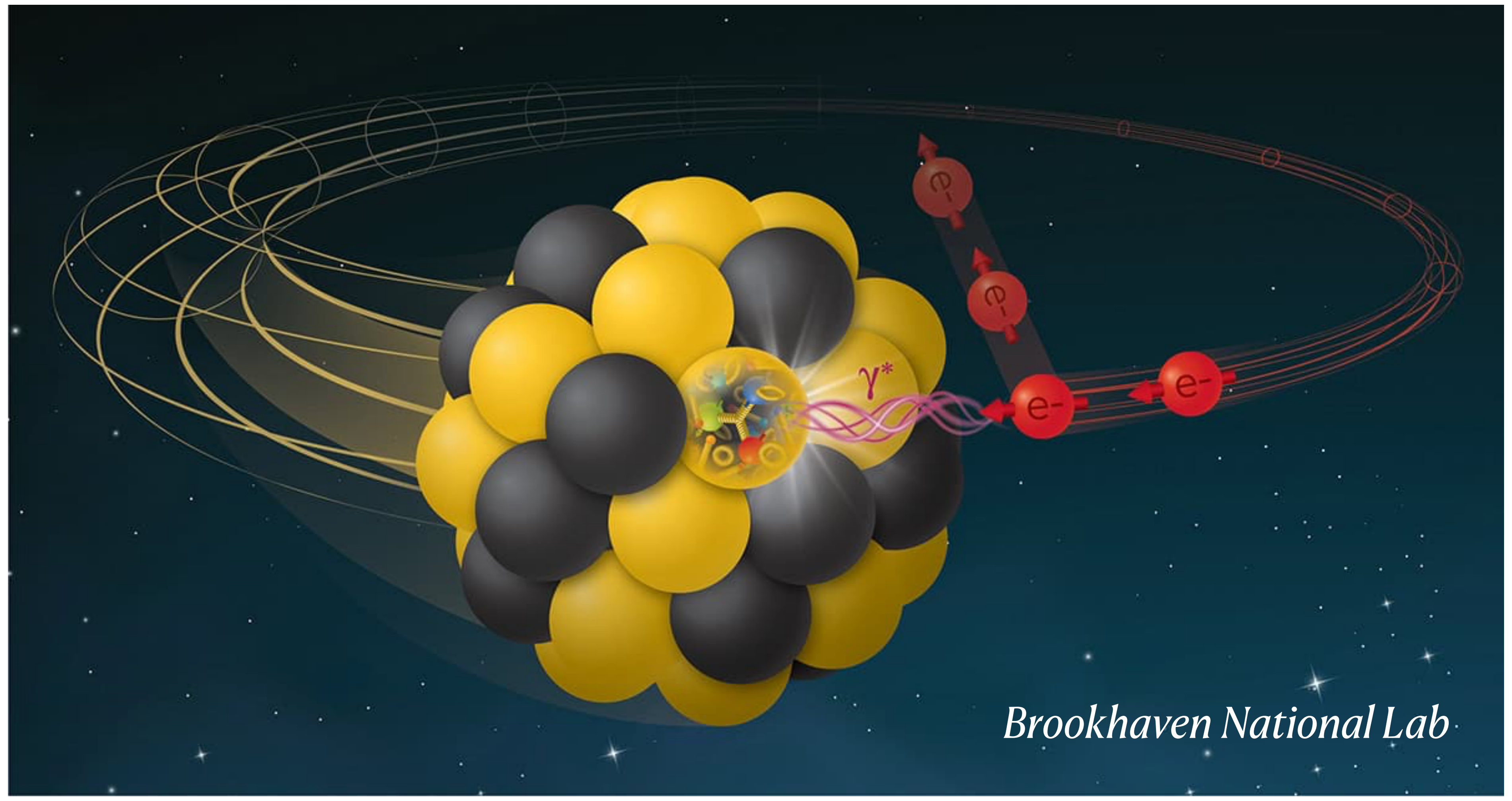
Brookhaven National Lab

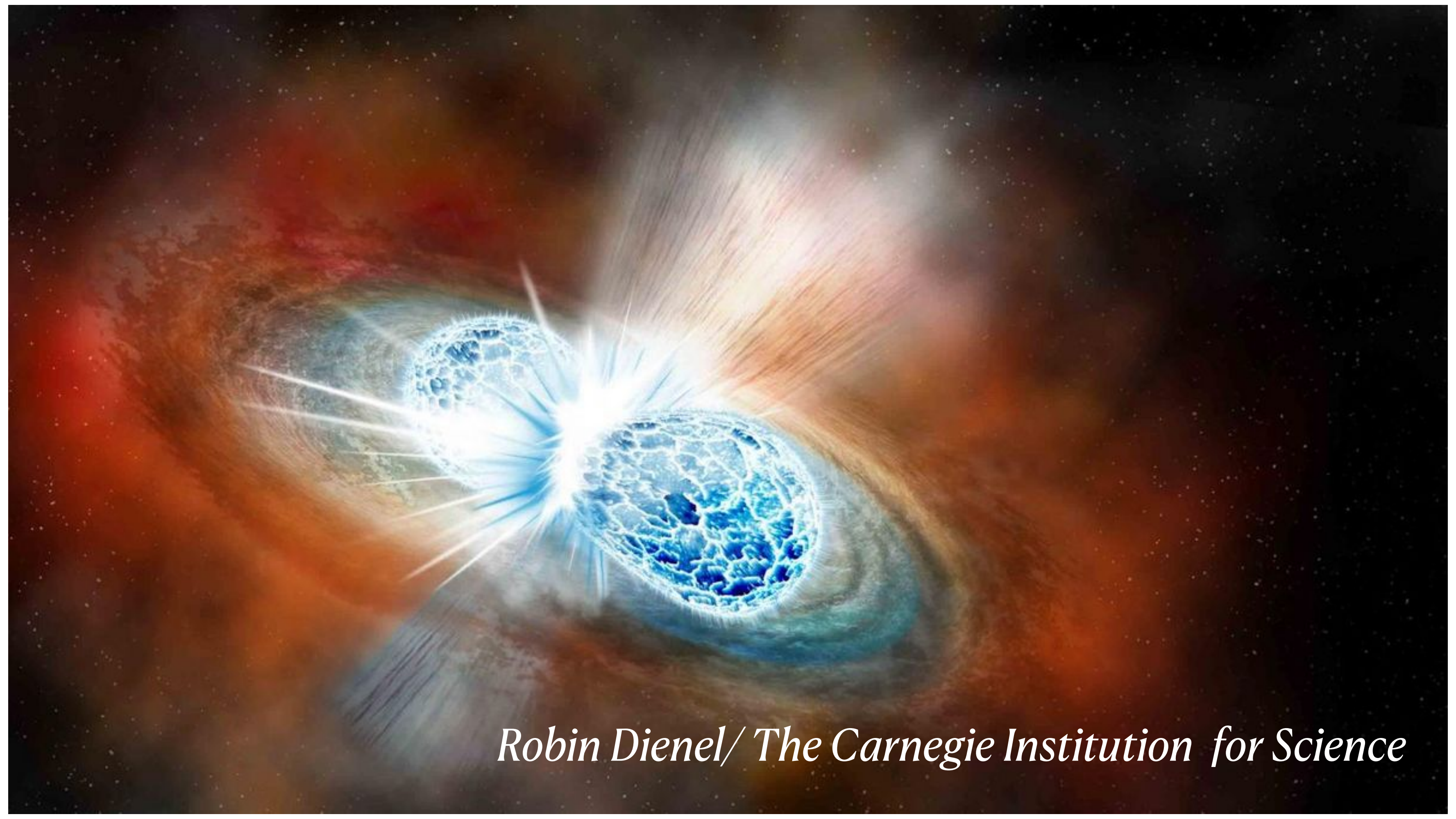
Robin Dienel/ The Carnegie Institution for Science

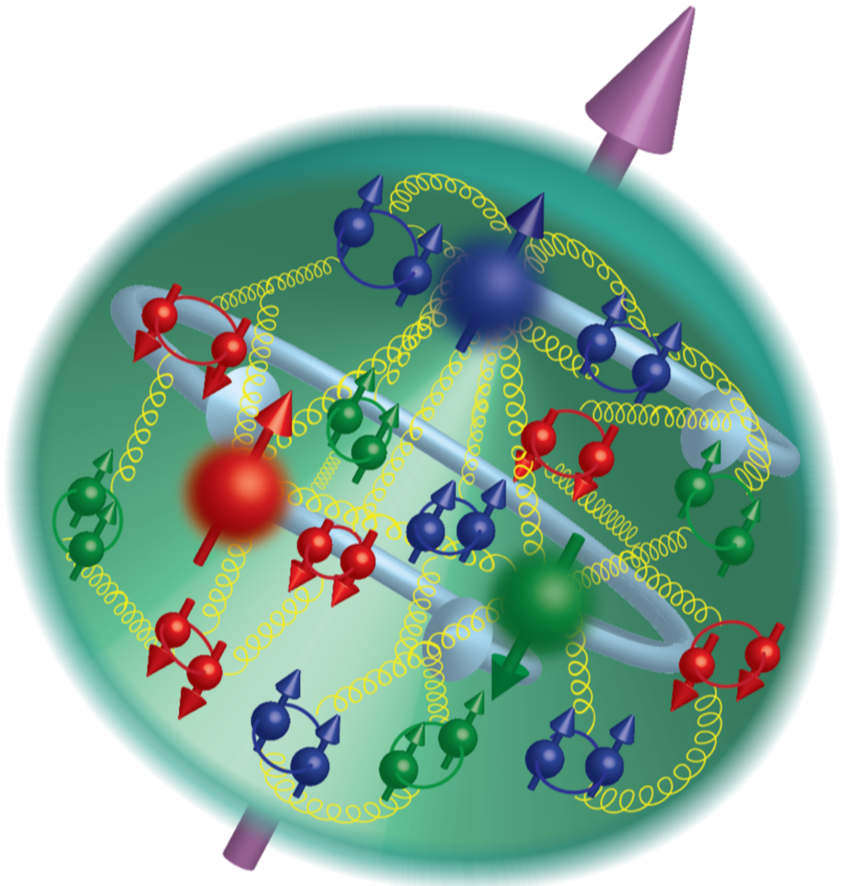
Argonne National Lab

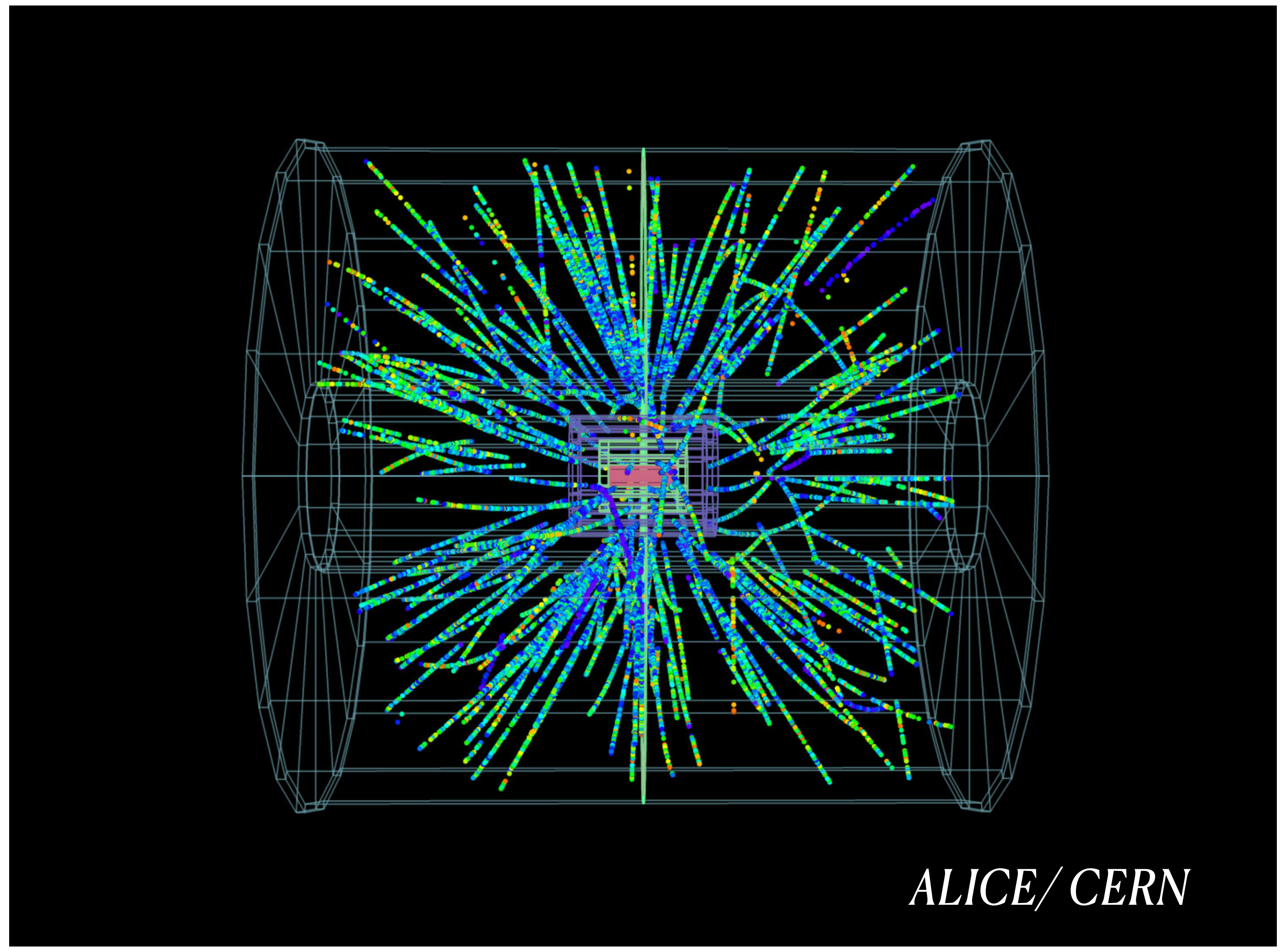
ALICE/ CERN

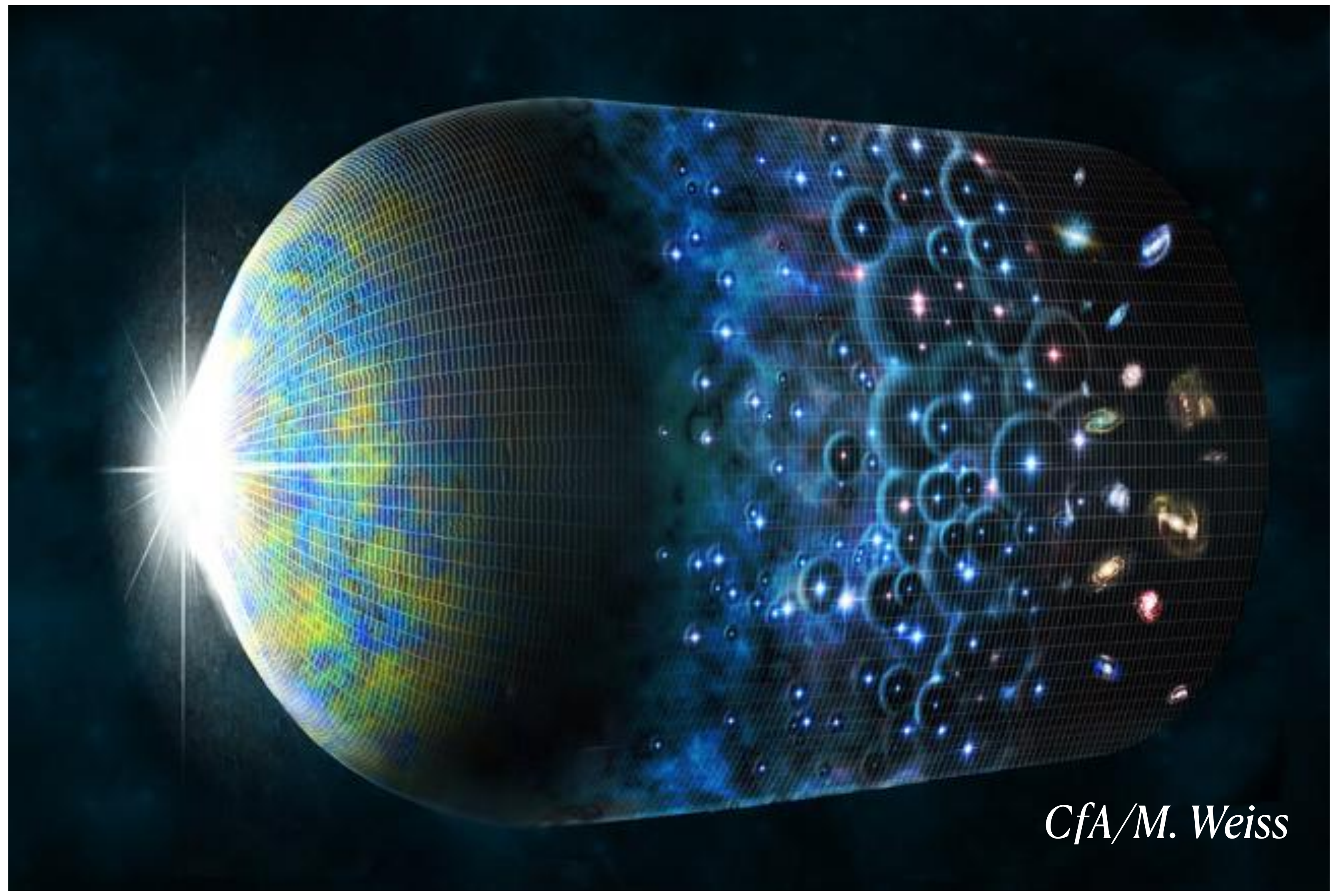
CfA/M. Weiss

"Nature isn't classical, dammit, and if you want to make a simulation of nature, you'd better make it quantum mechanical."

- Richard Feynman

The degrees of freedom of a quantum field theory can be efficiently encoded into quantum simulator degrees of freedoms.

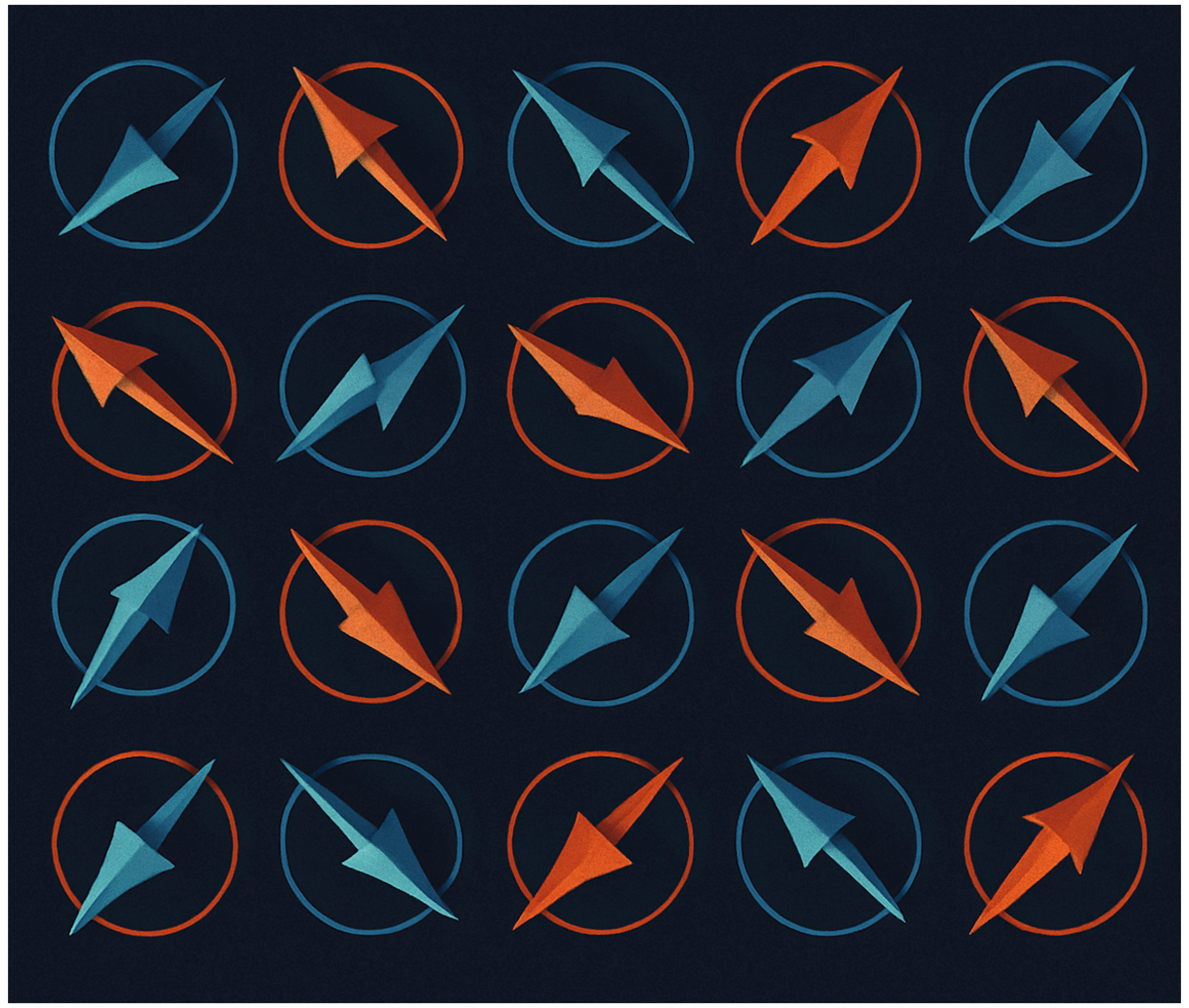

“Nature isn’t classical, dammit, and if you want to make a simulation of nature, you’d better make it quantum mechanical.”

- Richard Feynman

Phenomenon of interest

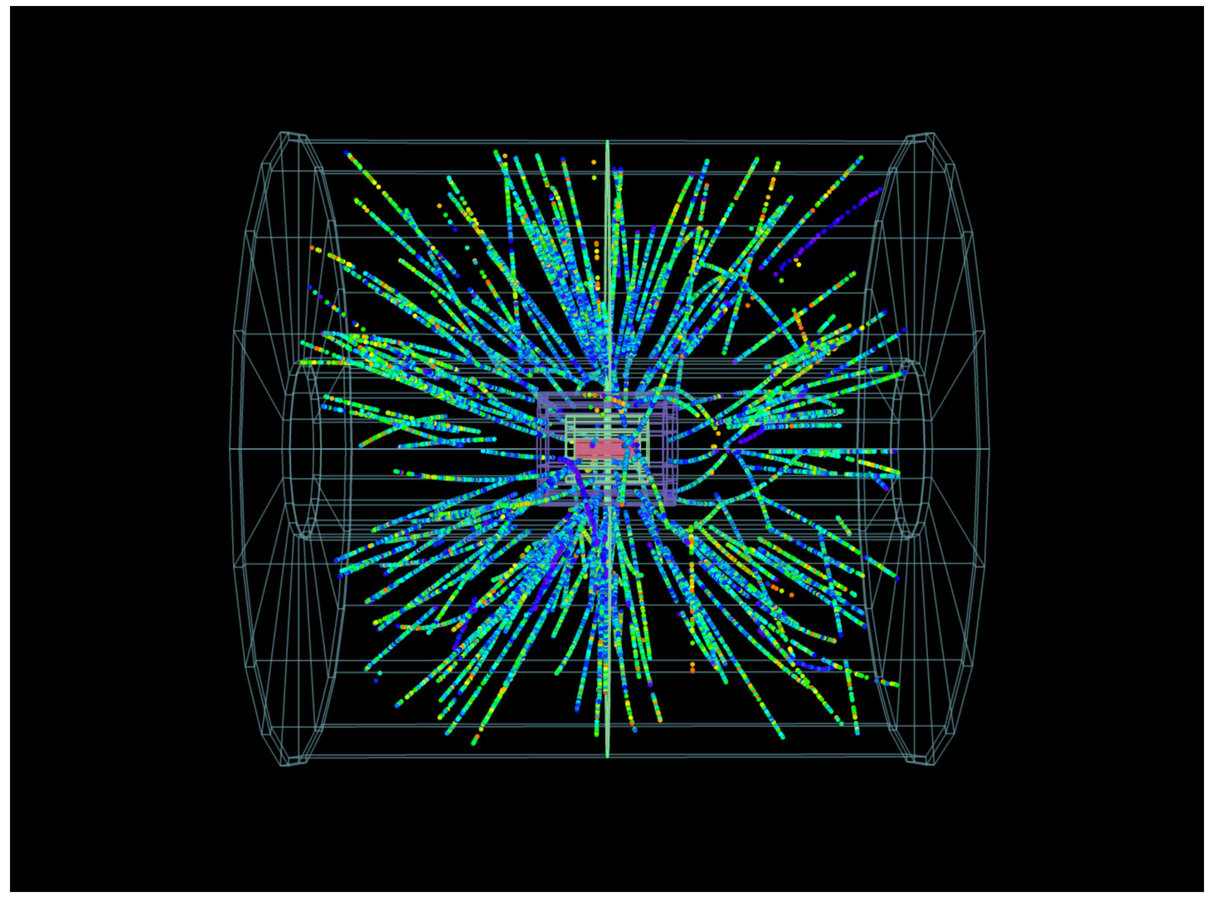

Quantum simulation

$$|\psi\rangle_{\text{in}} \rightarrow e^{-i\hat{H}t} \rightarrow \langle \hat{\mathcal{O}}(t) \rangle$$

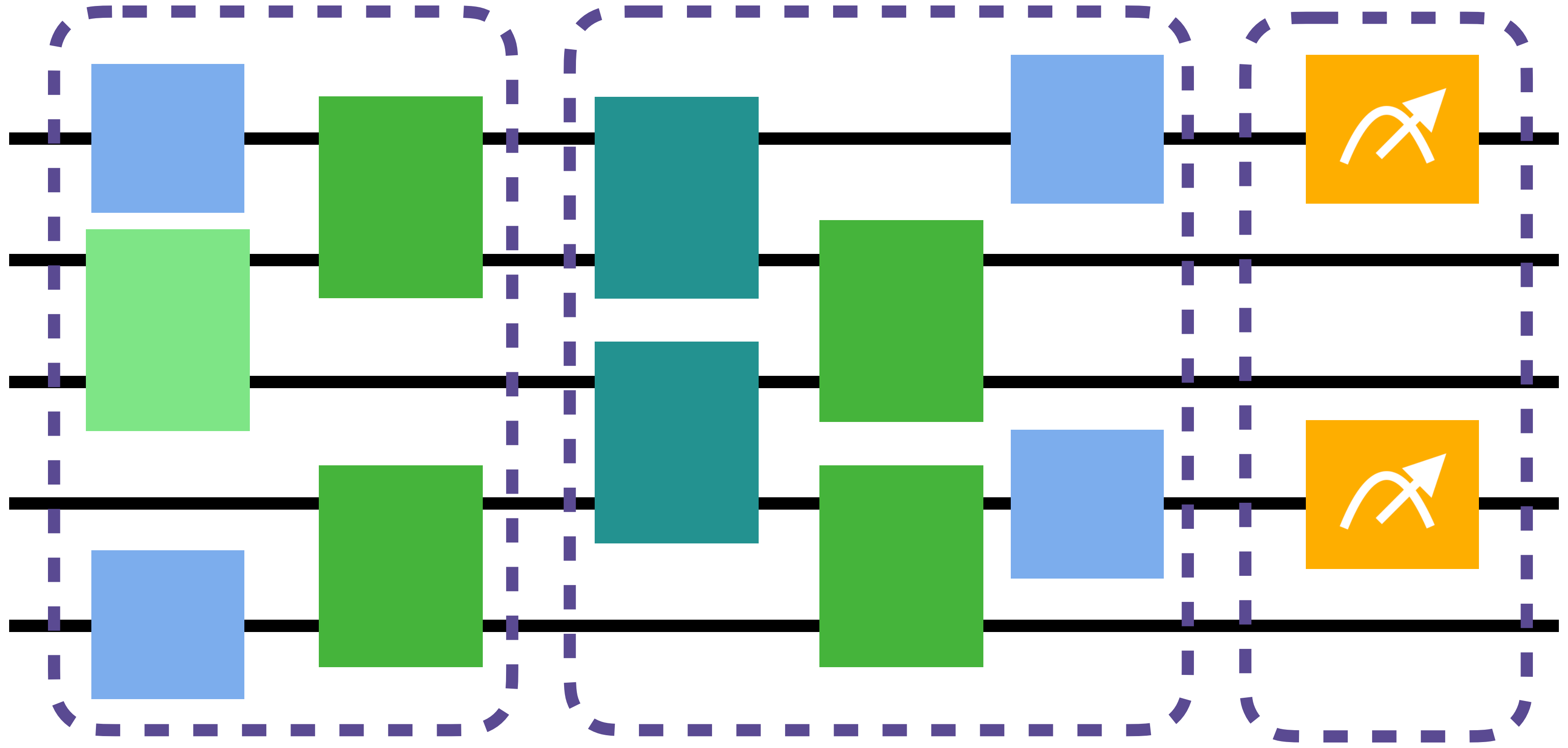

"Nature isn't classical, dammit, and if you want to make a simulation of nature, you'd better make it quantum mechanical."

- Richard Feynman

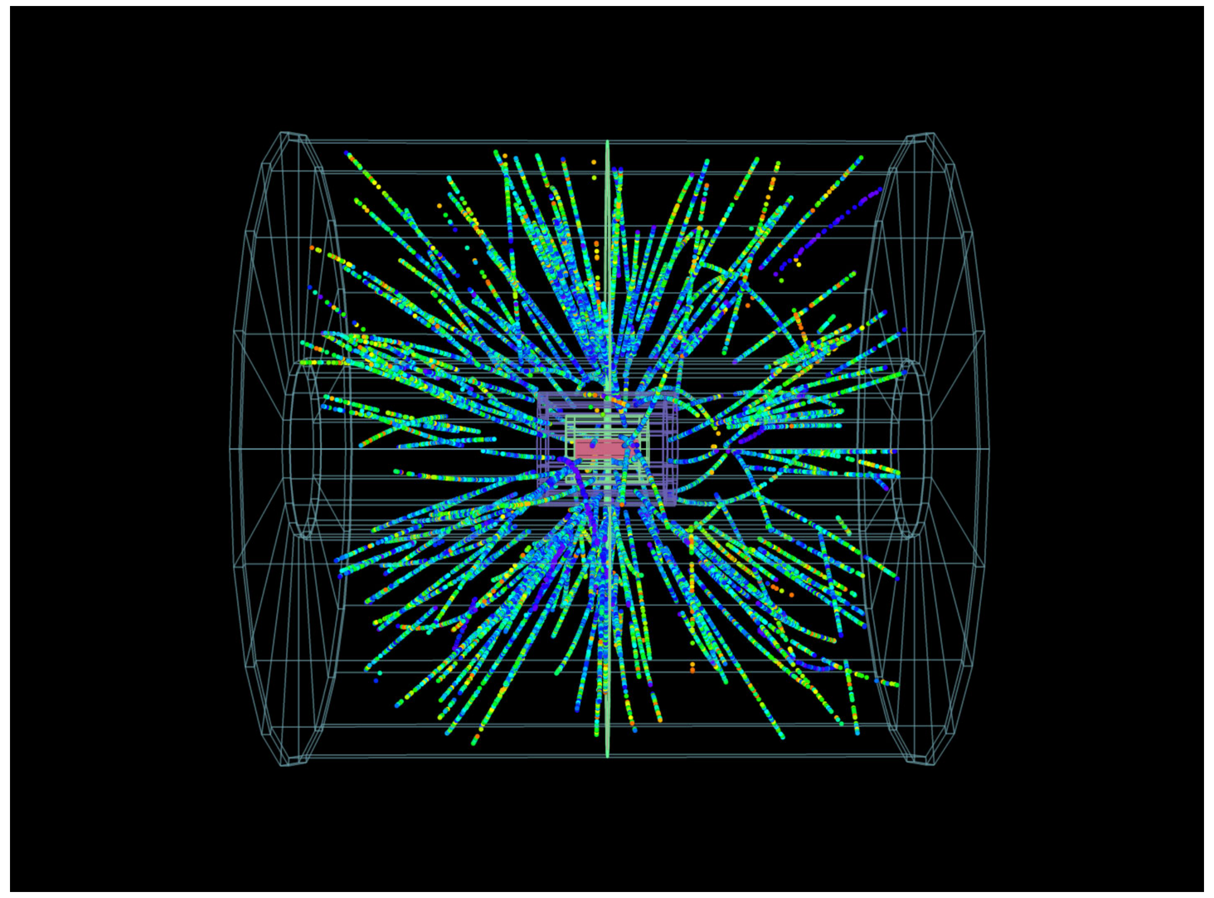

$$|\psi\rangle_{\text{in}} \rightarrow e^{-i\hat{H}t} \rightarrow \langle\hat{\mathcal{O}}(t)\rangle$$

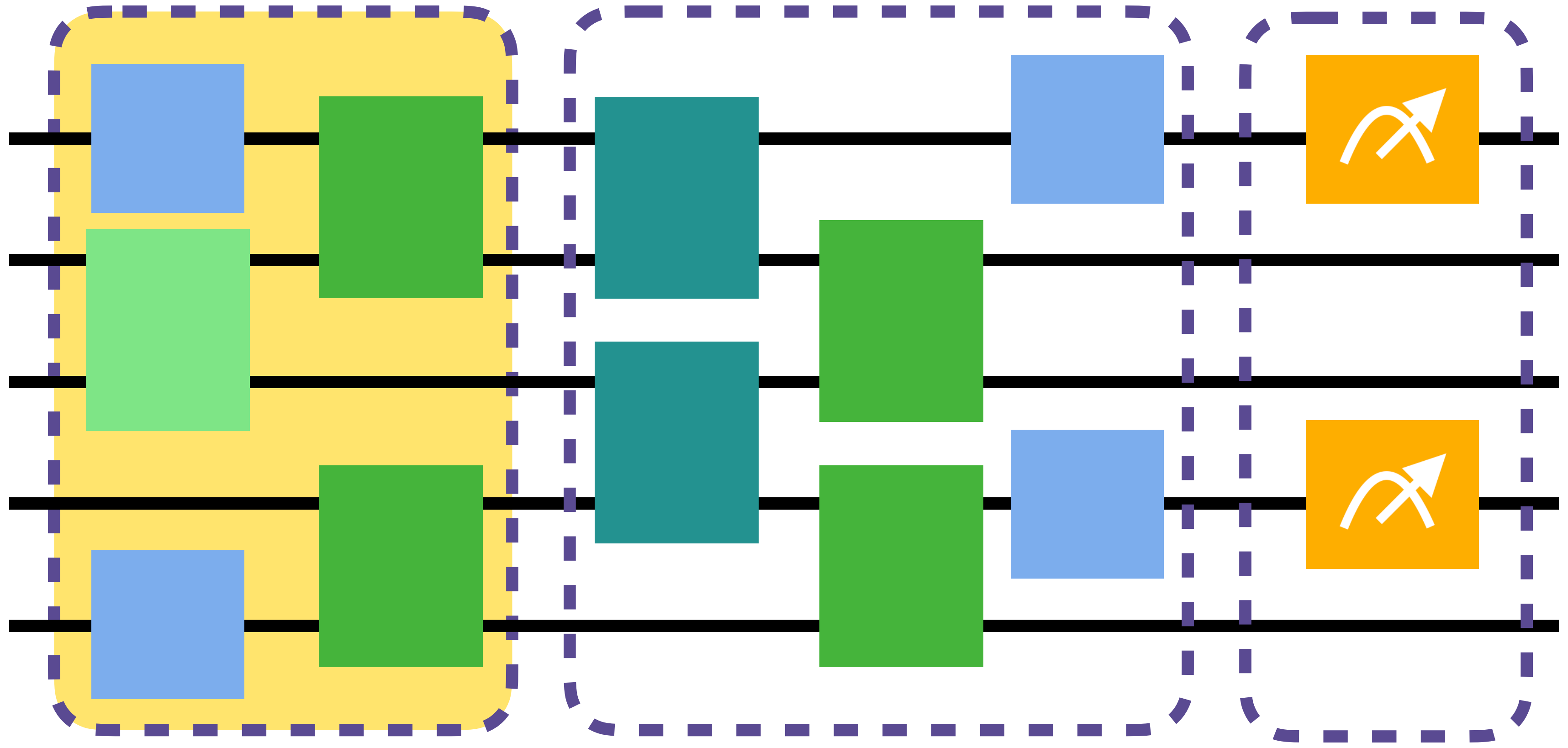

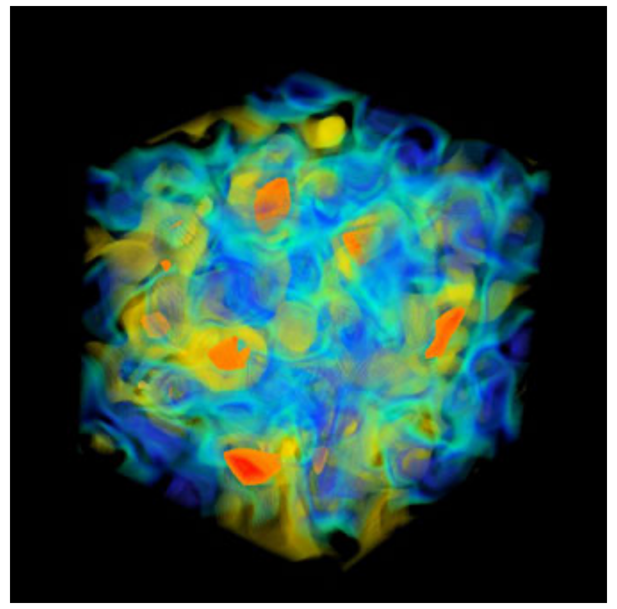

The first step in a quantum simulation is the preparation of an initial state.

This routine typically involves the preparation of an interacting ground state.

Direct methods

$$|\Omega\rangle$$

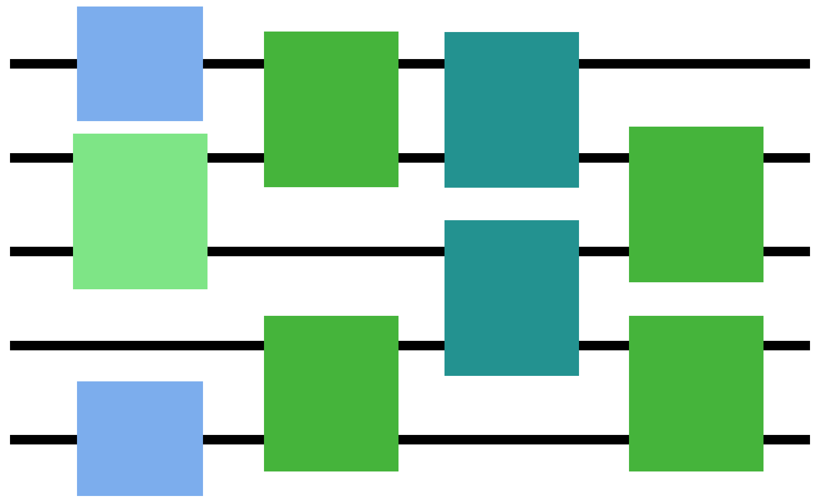

Known ground-state
(of free/ analytically solvable theory, or obtained from exact diagonalization)

Translation to quantum circuit
(map wavefunction to quantum-circuit using classical algorithm)

Ground-state quantum circuit
(implement classically-compiled quantum circuit on hardware)

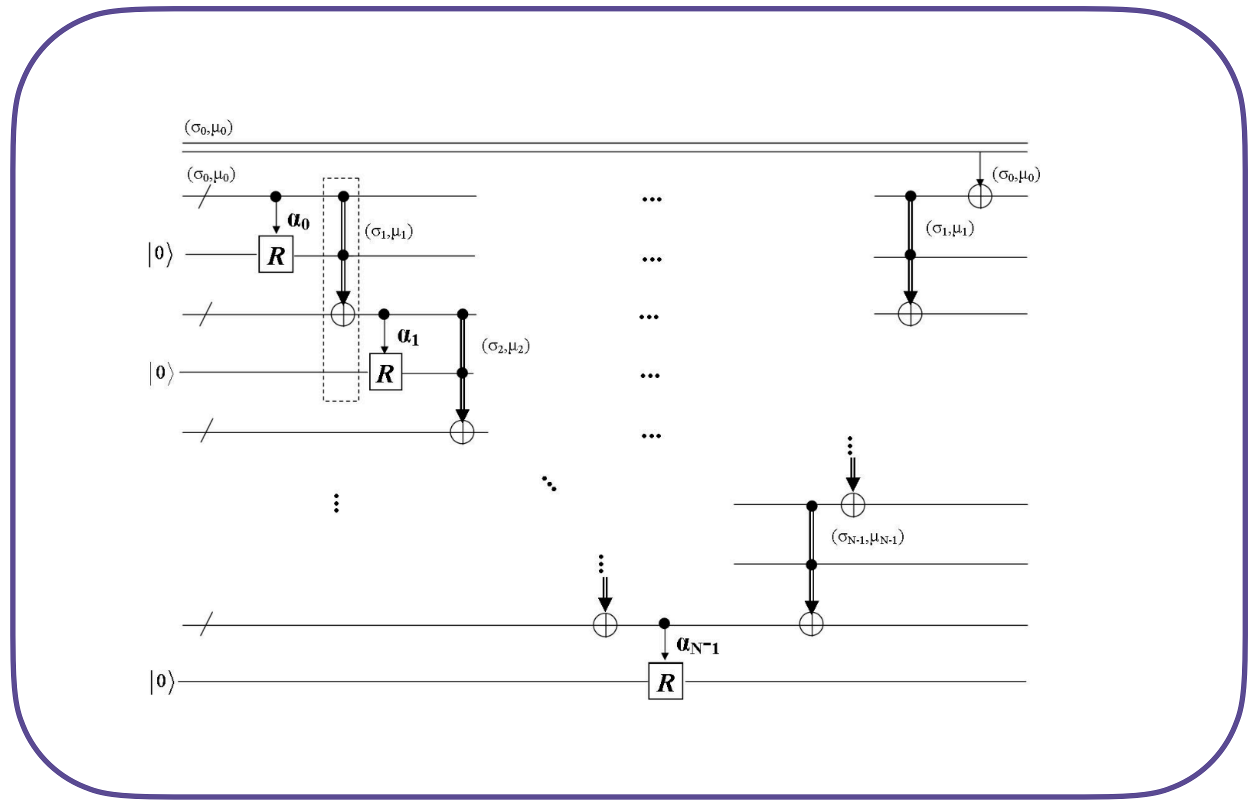

Kitaev & Webb ’08

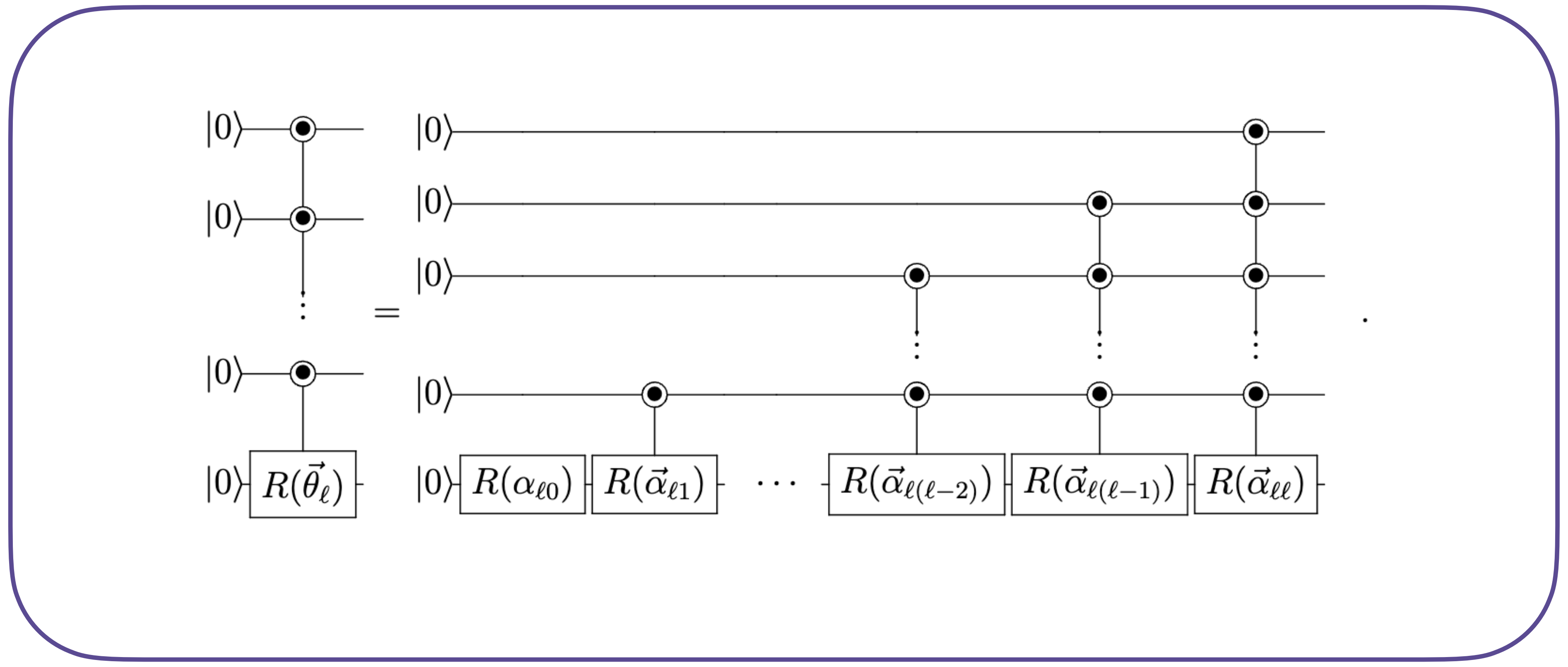

Klco & Savage ’20

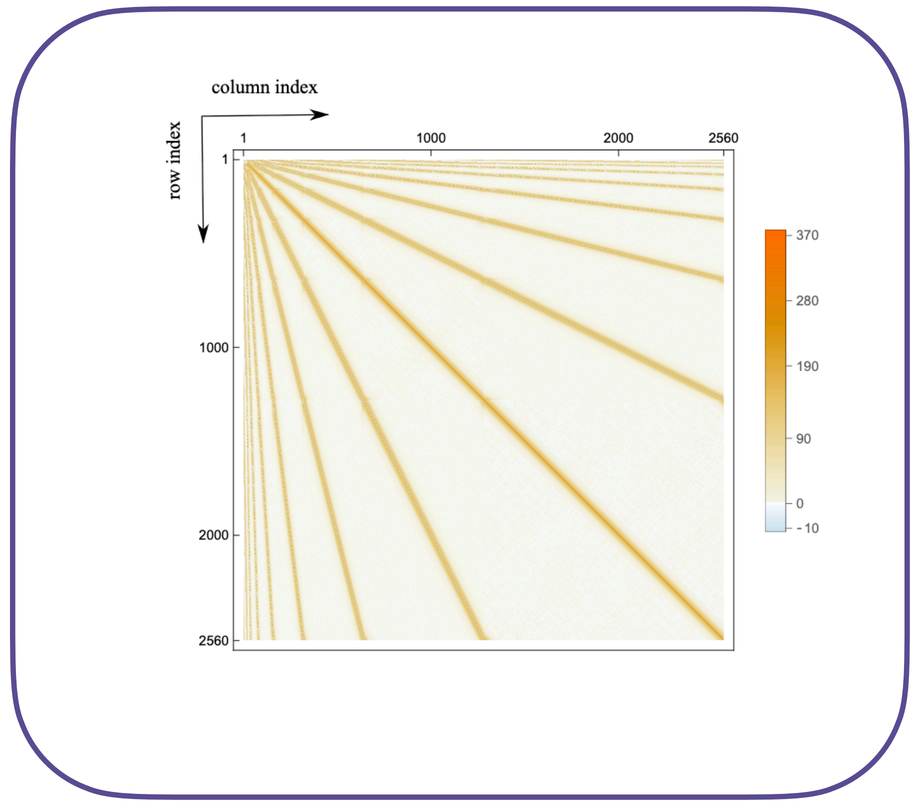

Bagherimehrab+ ’22

Exact quantum methods

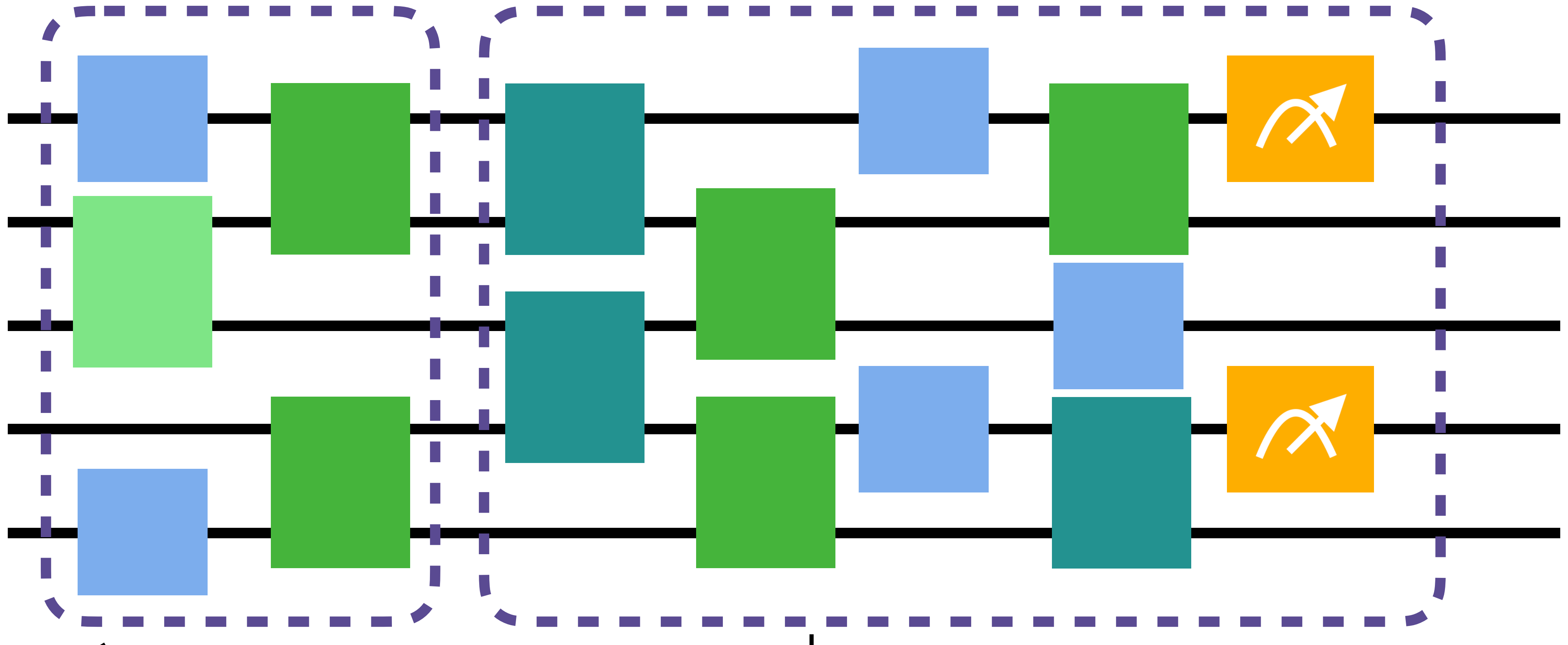

$|\psi_0\rangle$

Trial state
(Easily prepared, typically has non-trivial overlap with ground state of interest)

→

Quantum routine
(real/ imaginary time evolution, iterative filtering, projective measurements etc., may also involve classical mid- or post-circuit processing)

→

Ground-state quantum circuit

- While these algorithms come with provable guarantees for accuracy and optimality, they require deep coherent quantum circuits.
- Hence, they are more suitable for the far-term fault-tolerant era.

Heuristic hybrid methods

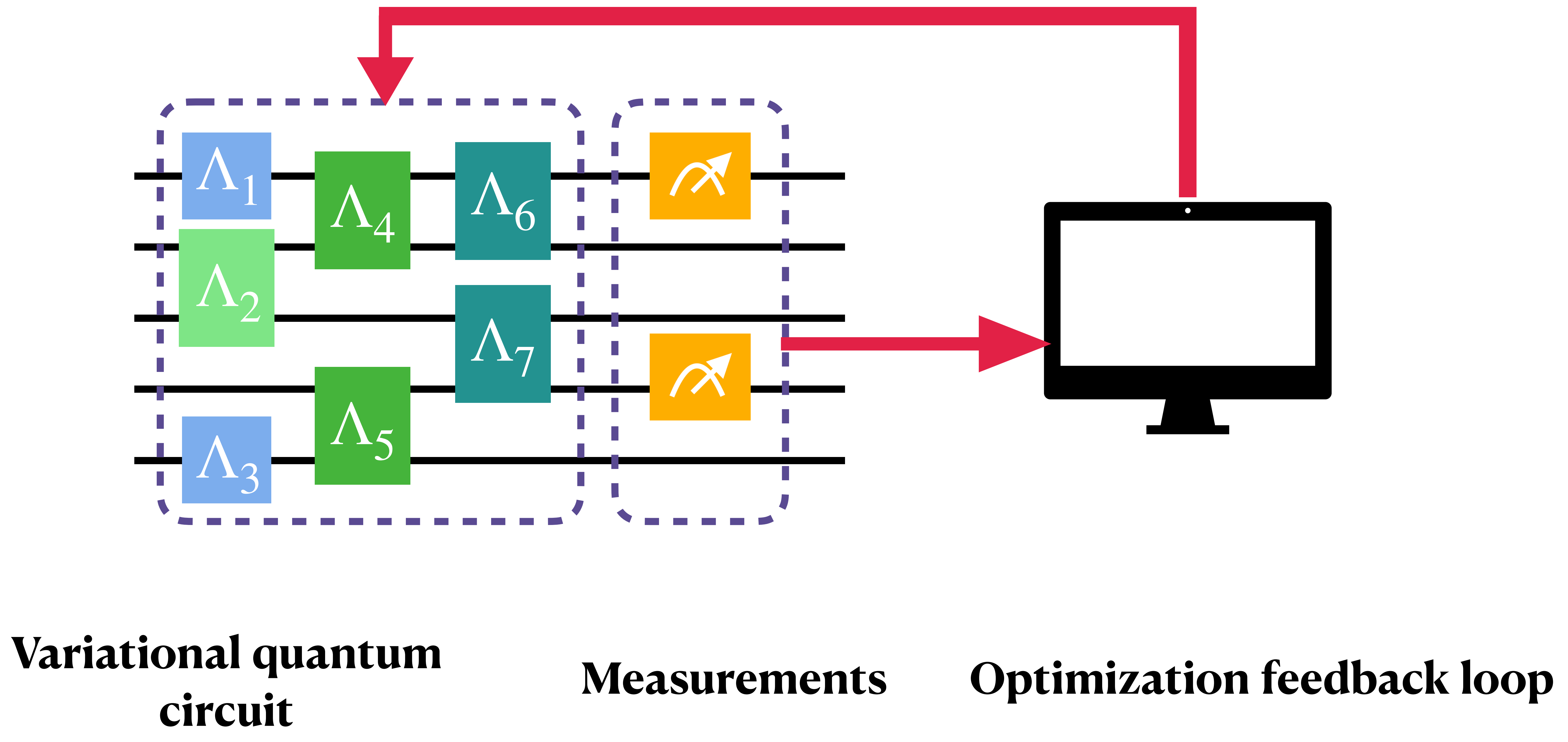

- Some quantum computing cost is traded off by the classical computing cost of optimization, resulting in shallower circuits.
- This makes this method more appropriate for the near-term era.
- However, there are typically no guarantees for the accuracy and efficiency of this procedure and its success critically depends upon an appropriate choice of circuit ansatz.
- Furthermore, statistical noise from quantum measurements aggravates barren plateaus.

An opportunity

Hadron Spectrum

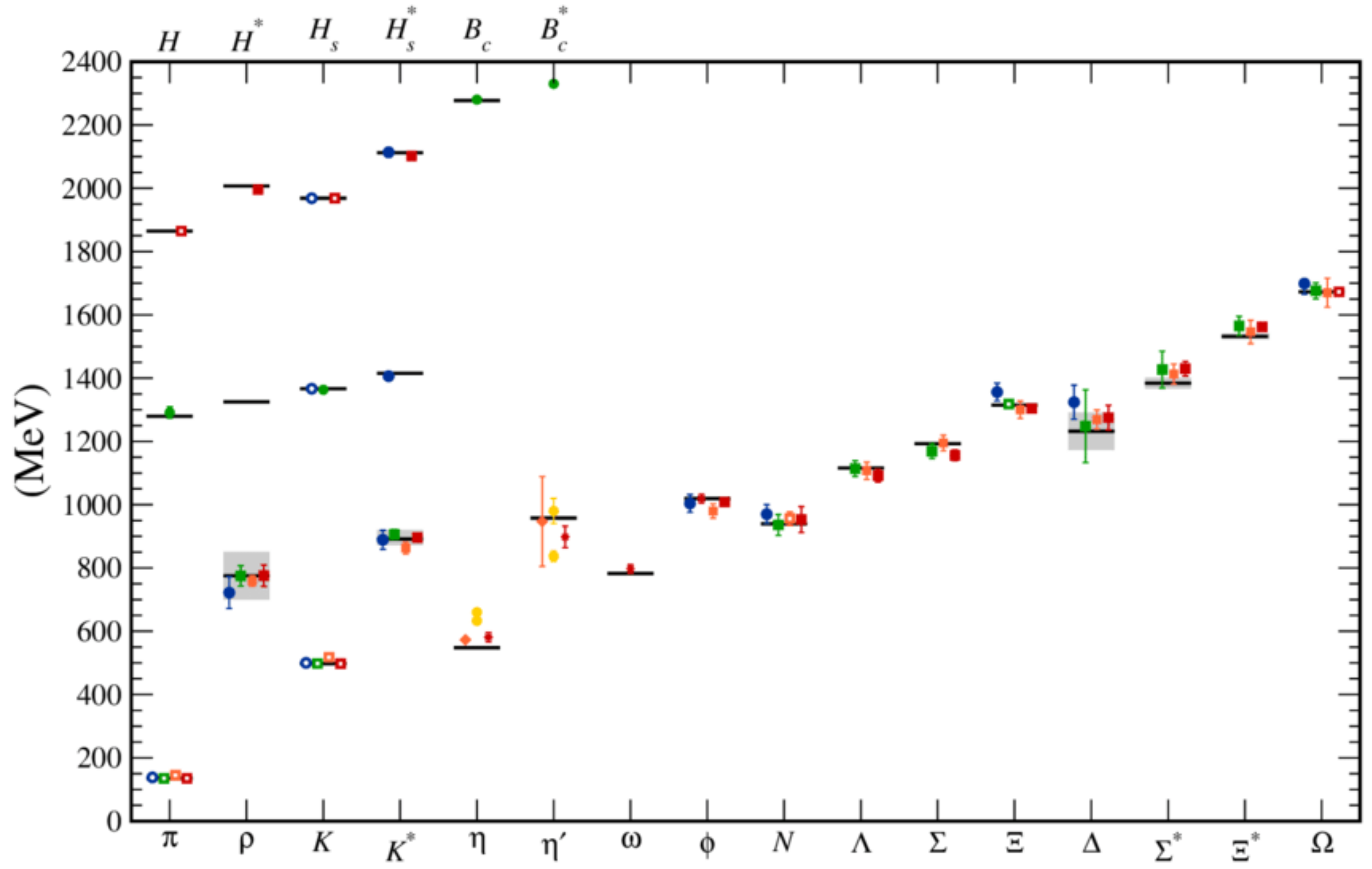

[1]

Path Integral Monte Carlo (PIMC) methods like lattice QCD are a rich source of ground-state data.

Structure

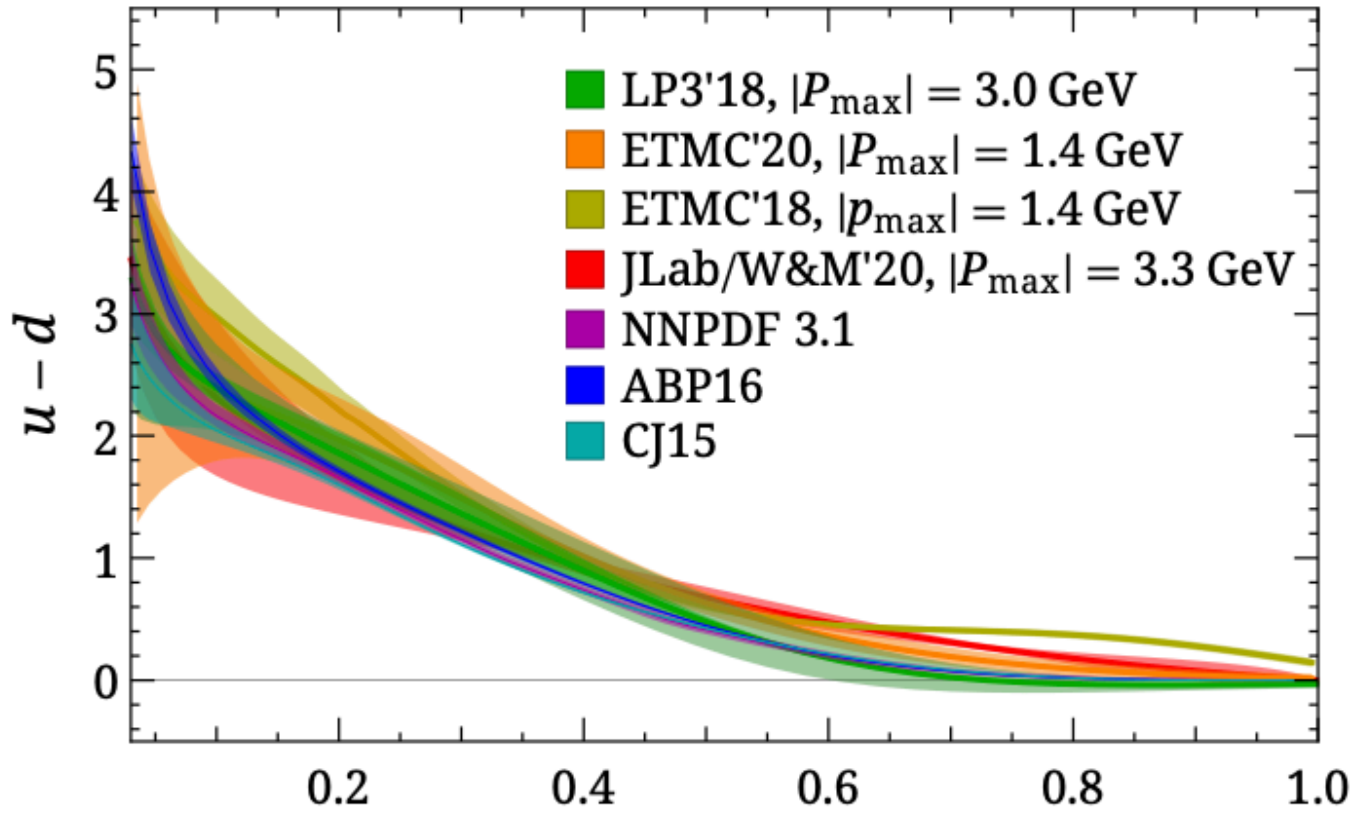

(Summary of lattice calculations of isovector unpolarized quark PDFs from various collaborations)

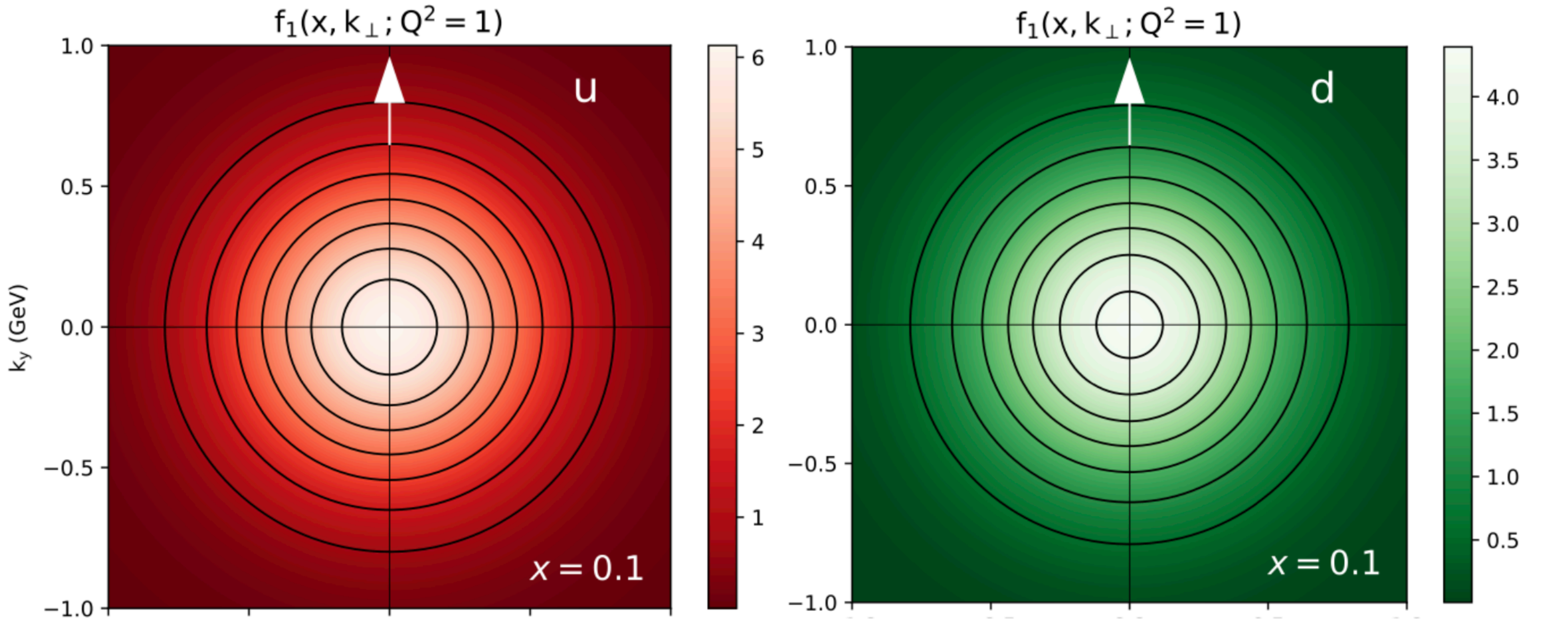

[2]

(Quark density for an unpolarized proton moving towards the viewer for the up quark on the left and down quark on the right)

[1] Kronfeld, A. S. (2012). *Annual Review of Nuclear and Particle Science*, *62*, 265-284.
[2] Constantinou, M., Courtoy, A., Ebert, M. A., Engelhardt, M., Giani, T., Hobbs, T., ... & Zhang, R. (2021). *Progress in Particle and Nuclear Physics*, *121*, 103908.

From lattice QCD to ground states for simulation?

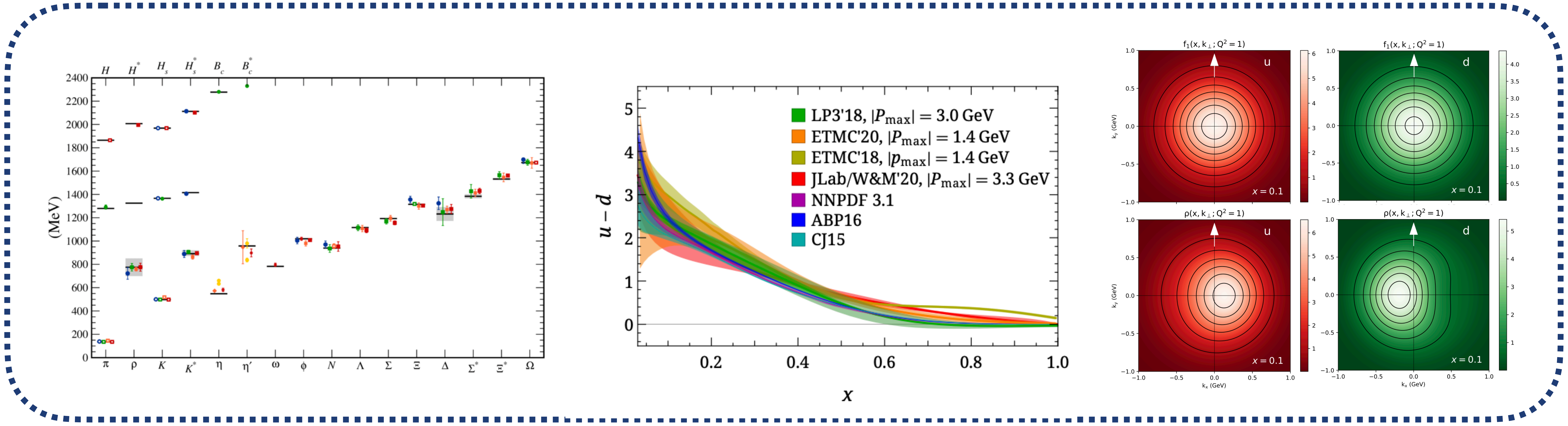

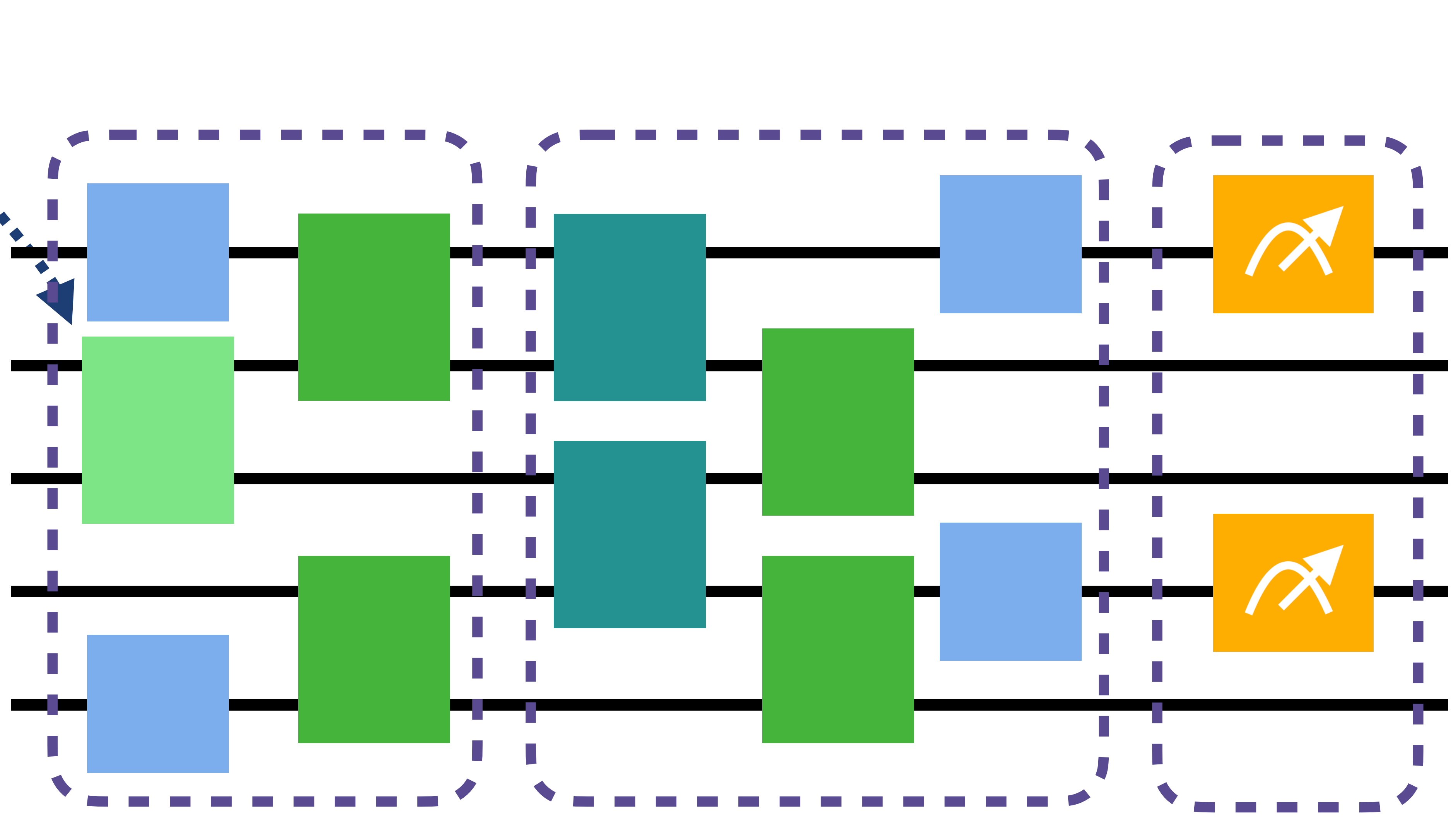

Non-trivial to make a connection between

Euclidean Monte Carlo data

and

Minkowski wavefunctions

in general, and for QCD in particular.

Classically determined quantum circuits

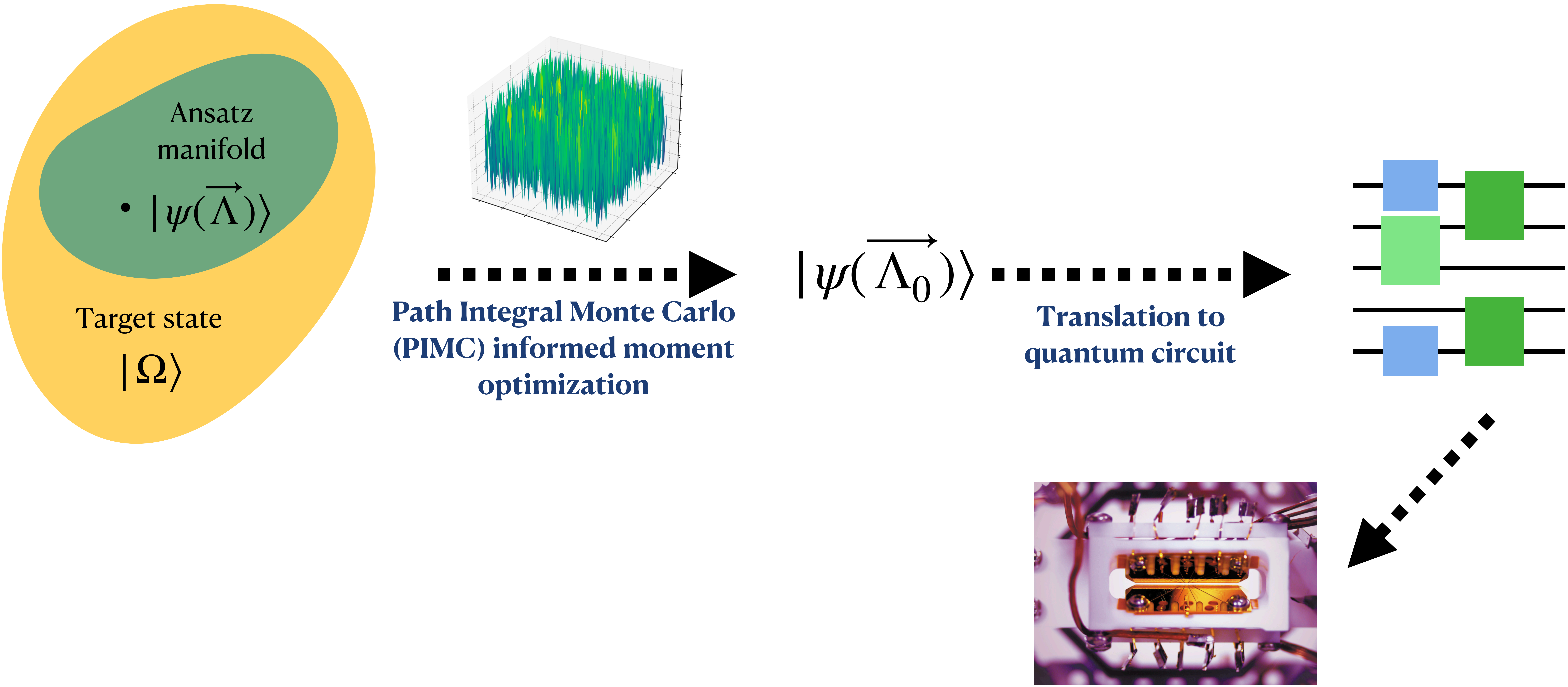

Trapped ion quantum computer from
Monroe Lab (UMD, 2016)

Classically determined quantum circuits

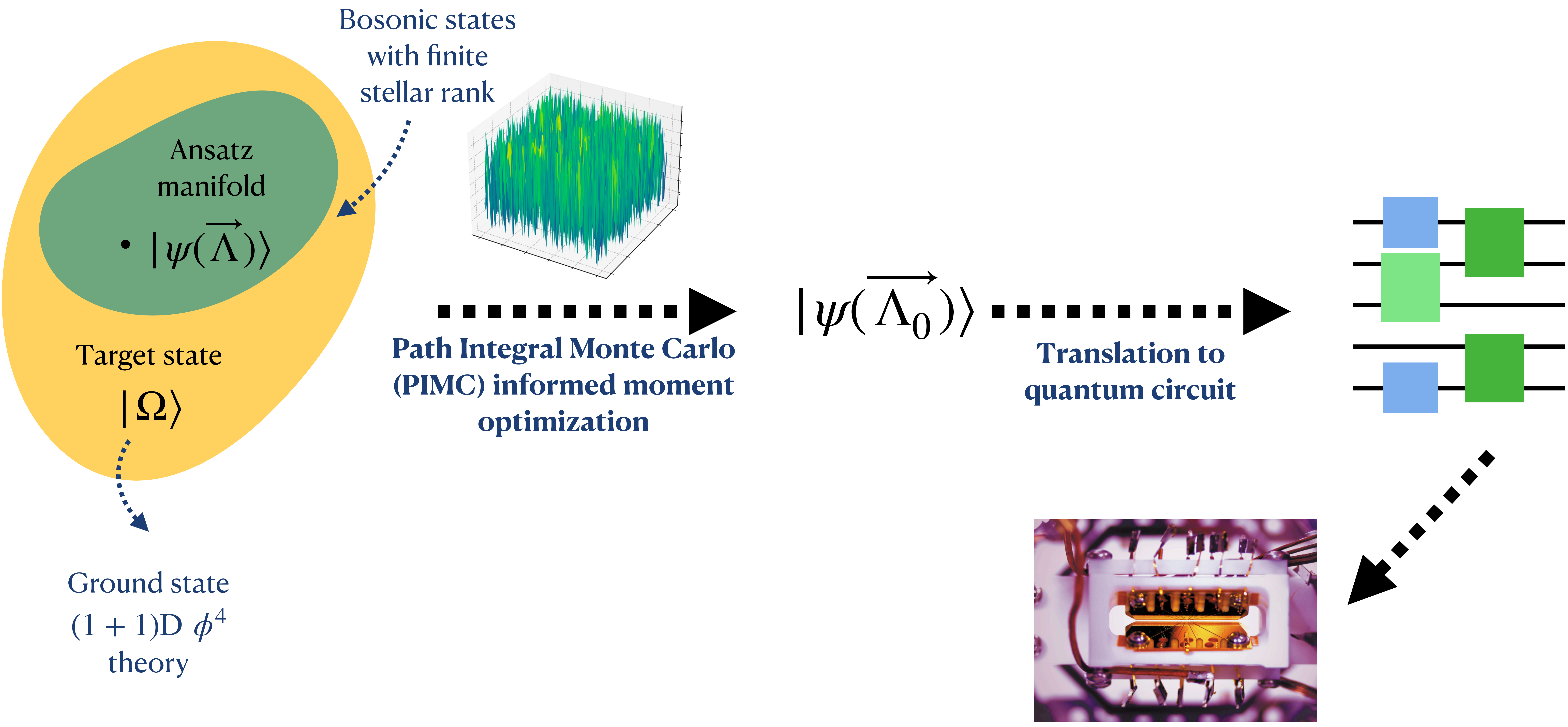

Trapped ion quantum computer from Monroe Lab (UMD, 2016)

Classically determined quantum circuits

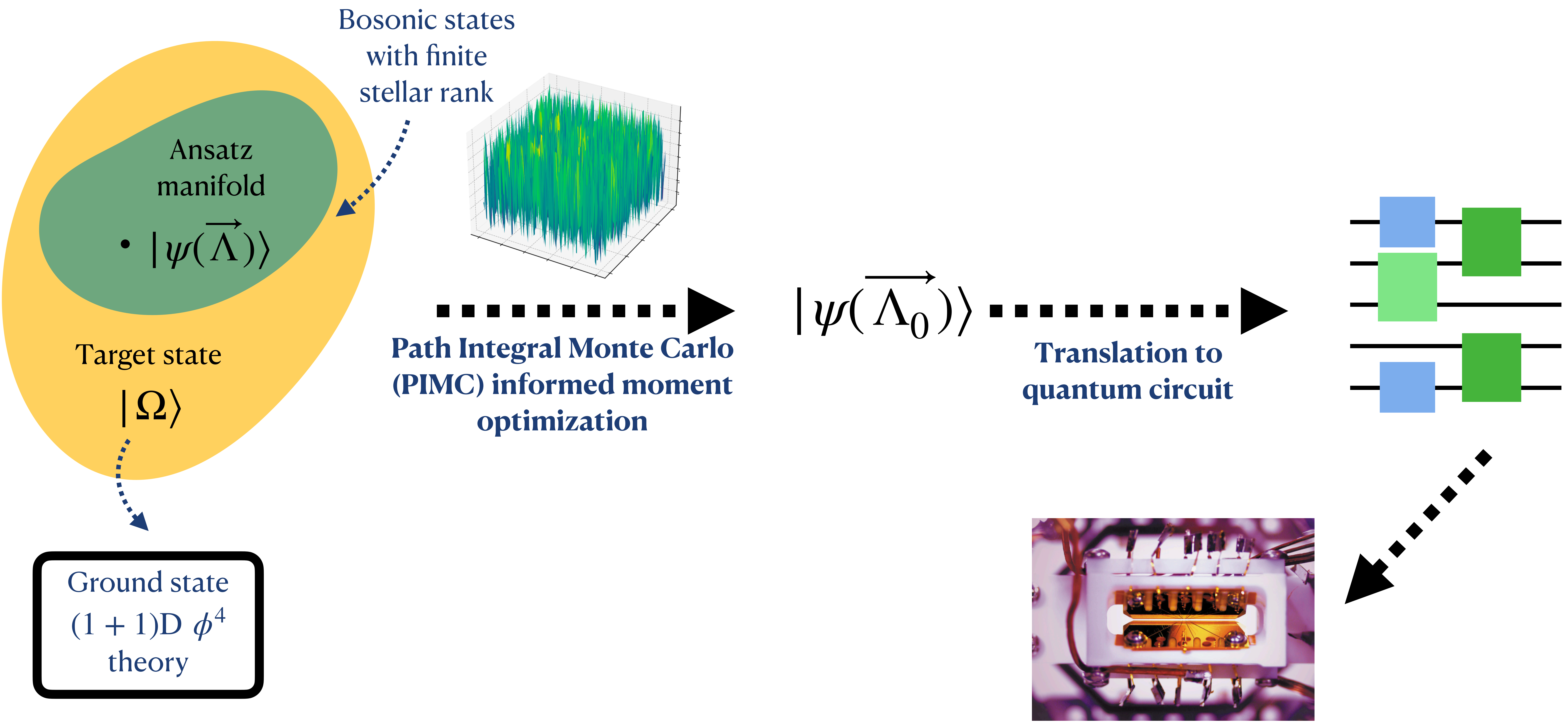

Trapped ion quantum computer from Monroe Lab (UMD, 2016)

Ground state of (1 + 1)D ϕ^4 theory

$$\hat{H} = \sum_{n=0}^{N-1} \left(\frac{\hat{\pi}_n^2}{2} + \frac{(\hat{\phi}_{n+1} - \hat{\phi}_n)^2}{2} + \frac{1}{2} m^2 \hat{\phi}_n^2 + \frac{\lambda}{4} \hat{\phi}_n^4 \right)$$

Parity, time-reversal, cyclic translation, and inversion symmetric.

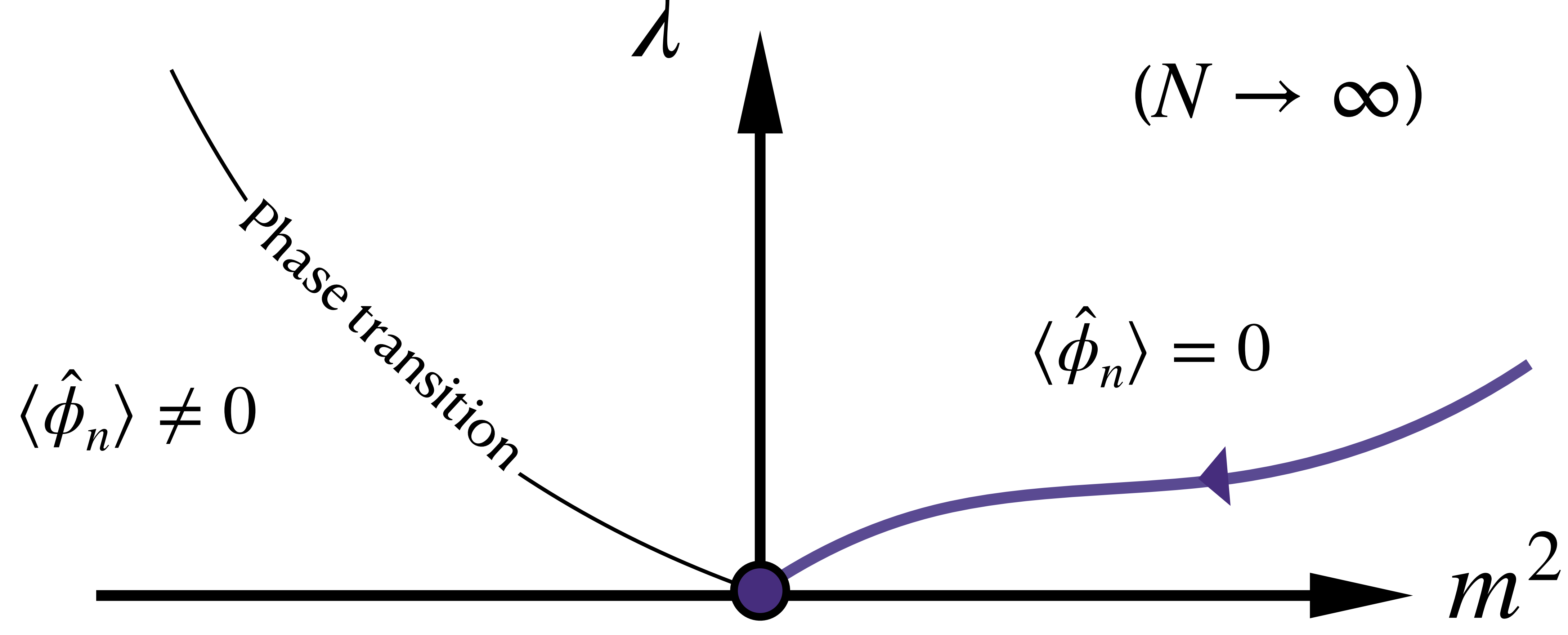

Continuum limit:

$m^2, \lambda \to 0{,}0$ along some line of constant physics.

Ground state of (1 + 1)D ϕ^4 theory

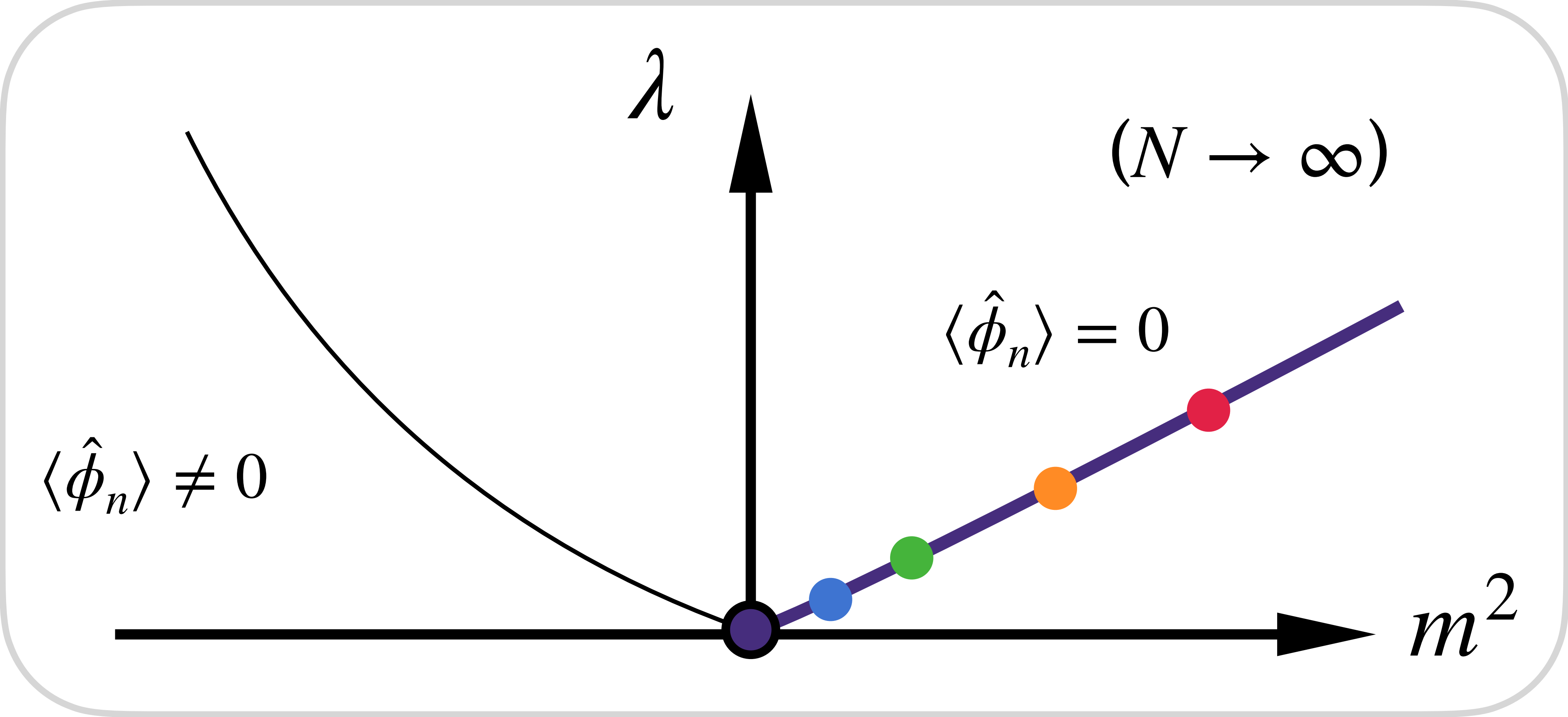

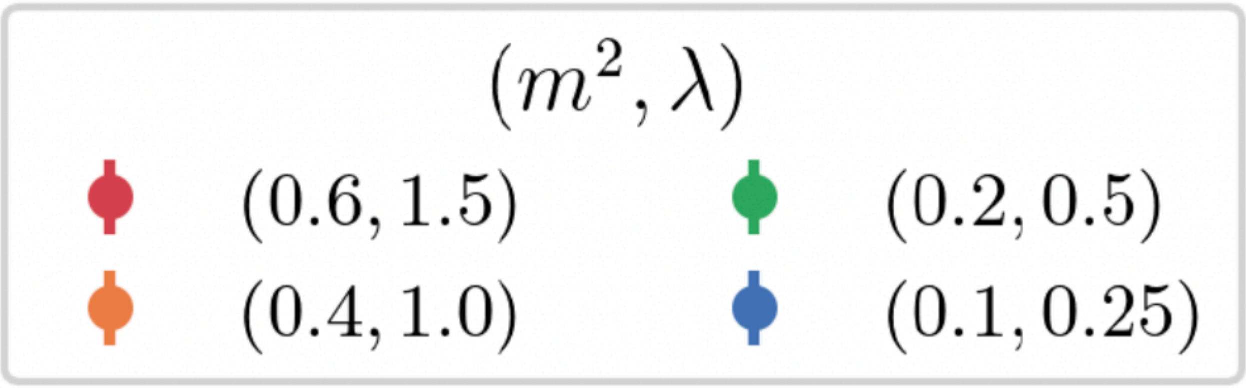

Correlations

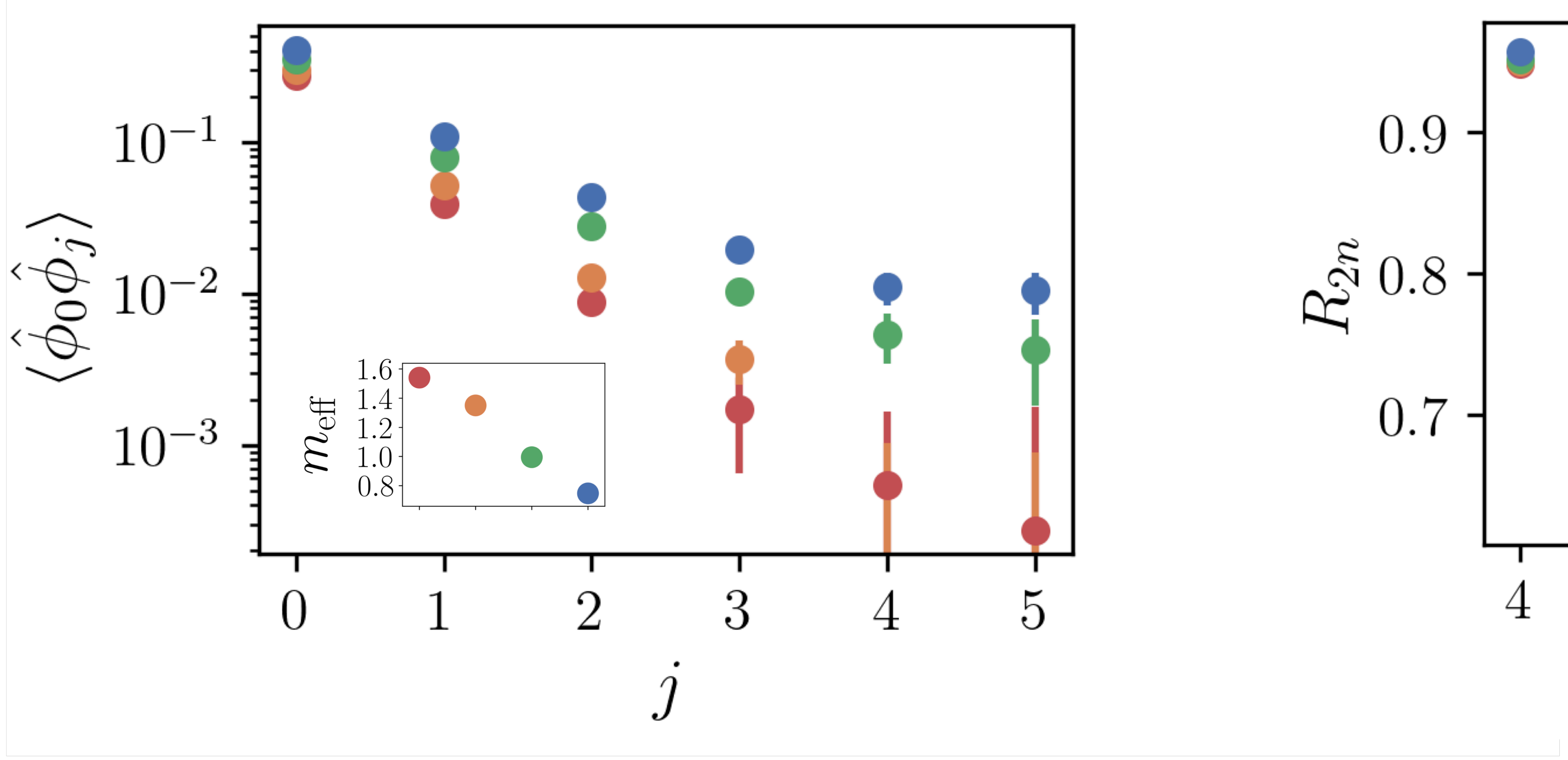

Non-Gaussianity

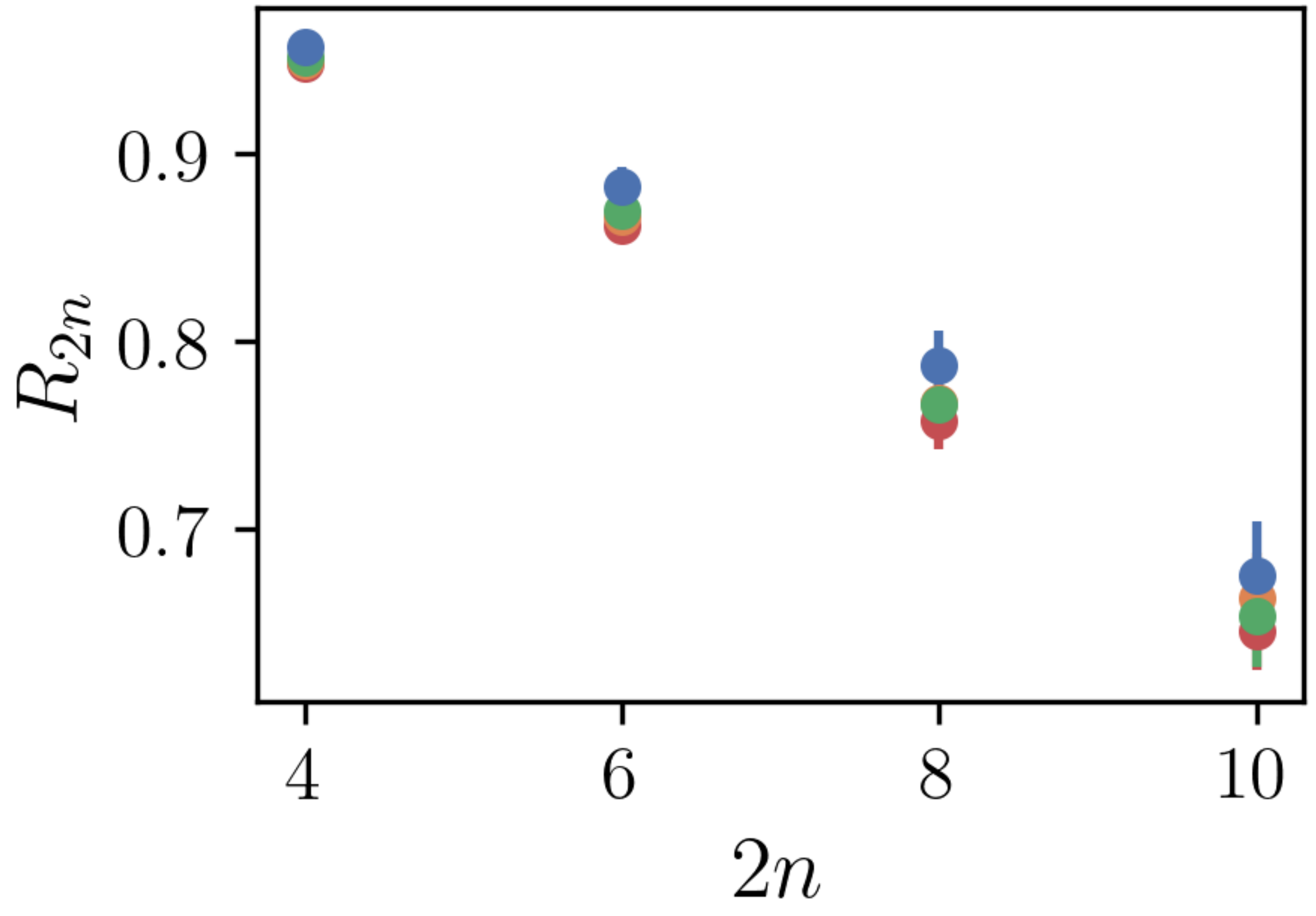

$$R_{2n} = \frac{\langle \hat{\phi}^{2n} \rangle}{(2n-1)!!\langle \hat{\phi}^2 \rangle^n}$$

Classically determined quantum circuits

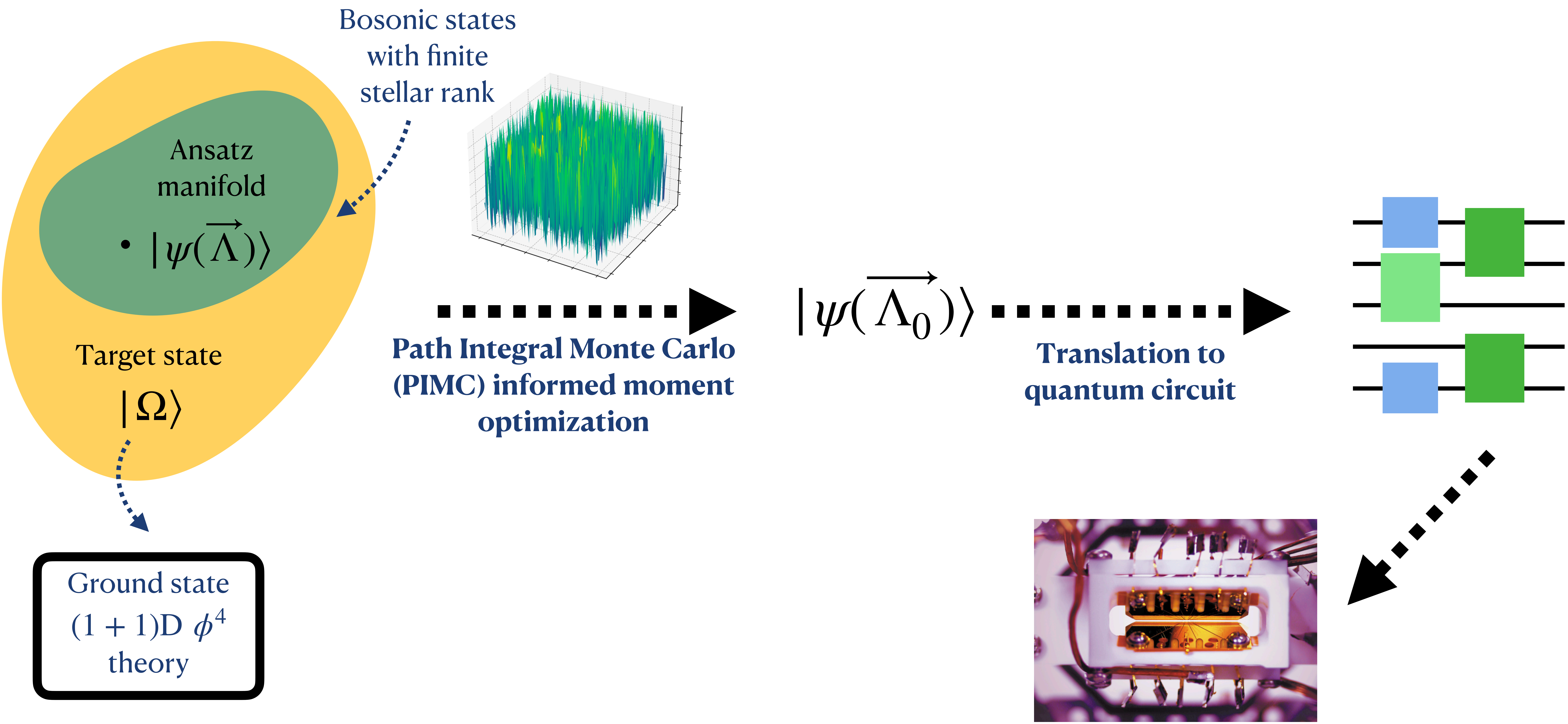

Trapped ion quantum computer from
Monroe Lab (UMD, 2016)

Classically determined quantum circuits

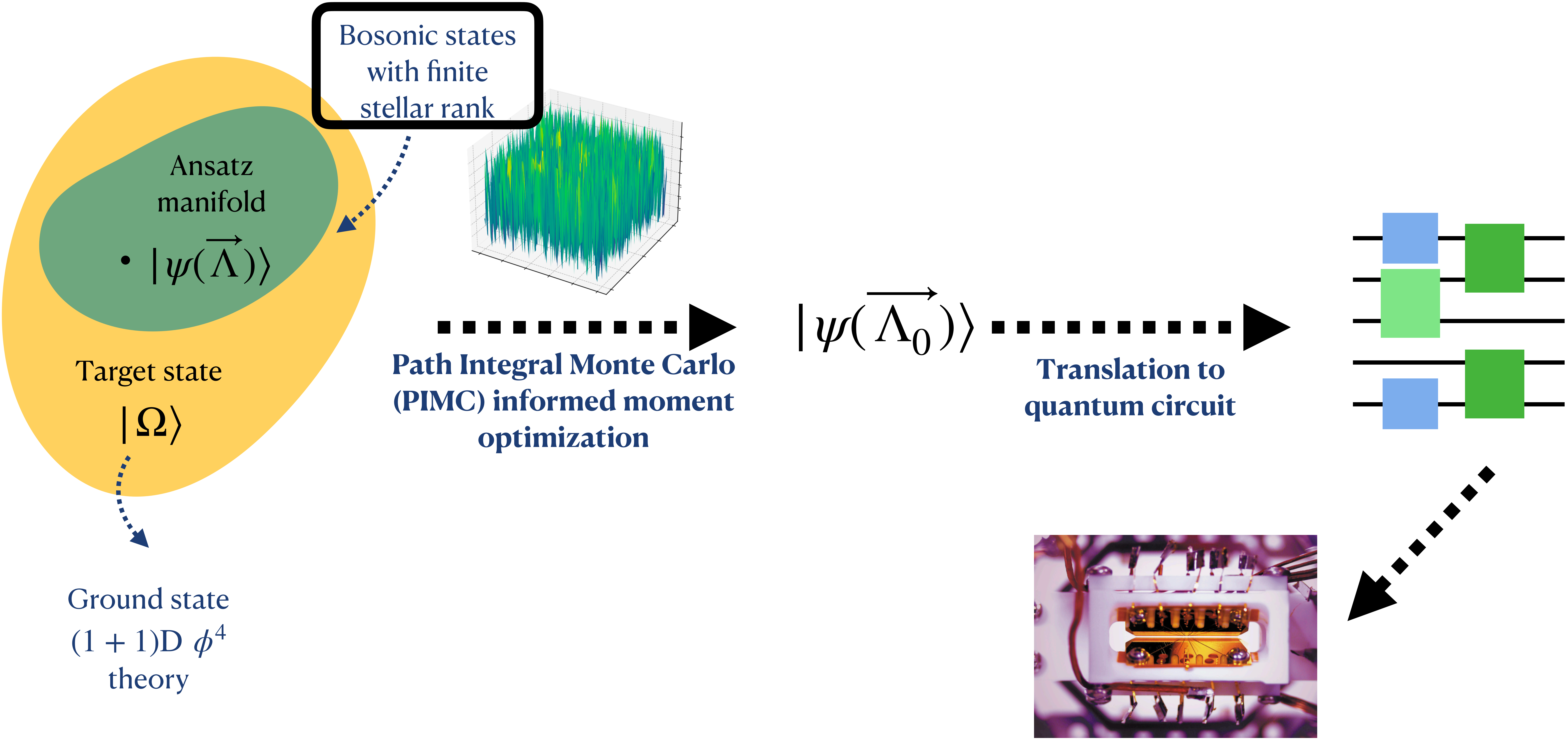

Trapped ion quantum computer from Monroe Lab (UMD, 2016)

Finite-stellar rank states

Most pure states of N bosonic modes have the decomposition

$$|\psi\rangle_R = \hat{U}_G |C\rangle_R$$

Gaussian unitary transformation

Core state

$$|C\rangle_R = \sum_{\substack{\vec{n} = n_0, \ldots, n_{N-1} \\ \text{sum}(\vec{n}) \leq R}} c_{\vec{n}} \, |\vec{n}\rangle$$

$R \in \mathbb{N} \cup \{0\}$ is the **stellar rank** of this state.

States which do not admit the above decomposition are said to have an infinite rank.

Chabaud, U., Markham, D., & Grosshans, F. (2020). Stellar representation of non-Gaussian quantum states. *Physical Review Letters*, *124*(6), 063605.

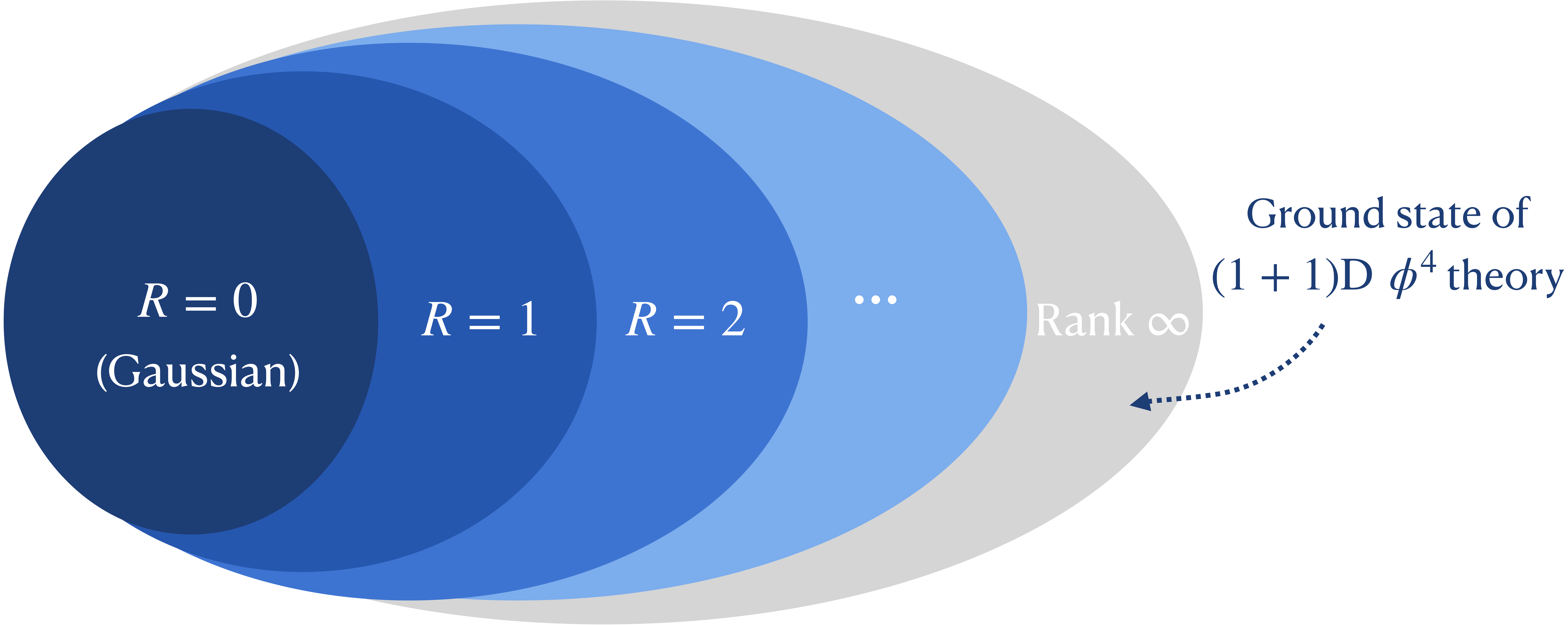

Finite rank states can get arbitrarily close to infinite-rank states (in trace distance).

Thus, we will use finite rank states to approximate the infinite rank ground state.

Chabaud, U., Markham, D., & Grosshans, F. (2020). Stellar representation of non-Gaussian quantum states. *Physical Review Letters*, *124*(6), 063605.

The (R, Q) ansatz

$$|\psi\rangle_R = \hat{U}_G |C\rangle_R \;\rightarrow\; |\psi\rangle_{R,Q} = \otimes_{j=0}^{N-1} \hat{U}_{G,j} |C\rangle_{R,Q}$$

$$U_{G,j} = \hat{S}_j(r)$$

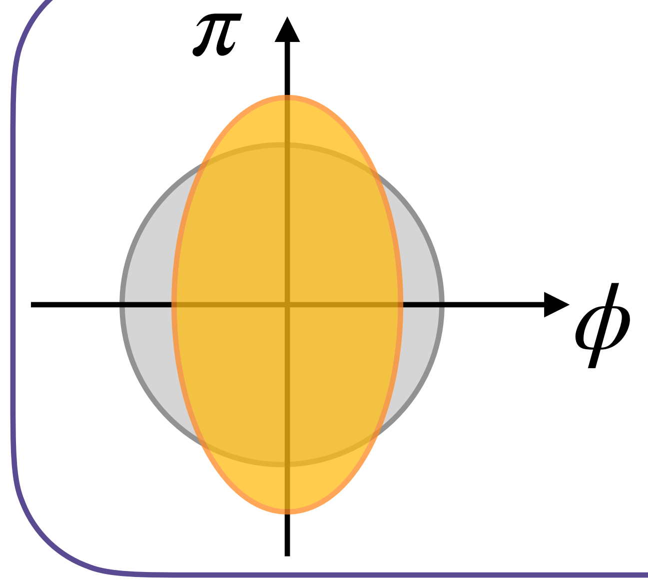

Squeezing

$$\hat{S}(r) = e^{\frac{r}{2}[(\hat{a}^\dagger)^2 - \hat{a}^2]}$$

$$|C\rangle_{R,Q} = \sum_{\substack{\vec{n} = n_0, \ldots, n_{N-1} \\ \mathrm{sum}(\vec{n}) \leq R \\ \mathrm{span}(\vec{n}) \leq Q \leq N/2}} c_{\vec{n}} \; |\vec{n}\rangle$$

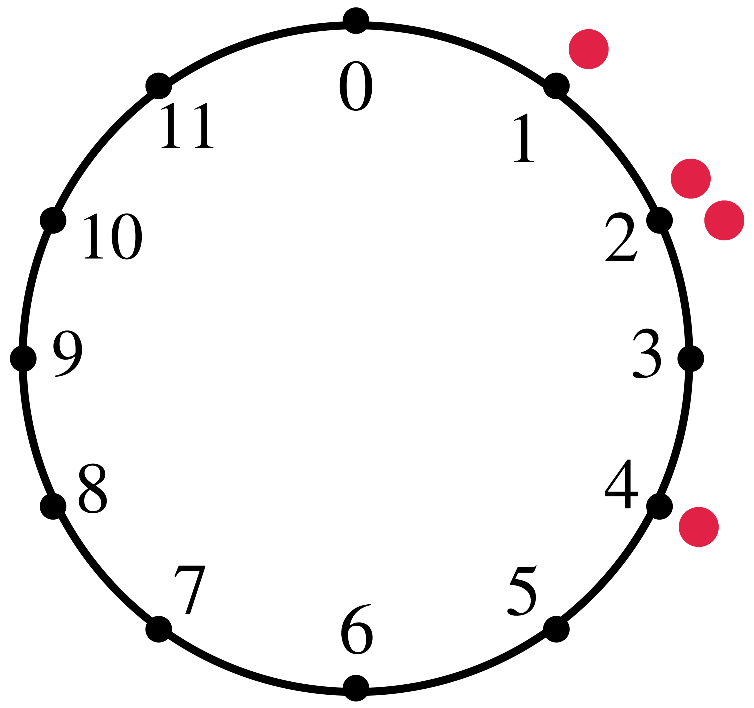

$\vec{n} = (0,1,2,0,1,0,0,0,0,0,0,0)$

$\mathrm{span}(\vec{n}) = 3$

(All non-zero excitations reside between sites j and $j+3$)

- The variational parameters are r and $c_{\vec{n}}$.
- The above simplifications result in an $O(Q^2|c_{R,Q}|^2)$ complexity for the classical computation of low-order expectation values. $N|c_{R,Q}|$ is the number of terms in the superposition $|C\rangle_{R,Q}$.

The Gaussian Effective Potential (GEP) ansatz

$$|\psi\rangle_R = \hat{U}_G\,|\,C\rangle_R \;\;\rightarrow\;\; |\psi\rangle_{\mathrm{GEP}} = \hat{U}_{\mathrm{GEP}}\,|\,\vec{0}\rangle$$

- $\hat{U}_{\mathrm{GEP}}$ is the ground-state of a free scalar field theory with bare mass μ, which is the variational parameter.
- The ground state of a $\lambda\phi^4$ theory with bare mass m can be approximated by that of a free scalar field theory with a different mass μ.

Classically determined quantum circuits

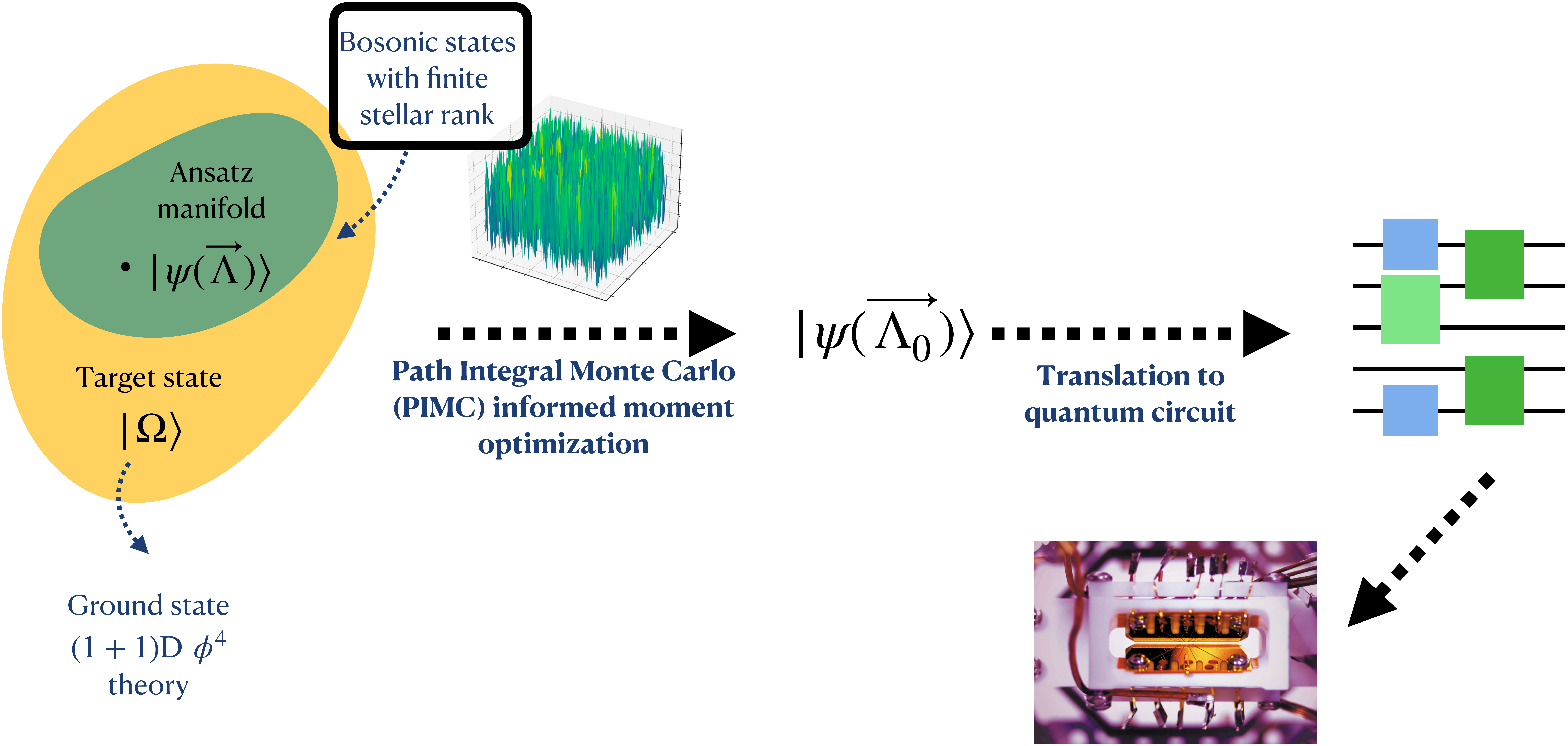

Trapped ion quantum computer from Monroe Lab (UMD, 2016)

Classically determined quantum circuits

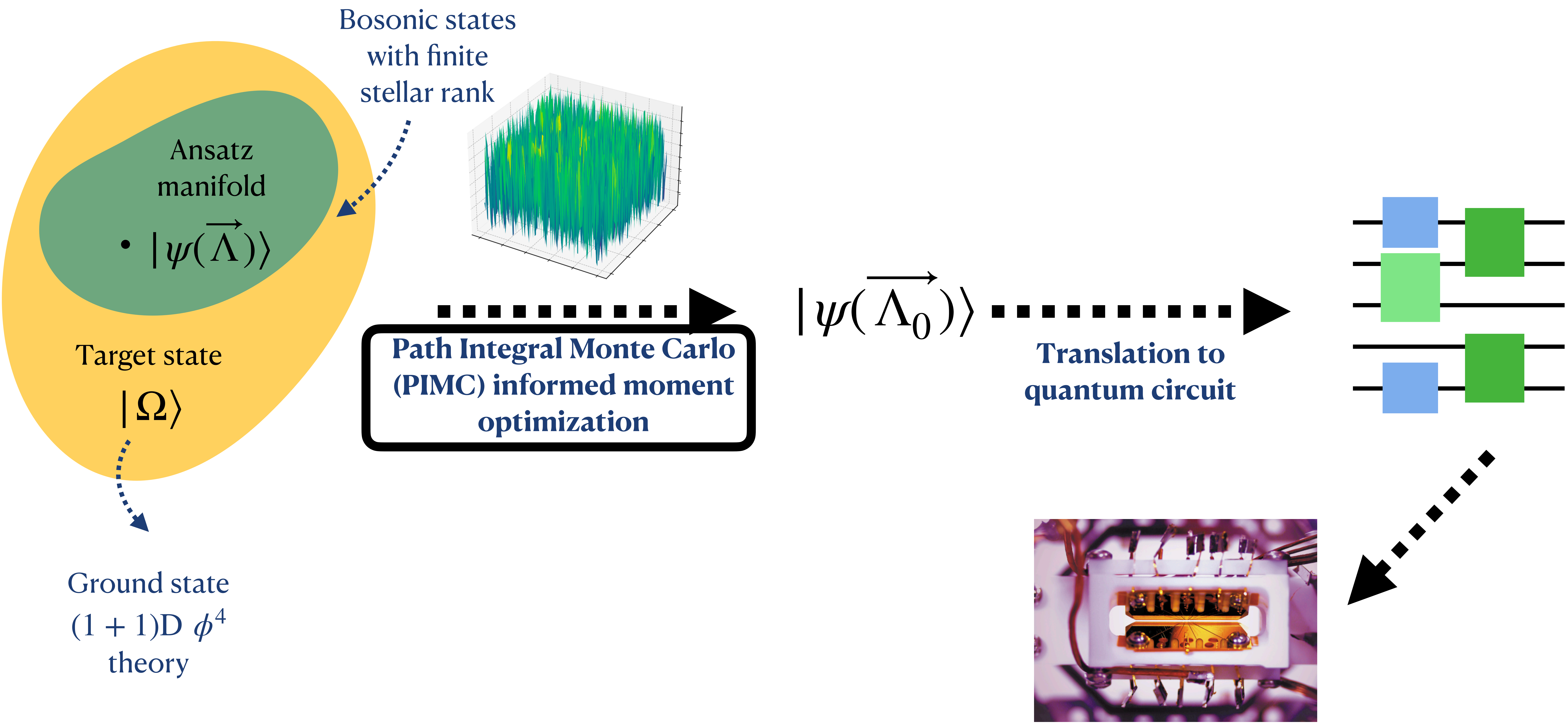

Trapped ion quantum computer from Monroe Lab (UMD, 2016)

Energy minimization

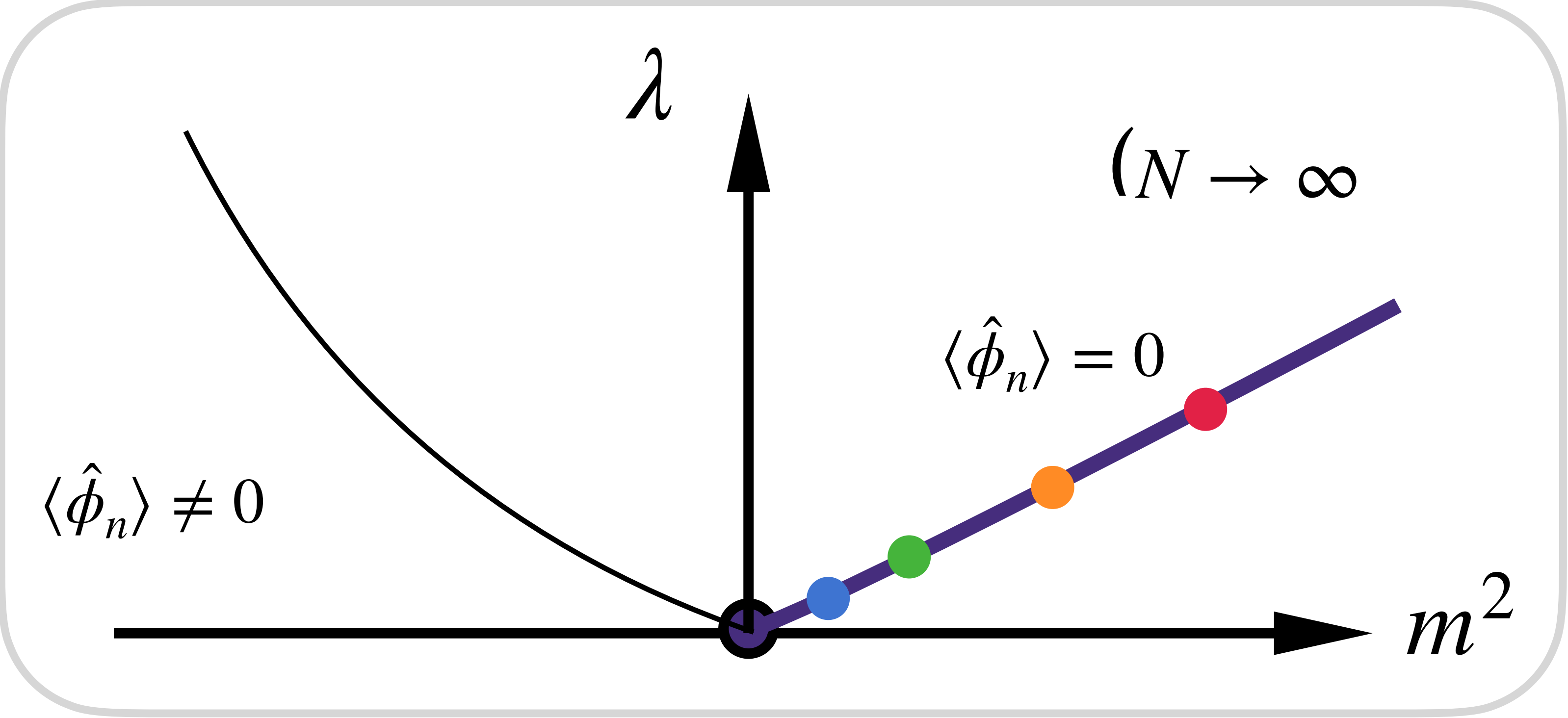

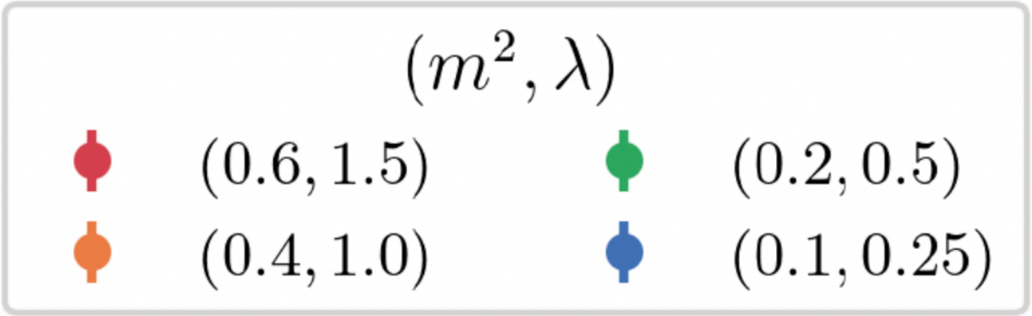

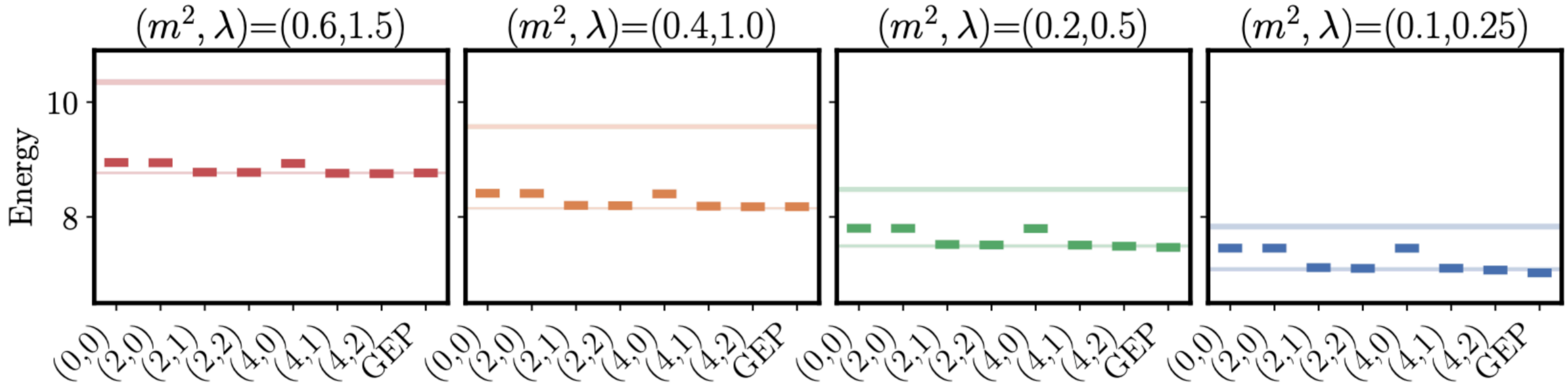

Energy minimization: Two-point functions

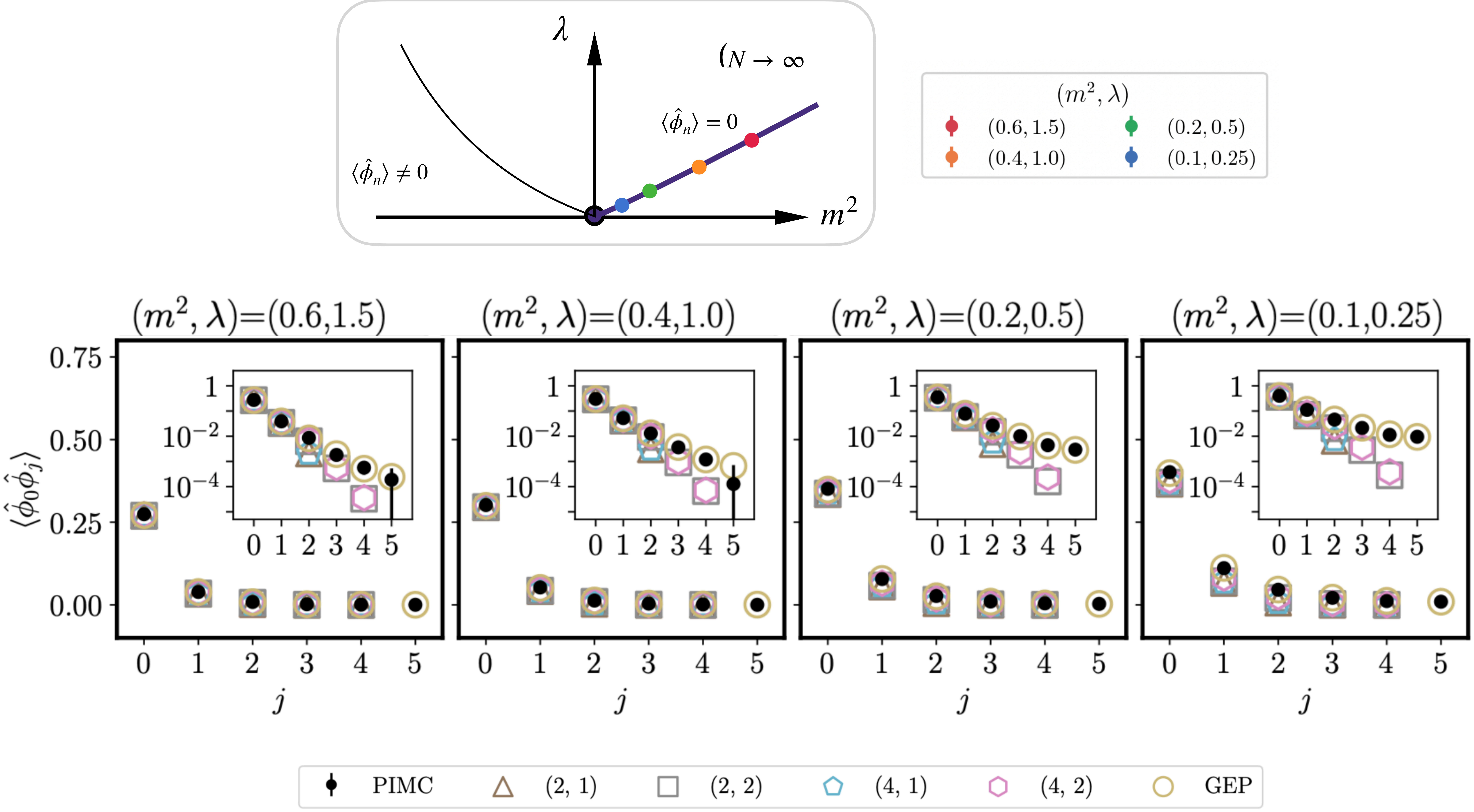

Energy minimization: Moment ratios

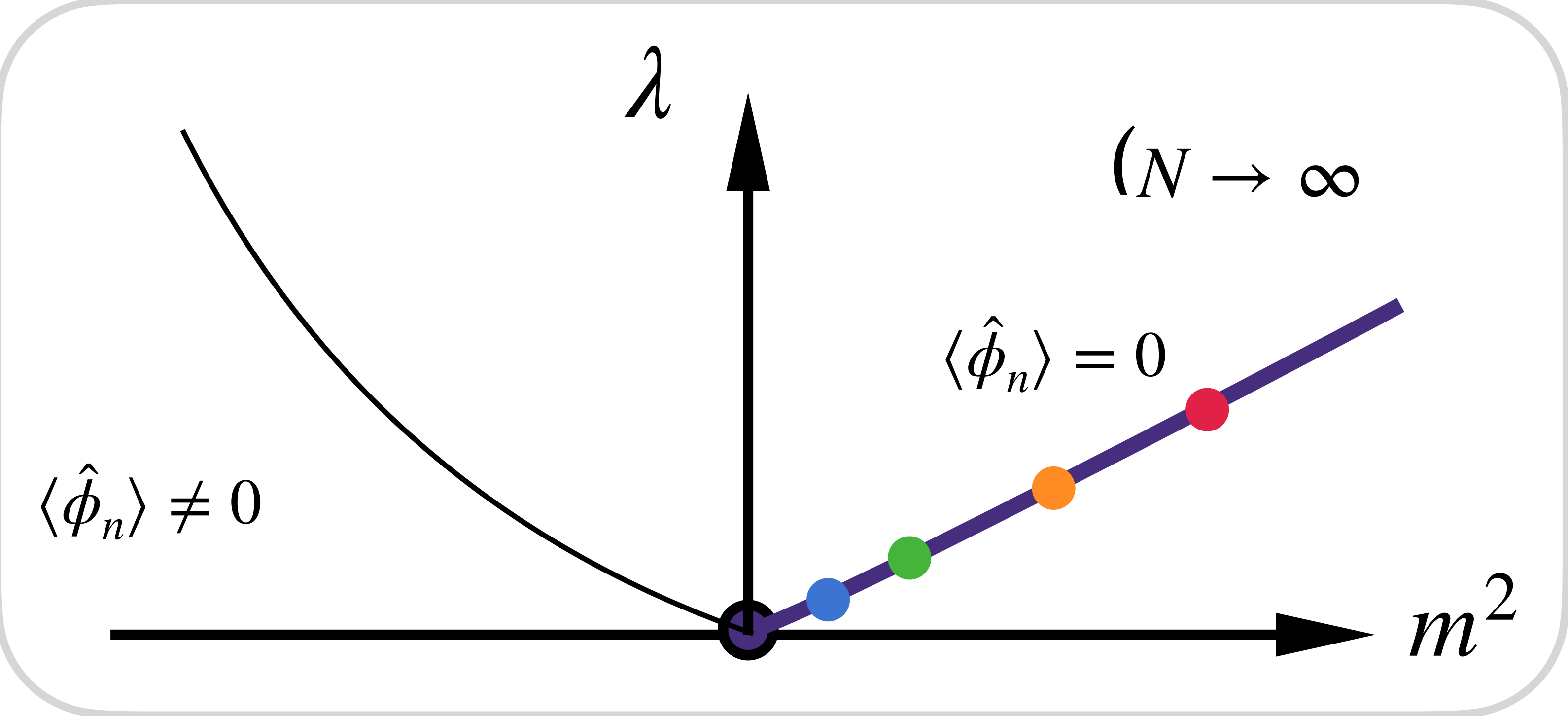

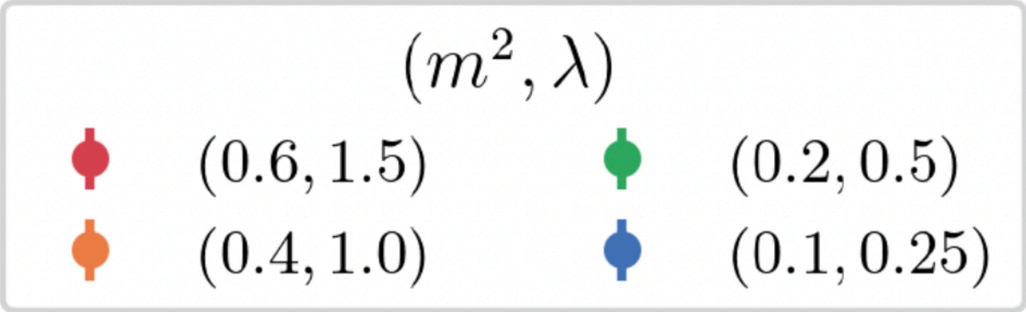

$$R_{2n} = \frac{\langle \hat{\phi}^{2n} \rangle}{(2n-1)!!\langle \hat{\phi}^2 \rangle^n}$$

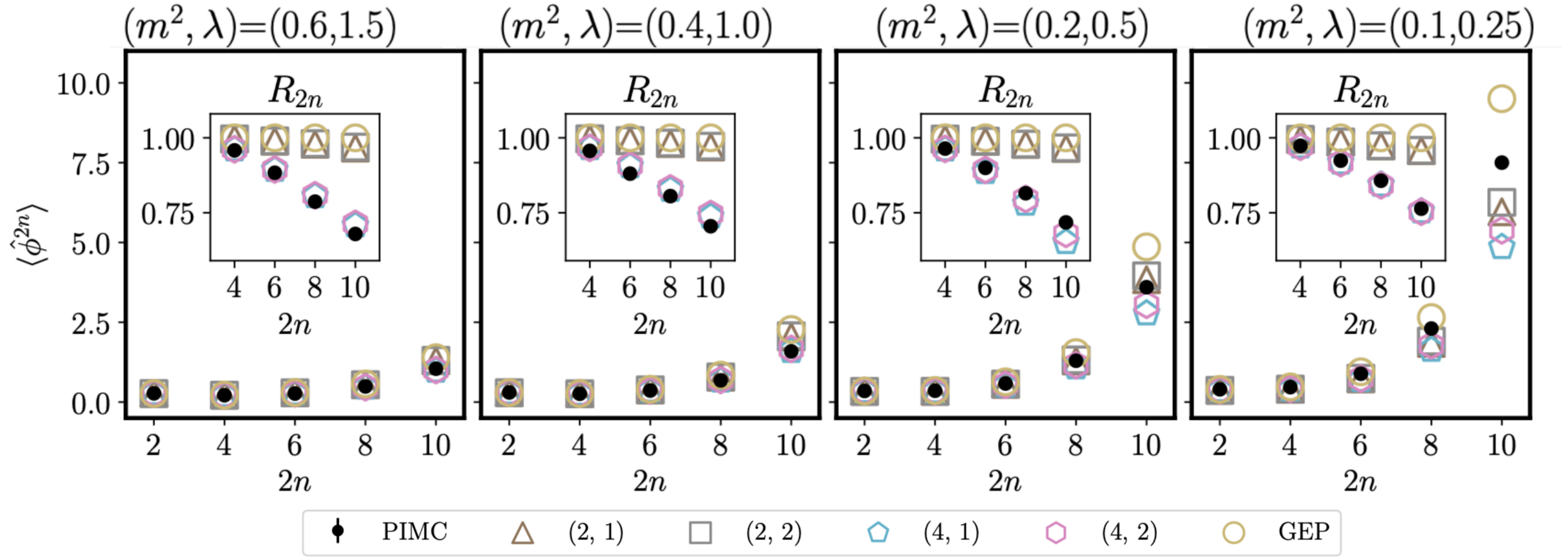

Moment optimization

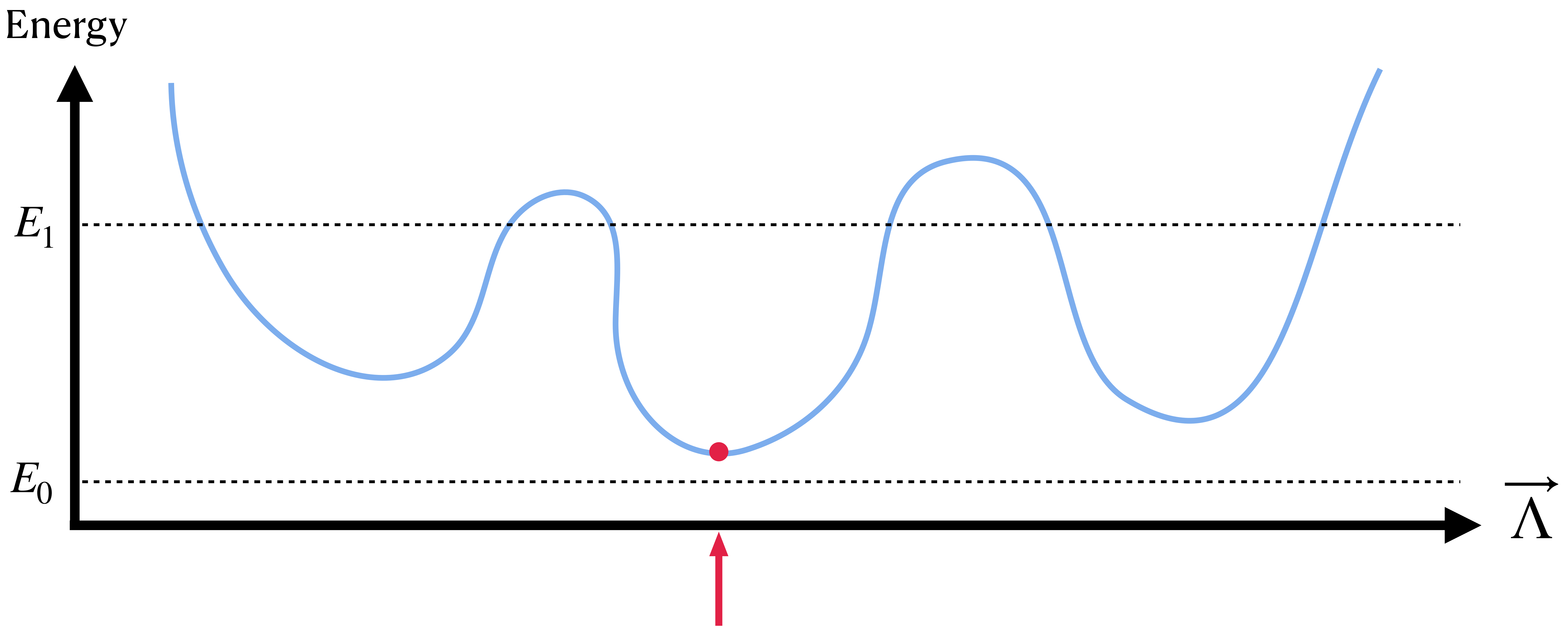

$$\vec{\Lambda}_0 = \mathrm{argmin}_{\vec{\Lambda}} \left[\langle \psi(\vec{\Lambda}) \,|\, \hat{H} \,|\, \psi(\vec{\Lambda}) \rangle \right]$$

Moment optimization

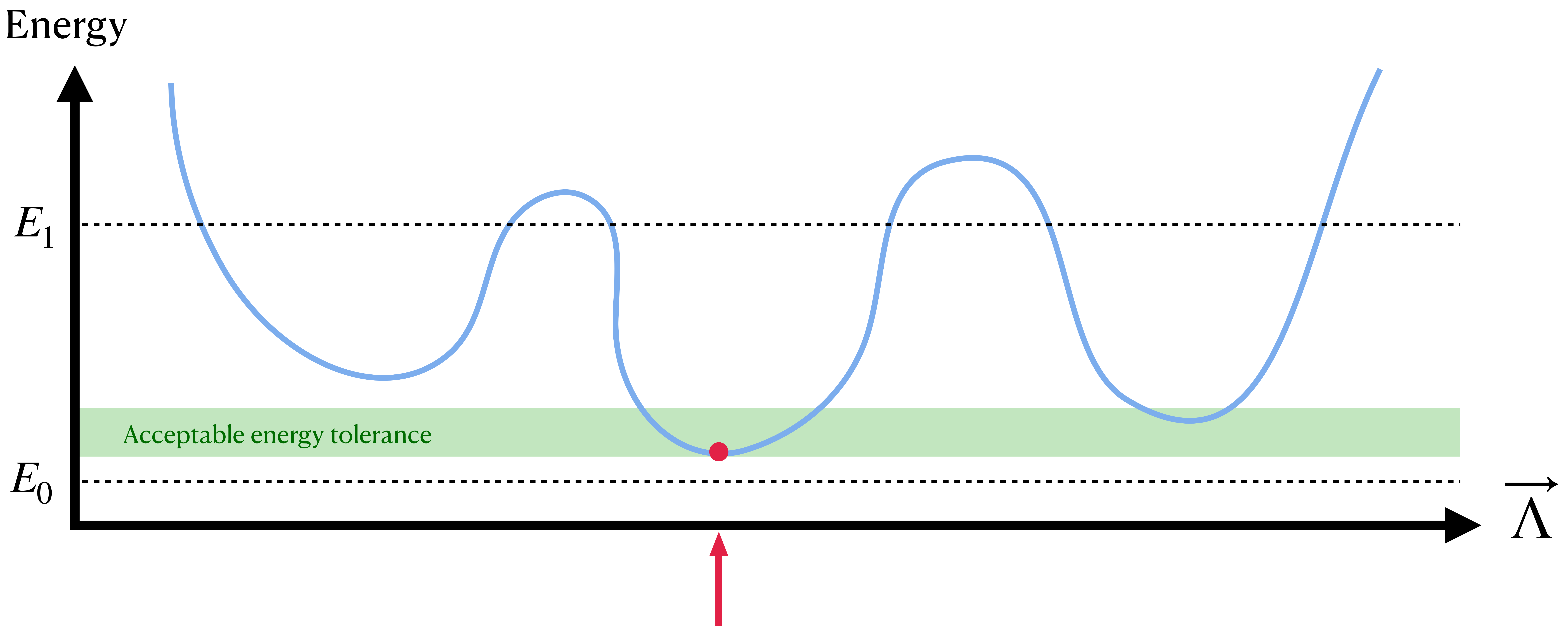

$$\vec{\Lambda}_0 = \mathrm{argmin}_{\vec{\Lambda}} \left[\langle \psi(\vec{\Lambda}) \,|\, \hat{H} \,|\, \psi(\vec{\Lambda}) \rangle \right]$$

Moment optimization

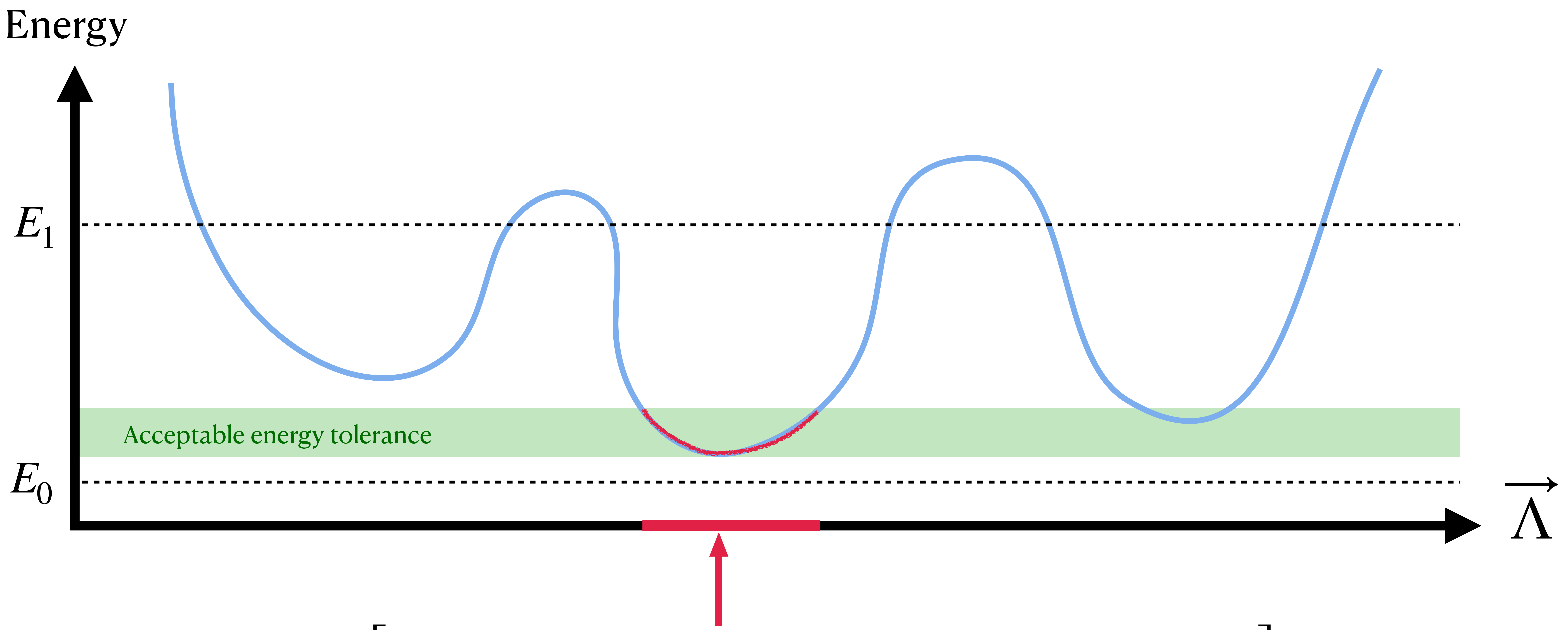

$$\vec{\Lambda}_0 = \mathrm{argmin}_{\vec{\Lambda}} \left[\langle \psi(\vec{\Lambda}) | \hat{H} | \psi(\vec{\Lambda}) \rangle + \sum_{\hat{O} \in \mathcal{T}} w_{\hat{O}} \left(\langle \psi(\vec{\Lambda}) | \hat{O} | \psi(\vec{\Lambda}) \rangle - \langle \Omega | \hat{O} | \Omega \rangle \right)^2 \right]$$

Varying the set of "target moments" $\mathcal{T}$ and weights $w_{\hat{O}}$ enables exploration of acceptable regions in parameter space.

Euclidean-Monte-Carlo-informed Moment optimization

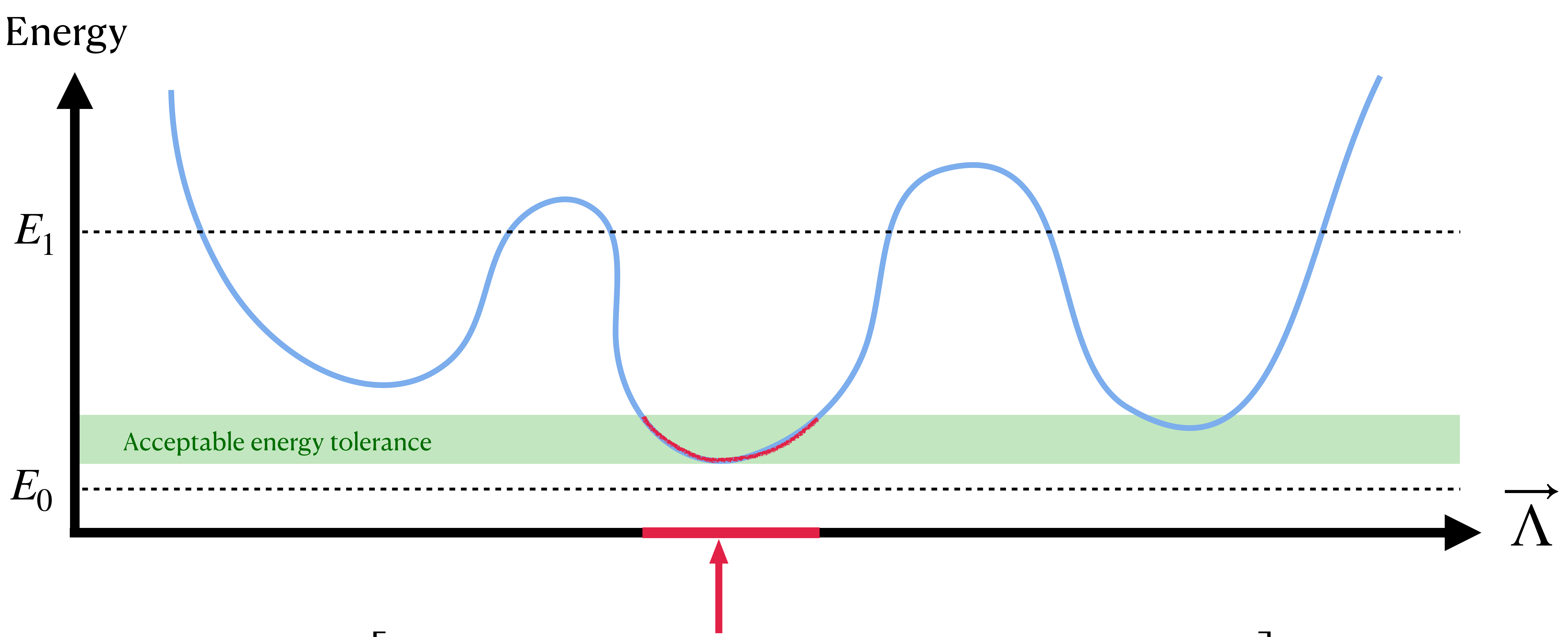

$$\vec{\Lambda}_0 = \text{argmin}_{\vec{\Lambda}} \left[\langle \psi(\vec{\Lambda}) | \hat{H} | \psi(\vec{\Lambda}) \rangle + \sum_{\hat{O} \in \mathcal{T}} w_{\hat{O}} \left(\langle \psi(\vec{\Lambda}) | \hat{O} | \psi(\vec{\Lambda}) \rangle - \langle \Omega | \hat{O} | \Omega \rangle \right)^2 \right]$$

Ground-state moments $\langle \Omega | \hat{O} | \Omega \rangle$ can be sourced from Euclidean Monte Carlo methods.

Optimization of two-point functions

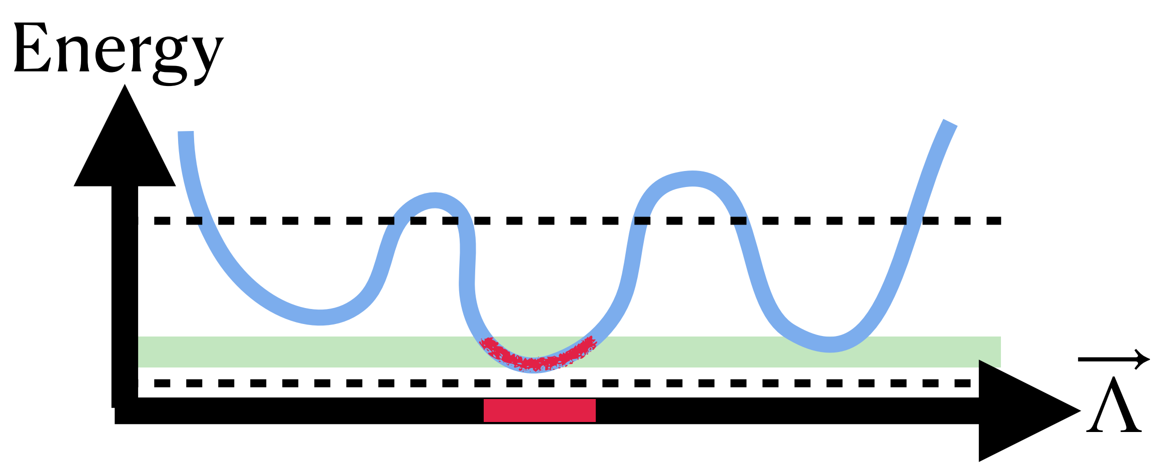

$$\vec{\Lambda}_0 = \mathrm{argmin}_{\vec{\Lambda}} \left[\langle \psi(\vec{\Lambda}) | \hat{H} | \psi(\vec{\Lambda}) \rangle + w \sum_{\hat{O} \in \mathcal{T}} \left(\langle \psi(\vec{\Lambda}) | \hat{O} | \psi(\vec{\Lambda}) \rangle - \langle \Omega | \hat{O} | \Omega \rangle \right)^2 \right]$$

Choose $\mathcal{T} = \{\hat{\phi}_0 \hat{\phi}_4\}$ and the $(R, Q) = (2,2)$ ansatz.

Optimization of two-point functions

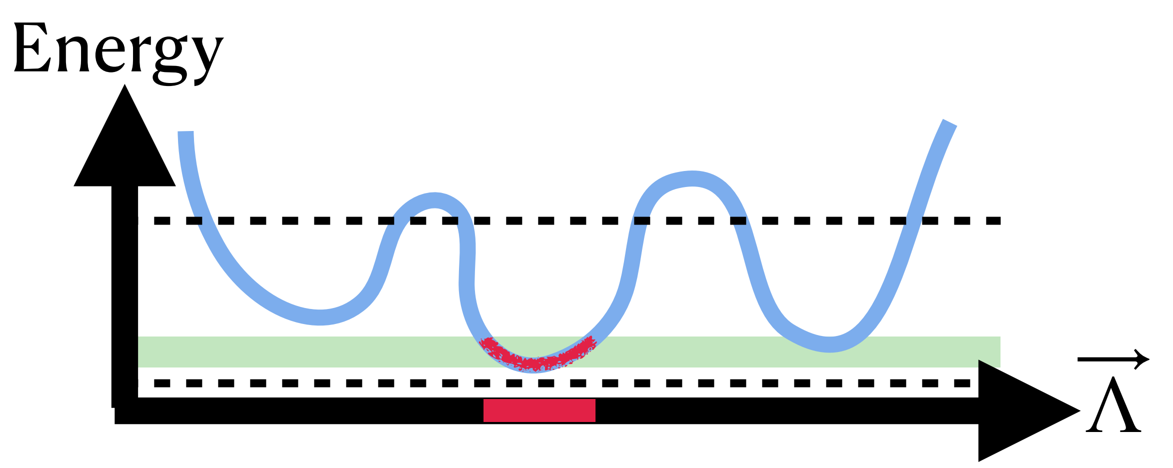

$$\vec{\Lambda}_0 = \text{argmin}_{\vec{\Lambda}} \left[\langle \psi(\vec{\Lambda}) | \hat{H} | \psi(\vec{\Lambda}) \rangle + w \sum_{\hat{O} \in \mathcal{T}} \left(\langle \psi(\vec{\Lambda}) | \hat{O} | \psi(\vec{\Lambda}) \rangle - \langle \Omega | \hat{O} | \Omega \rangle \right)^2 \right]$$

Choose $\mathcal{T} = \{\hat{\phi}_0 \hat{\phi}_4\}$ and the $(R, Q) = (2,2)$ ansatz.

- Varying w leads to excursions in the parameter space.

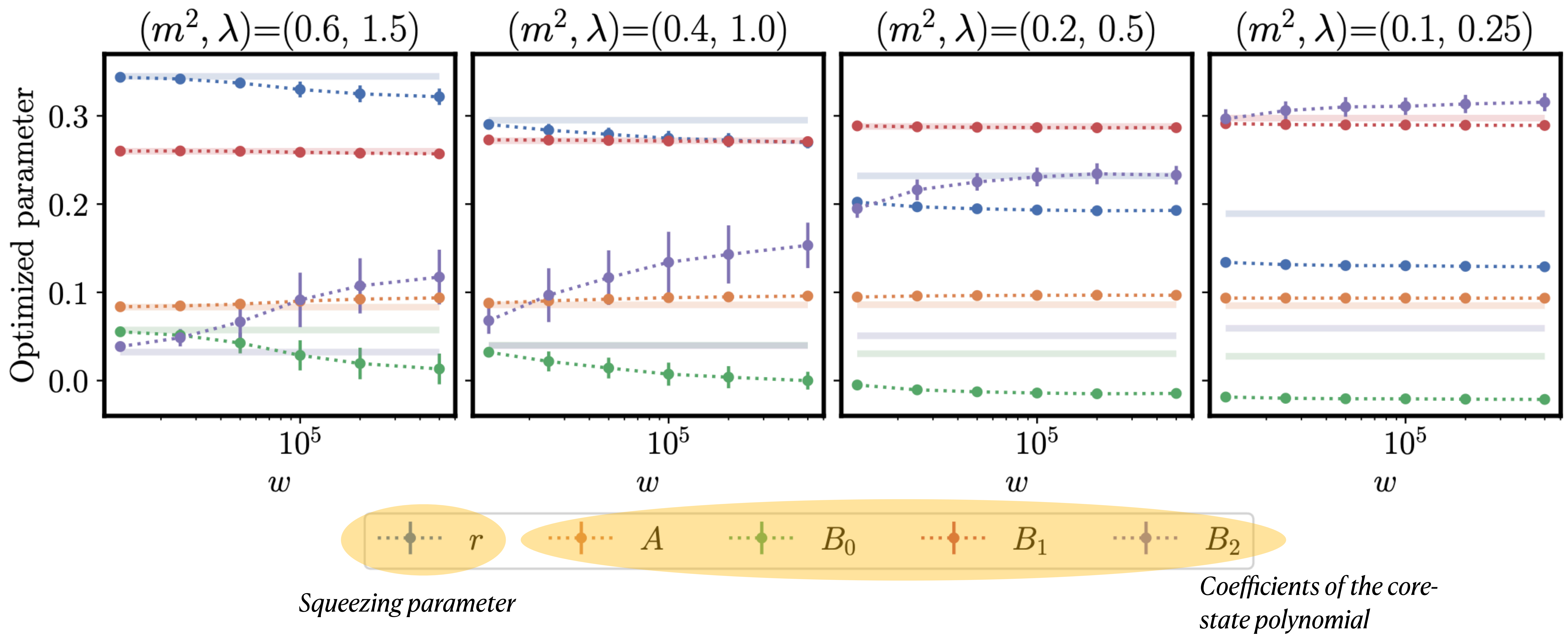

Optimization of two-point functions

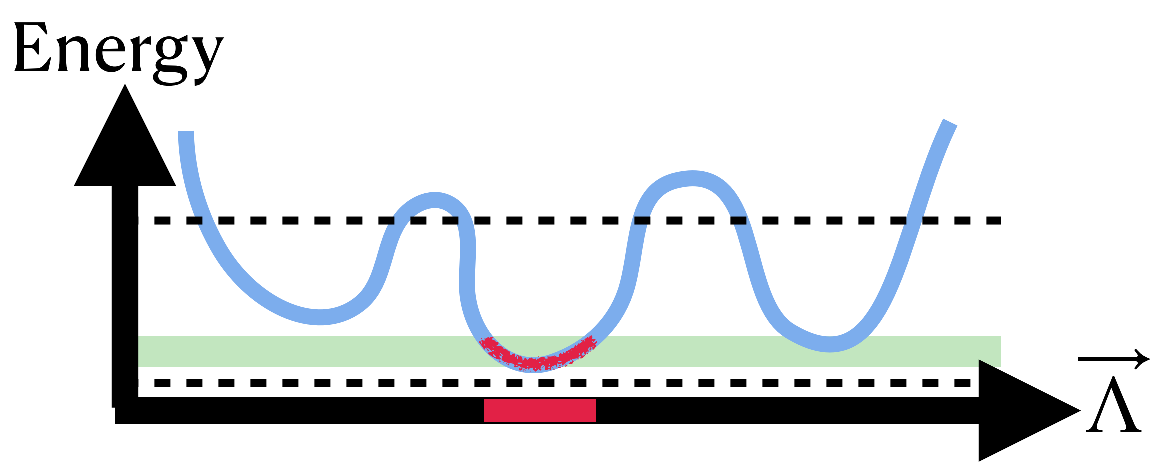

$$\vec{\Lambda}_0 = \text{argmin}_{\vec{\Lambda}}\left[\langle\psi(\vec{\Lambda})|\hat{H}|\psi(\vec{\Lambda})\rangle + w\sum_{\hat{O}\in\mathscr{T}}\left(\langle\psi(\vec{\Lambda})|\hat{O}|\psi(\vec{\Lambda})\rangle - \langle\Omega|\hat{O}|\Omega\rangle\right)^2\right]$$

Choose $\mathscr{T} = \{\hat{\phi}_0\hat{\phi}_4\}$ and the $(R, Q) = (2,2)$ ansatz.

- Varying w leads to excursions in the parameter space.
- Target-moment discrepancies go down with w

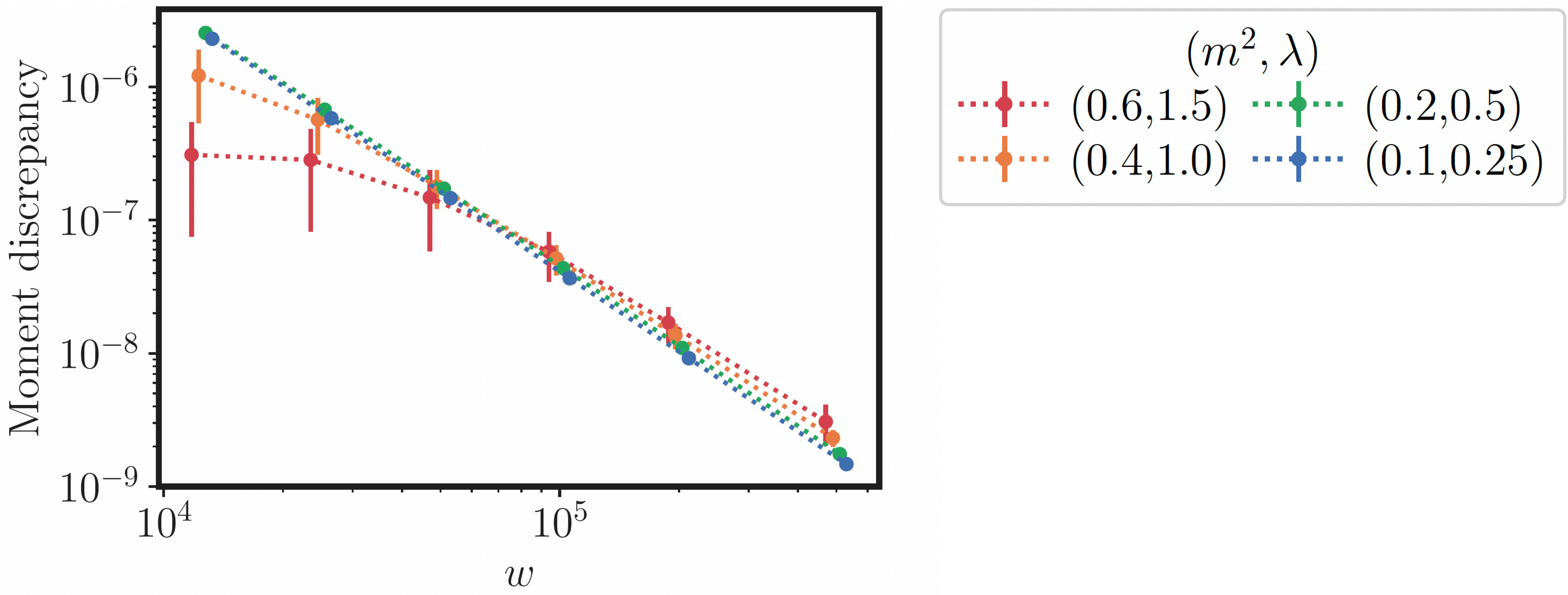

Optimization of two-point functions

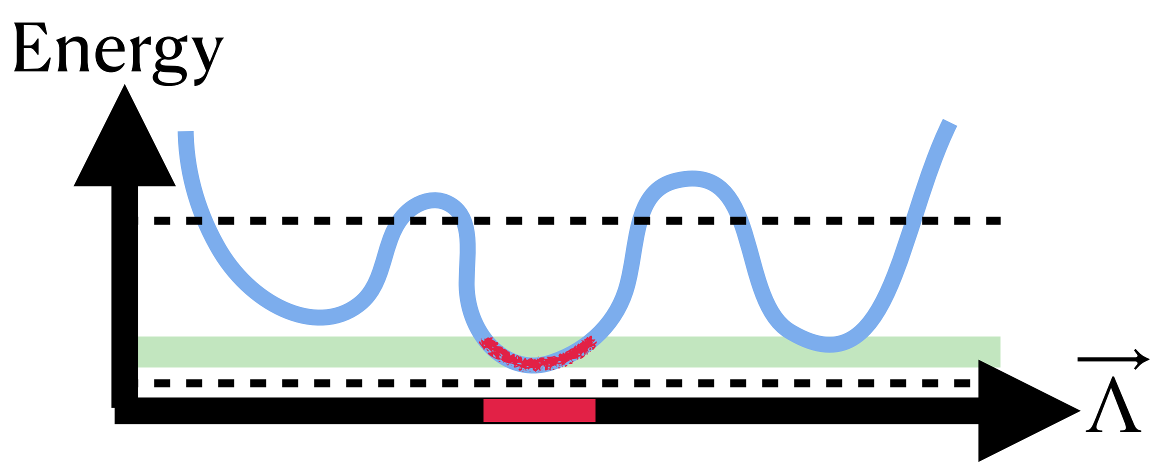

$$\vec{\Lambda}_0 = \text{argmin}_{\vec{\Lambda}} \left[\langle \psi(\vec{\Lambda}) | \hat{H} | \psi(\vec{\Lambda}) \rangle + w \sum_{\hat{O} \in \mathcal{T}} \left(\langle \psi(\vec{\Lambda}) | \hat{O} | \psi(\vec{\Lambda}) \rangle - \langle \Omega | \hat{O} | \Omega \rangle \right)^2 \right]$$

Choose $\mathcal{T} = \{\hat{\phi}_0 \hat{\phi}_4\}$ and the $(R, Q) = (2{,}2)$ ansatz.

- Varying w leads to excursions in the parameter space.
- Target-moment discrepancies go down with w at a negligible cost in energy for larger (m^2, λ) values.

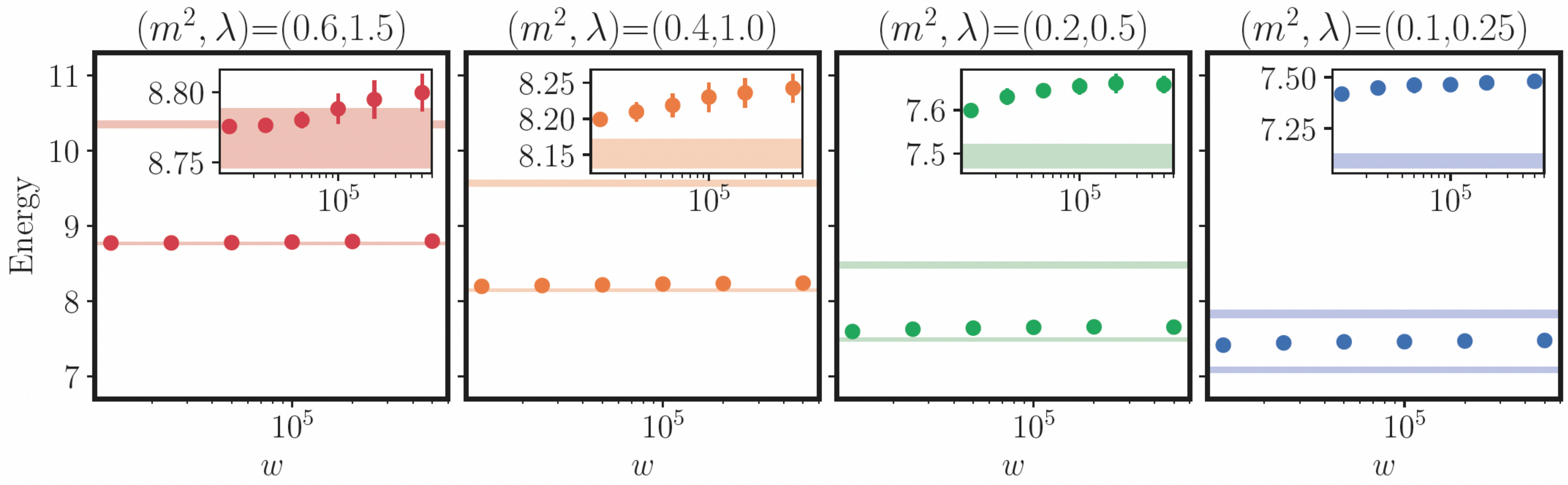

Optimization of two-point functions

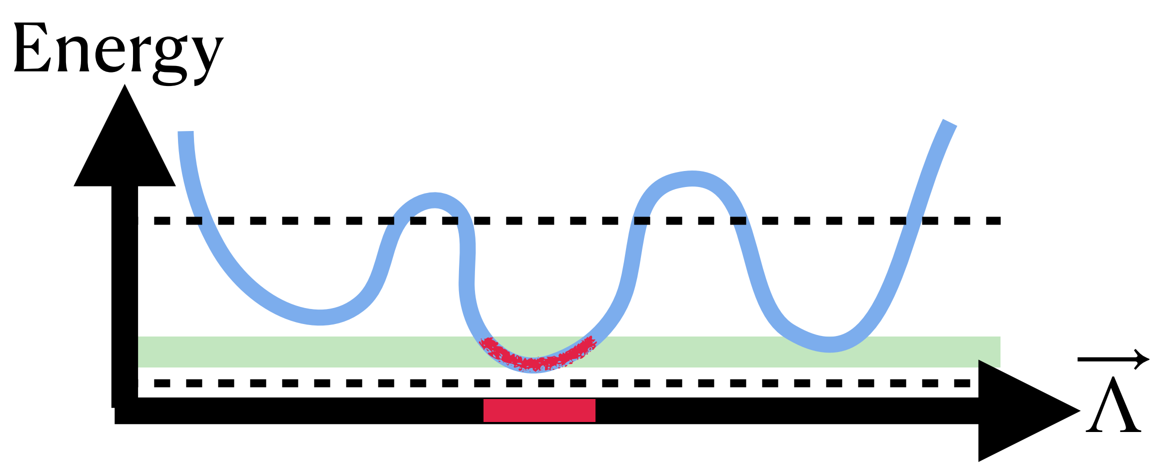

$$\vec{\Lambda}_0 = \mathrm{argmin}_{\vec{\Lambda}}\left[\langle\psi(\vec{\Lambda})\,|\,\hat{H}\,|\,\psi(\vec{\Lambda})\rangle + w\sum_{\hat{O}\in\mathcal{T}}\left(\langle\psi(\vec{\Lambda})\,|\,\hat{O}\,|\,\psi(\vec{\Lambda})\rangle - \langle\Omega\,|\,\hat{O}\,|\,\Omega\rangle\right)^2\right]$$

Choose $\mathcal{T} = \{\hat{\phi}_0\hat{\phi}_4\}$ and the $(R, Q) = (2{,}2)$ ansatz.

- Varying w leads to excursions in the parameter space.
- Target-moment discrepancies go down with w at a negligible cost in energy for larger (m^2, λ) values.
- **Crucially, there is a systematic improvement in the behavior of the two-point functions.**

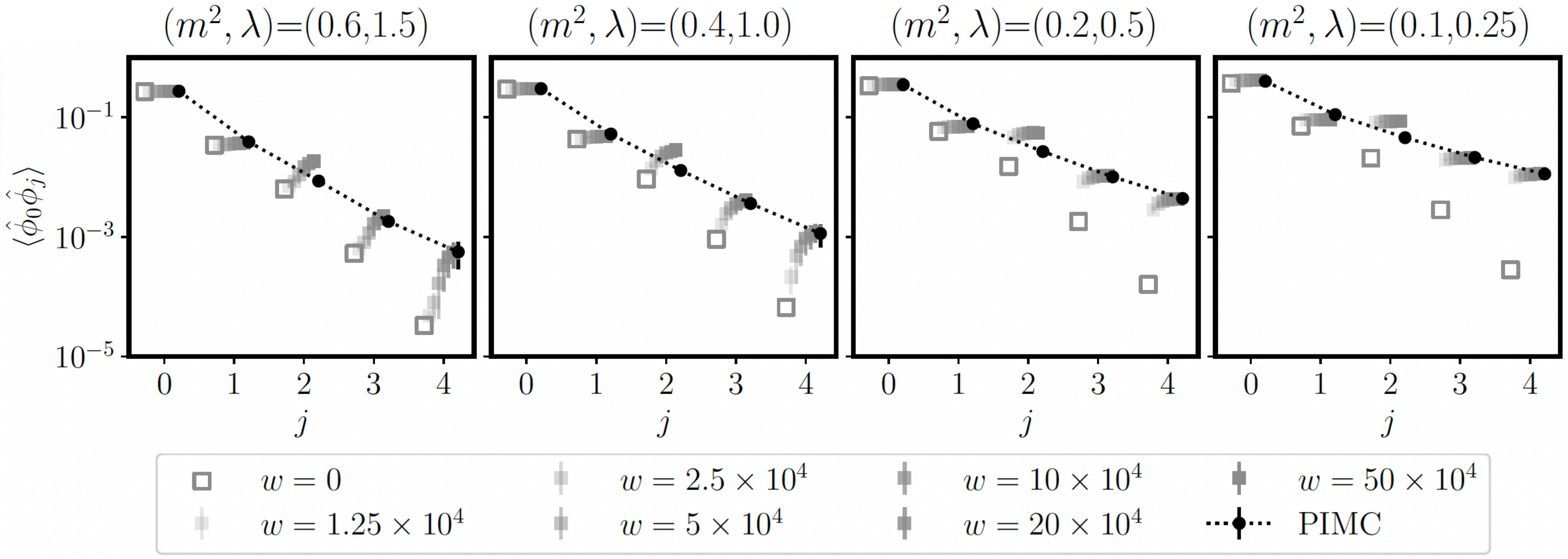

Optimization of two-point functions

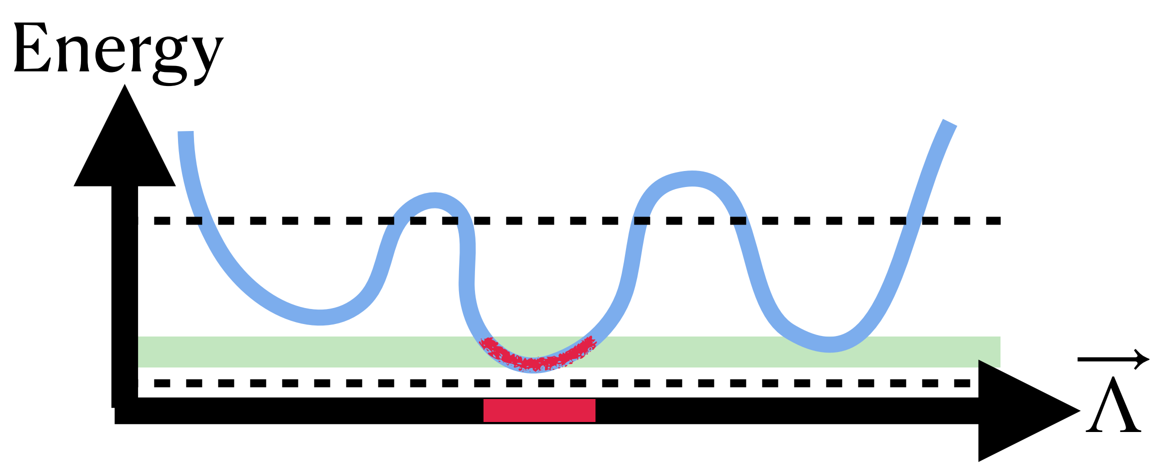

$$\vec{\Lambda}_0 = \text{argmin}_{\vec{\Lambda}} \left[\langle \psi(\vec{\Lambda}) | \hat{H} | \psi(\vec{\Lambda}) \rangle + w \sum_{\hat{O} \in \mathcal{T}} \left(\langle \psi(\vec{\Lambda}) | \hat{O} | \psi(\vec{\Lambda}) \rangle - \langle \Omega | \hat{O} | \Omega \rangle \right)^2 \right]$$

Choose $\mathcal{T} = \{\hat{\phi}_0 \hat{\phi}_4\}$ and the $(R, Q) = (2,2)$ ansatz.

- Varying w leads to excursions in the parameter space.
- Target-moment discrepancies go down with w at a negligible cost in energy for larger (m^2, λ) values.
- **Crucially, there is a systematic improvement in the behavior of the two-point functions.**
- However, the ansatz moment ratios do not capture the non-Gaussianity of the theory.

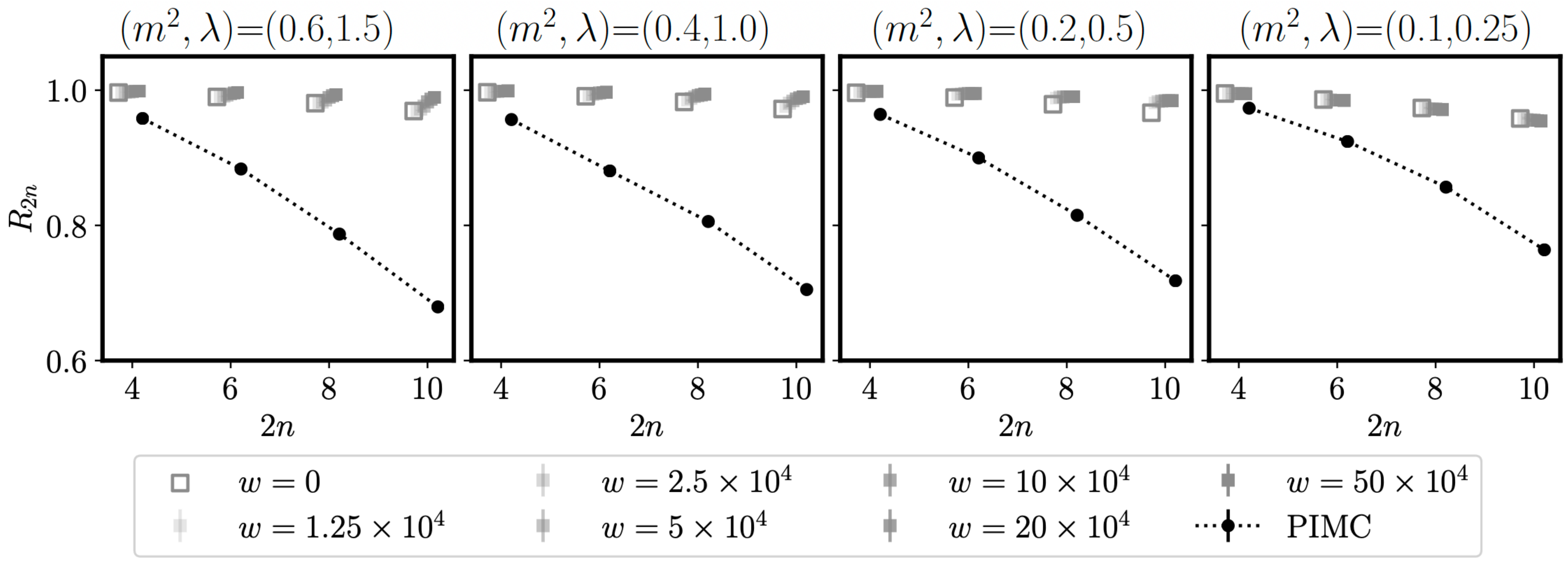

$$R_{2n} = \frac{\langle \hat{\phi}^{2n} \rangle}{(2n-1)!! \langle \hat{\phi}^2 \rangle^n}$$

Optimization of two-point functions

$$\mathscr{T} = \{\hat{\phi}_0 \hat{\phi}_4\}$$

$$R_{2n} = \frac{\langle \hat{\phi}^{2n} \rangle}{(2n-1)!!\langle \hat{\phi}^2 \rangle^n}$$

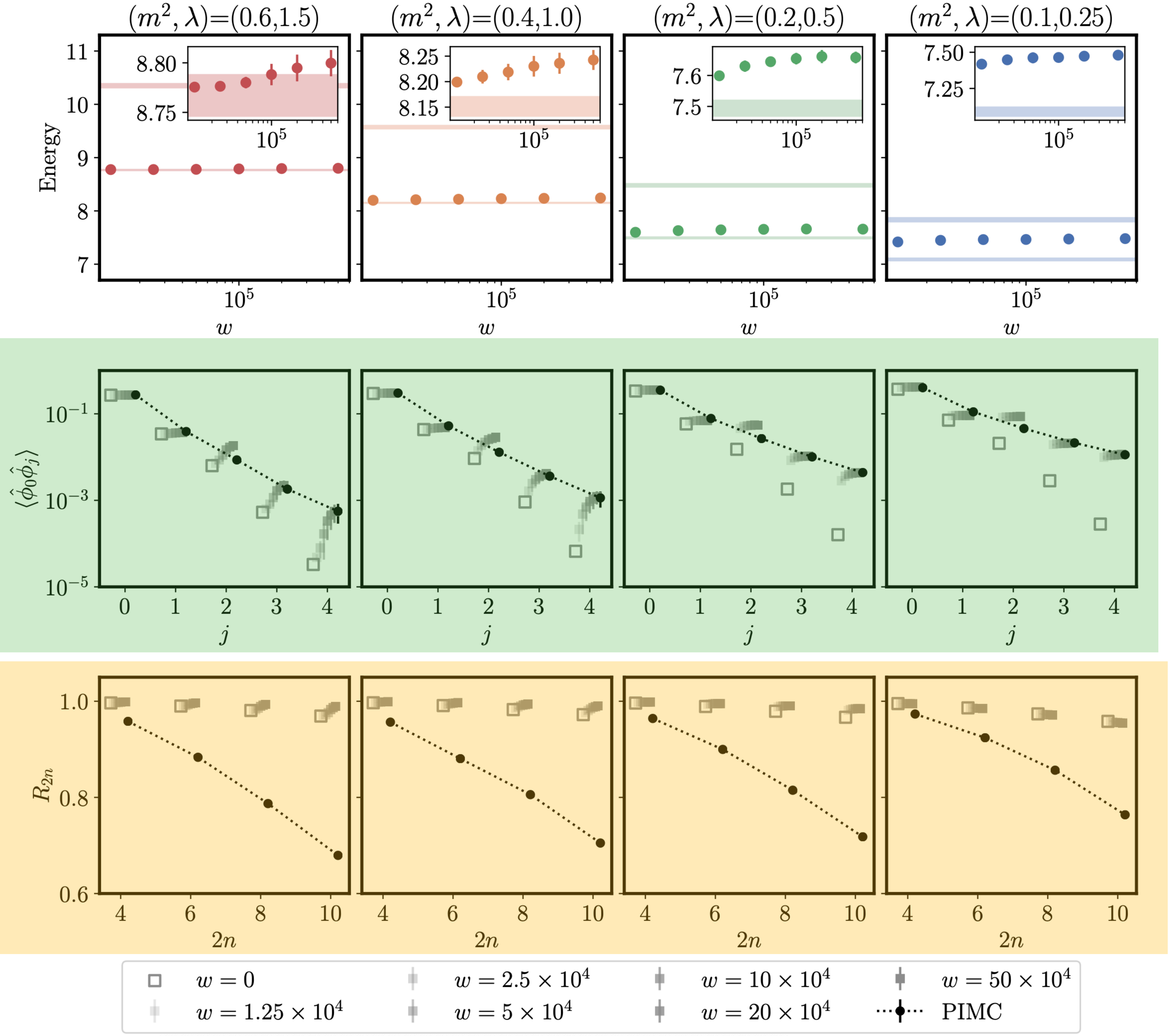

Ground-state two-point functions are captured more accurately.

Ground-state non-Gaussianity is captured no better than the minimum energy ansatz.

Optimization of moment ratios

$$\mathscr{T} = \{\hat{\phi}_0^6, \hat{\phi}_0^8, \hat{\phi}_0^{10}\}$$

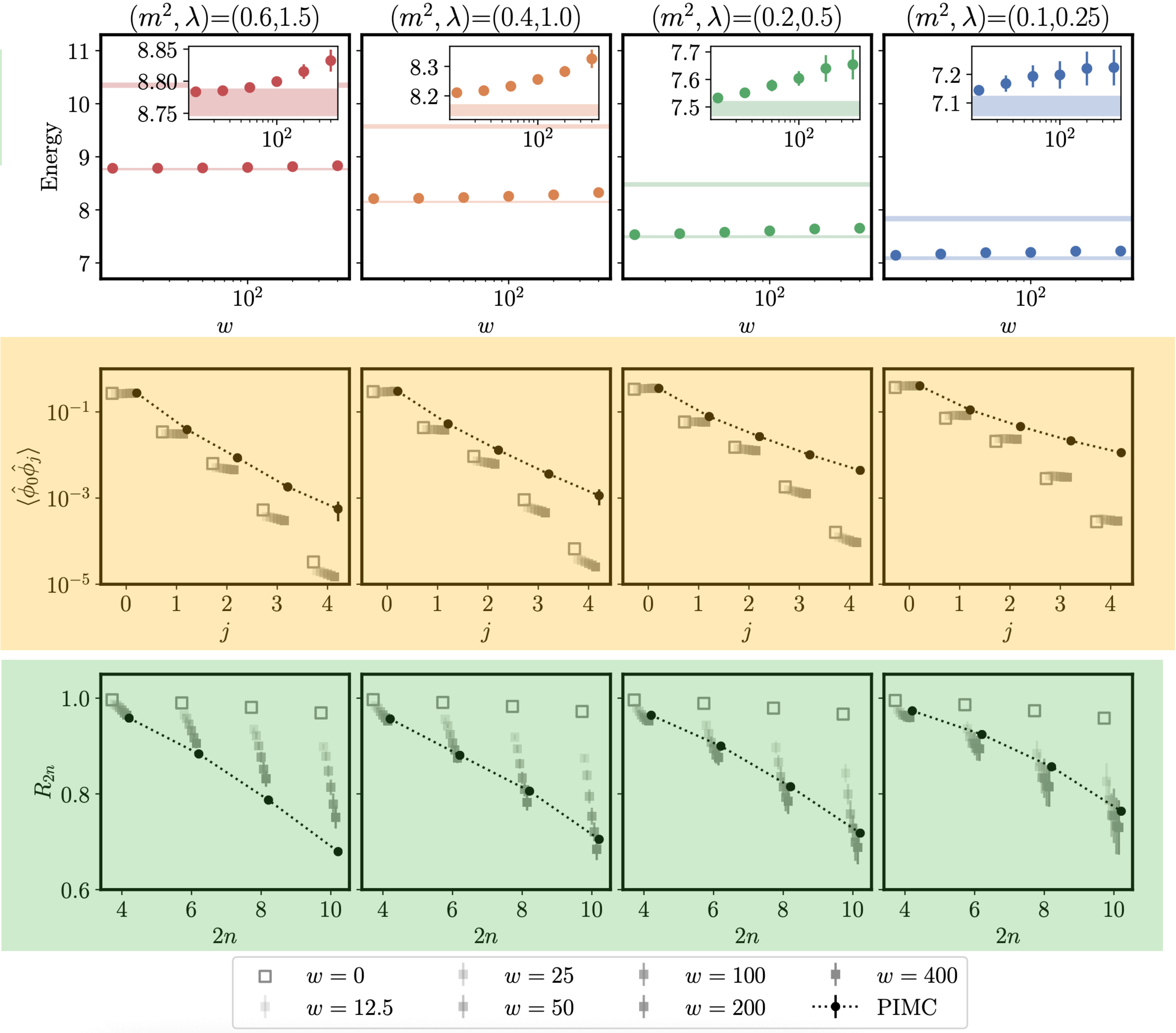

$$R_{2n} = \frac{\langle \hat{\phi}^{2n} \rangle}{(2n-1)!!\langle \hat{\phi}^2 \rangle^n}$$

Ground-state two-point functions are captured slightly less accurately.

Ground-state non-Gaussianity is captured more accurately.

Classically determined quantum circuits

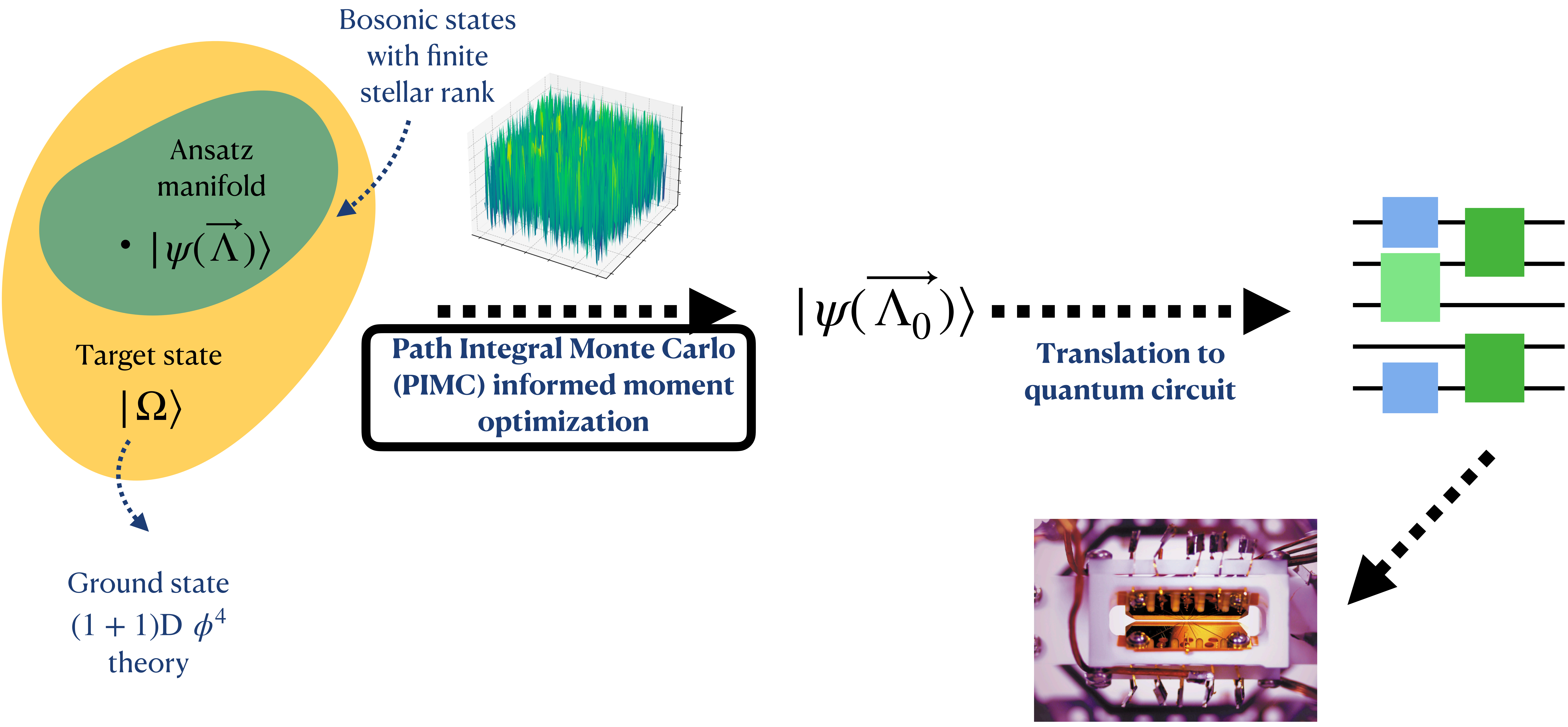

Trapped ion quantum computer from
Monroe Lab (UMD, 2016)

Classically determined quantum circuits

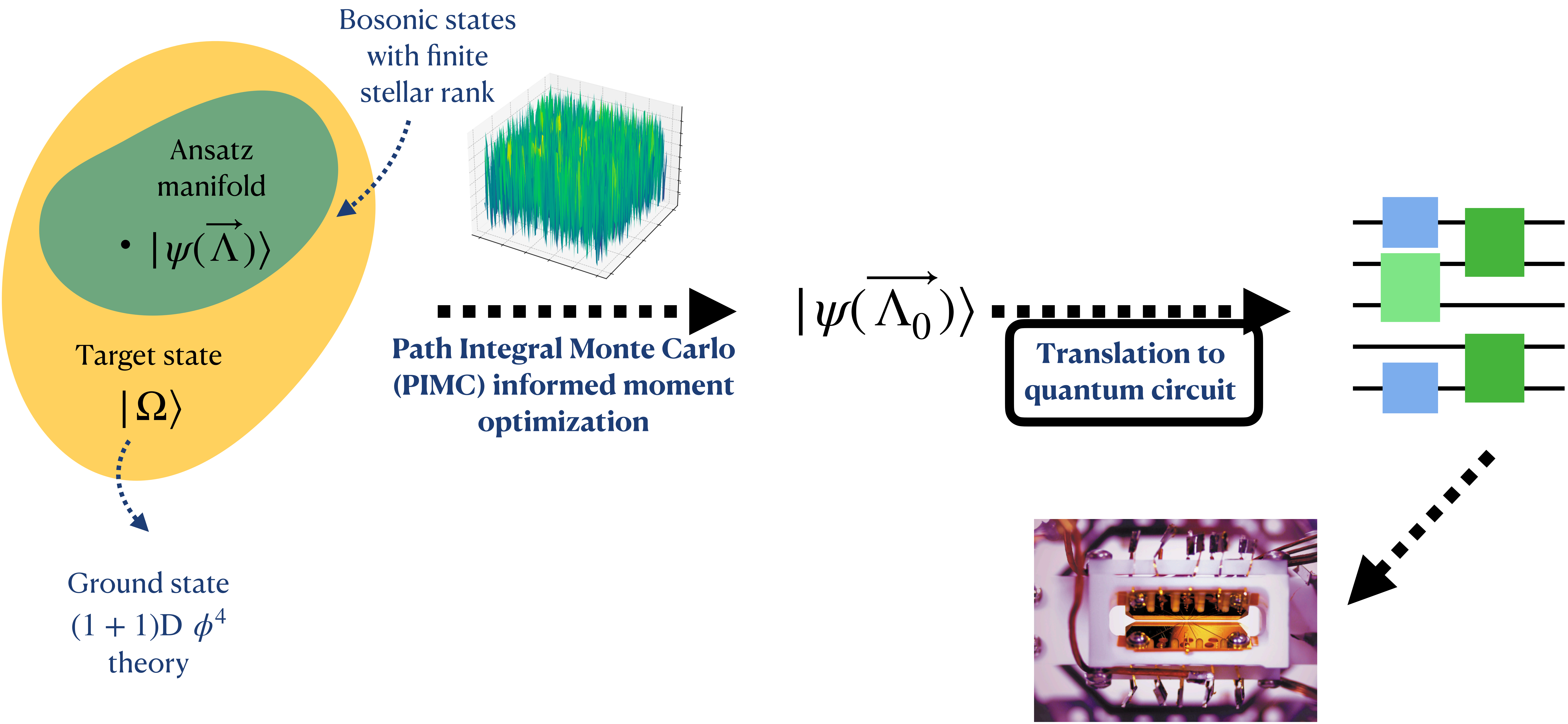

Trapped ion quantum computer from Monroe Lab (UMD, 2016)

Circuit encoding: Discrete variable

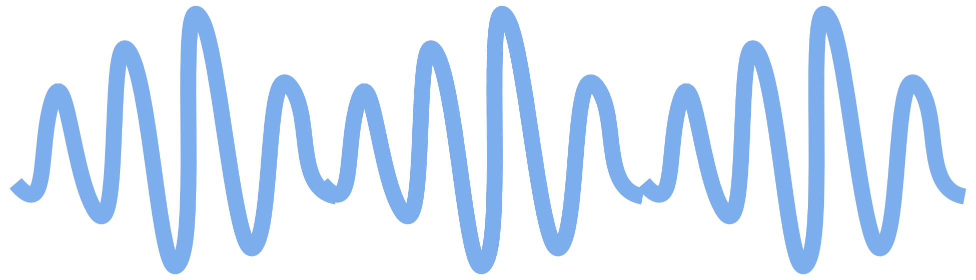

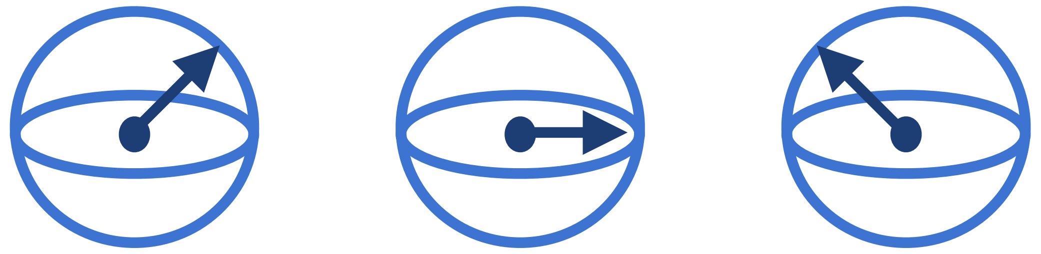

Mode 0 $\quad |n_0\rangle,\ n_0 \le \Lambda \quad \mapsto \quad \left\{ 0, 1, \vdots, \Lambda \right.$ $\quad |n_0\rangle_q \equiv |0_0, \ldots, 0_{n_0-1}, 1_{n_0}, 0_{n_0+1}, \ldots, 0_\Lambda\rangle$

Mode 1 $\quad |n_1\rangle,\ n_1 \le \Lambda \quad \mapsto \quad \left\{ 0, 1, \vdots, \Lambda \right.$ $\quad |n_1\rangle_q \equiv |0_0, \ldots, 0_{n_1-1}, 1_{n_1}, 0_{n_1+1}, \ldots, 0_\Lambda\rangle$

$\vdots \qquad \vdots$

Mode $N-1$ $\quad |n_1\rangle,\ n_1 \le \Lambda \quad \mapsto \quad \left\{ 0, 1, \vdots, \Lambda \right.$ $\quad |n_{N-1}\rangle_q \equiv |0_0, \ldots, 0_{n_1-1}, 1_{n_1}, 0_{n_1+1}, \ldots, 0_\Lambda\rangle$

$$|\vec{n}\rangle = |n_0, n_1, \ldots, n_{N-1}\rangle \quad \mapsto \quad |\vec{n}\rangle_q \equiv |n_0\rangle_q \otimes |n_1\rangle_q \otimes \ldots \otimes |n_{N-1}\rangle_q$$

Circuit encoding: Discrete variable

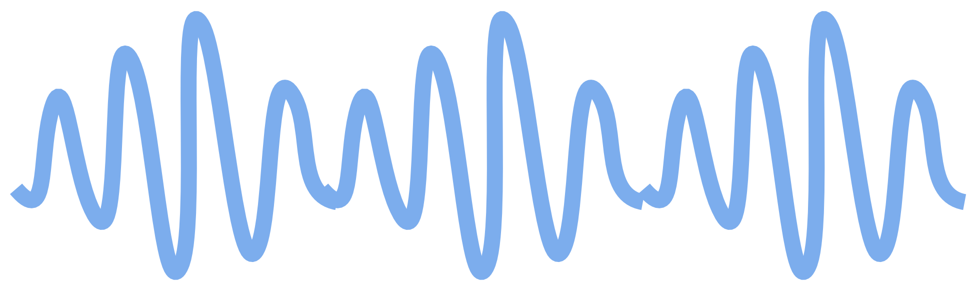

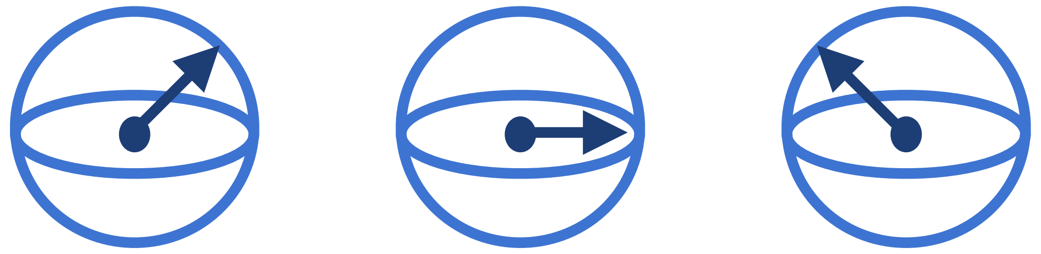

$$|\psi\rangle_{R,Q} = \hat{U}_G |C\rangle$$
$$= \hat{U}_G \sum_{\vec{n}}^{\bar{}} c_{\vec{n}} |\vec{n}\rangle$$

$$\mapsto$$

$$|\psi\rangle_{R,Q,q} \equiv [\hat{U}_G]_q \sum_{\vec{n}}^{\bar{}} c_{\vec{n}} |\vec{n}\rangle_q$$

Circuit encoding: Discrete variable

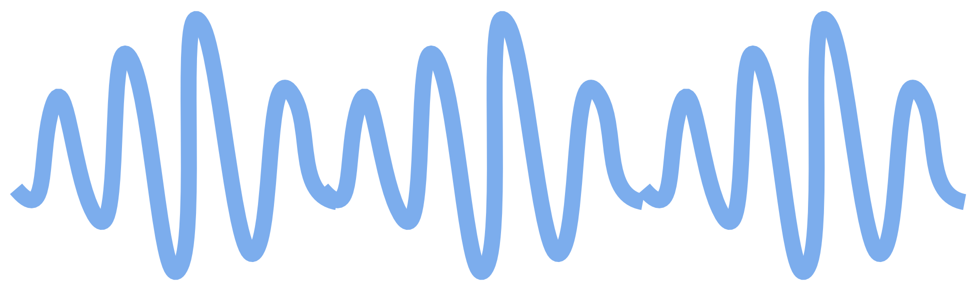

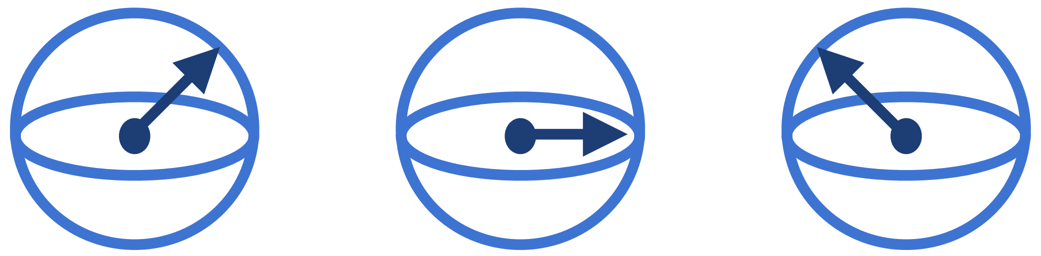

$$|\psi\rangle_{R,Q} = \hat{U}_G|C\rangle = \hat{U}_G \bar{\sum}_{\vec{n}} c_{\vec{n}}|\vec{n}\rangle \quad \mapsto \quad |\psi\rangle_{R,Q,q} \equiv [\hat{U}_G]_q \bar{\sum}_{\vec{n}} c_{\vec{n}}|\vec{n}\rangle_q$$

- The core state has a bounded support over Fock space.
- Thus, it can be represented exactly using $R+1$ qubits per mode.
- Using the sparse state preparation algorithm proposed by Gleinig et al., this state can be prepared using $O(N^2)$ CNOT gates and $O(N \log N)$ single qubit gates using an $O(N^3 \log N)$ complexity.

Circuit encoding: Discrete variable

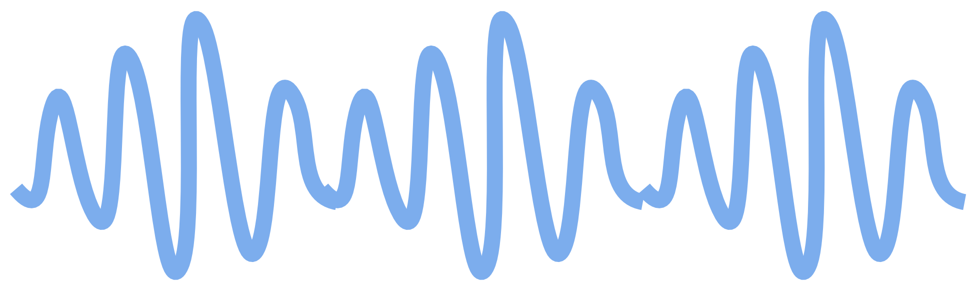

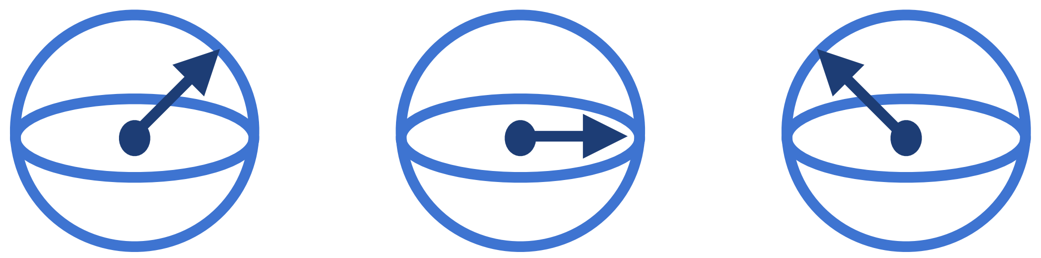

$$|\psi\rangle_{R,Q} = \hat{U}_G |C\rangle = \hat{U}_G \bar{\sum}_{\vec{n}} c_{\vec{n}} |\vec{n}\rangle \quad \mapsto \quad |\psi\rangle_{R,Q,q} \equiv [\hat{U}_G]_q \bar{\sum}_{\vec{n}} c_{\vec{n}} |\vec{n}\rangle_q$$

- The Gaussian unitary operation is $\hat{U}_G = \bigotimes_{j=0}^{N-1} \hat{S}_j(r)$, where $\hat{S}(r) = e^{\frac{r}{2}[(\hat{a}^\dagger)^2 - \hat{a}^2]}$.
- This operator extends the support of the core state to the entire bosonic Hilbert space.
- Thus, it can only be represented approximately on a discrete-variable platform.

Circuit encoding: Discrete variable

$$\hat{S}(r) = e^{\frac{r}{2}[(\hat{a}^\dagger)^2 - \hat{a}^2]}$$

$$= e^{\frac{r}{2}\sum_{n=0}^{\infty} \ell_n \left(|n+2\rangle\langle n| - |n\rangle\langle n+2| \right)}$$

Truncation

$$\hat{S}^{\Lambda}(r) = e^{\frac{r}{2}\sum_{n=0}^{\Lambda} \ell_n \left(|n+2\rangle\langle n| - |n\rangle\langle n+2| \right)}$$

Trotterization

$$\hat{S}^{\Lambda,K}(r) = \left(e^{-i\frac{r}{K}s_0^{\Lambda}} e^{-i\frac{r}{K}s_2^{\Lambda}} \right)^K \left(e^{-i\frac{r}{K}s_1^{\Lambda}} e^{-i\frac{r}{K}s_3^{\Lambda}} \right)^K$$

- Once a choice for the “circuit regulators”, namely the cutoff Λ and number of Trotter layers K is picked, the squeezing operator can be implemented using $O(\Lambda K)$ CNOT gates.
- We now describe the errors associated with both regularizations.

Circuit encoding: Discrete variable

$$\hat{S}(r) = e^{\frac{r}{2}([\hat{a}^{\dagger})^2 - \hat{a}^2]}$$

$$= e^{\frac{r}{2}\sum_{n=0}^{\infty}} \ell_n\left(|n+2\rangle\langle n| - |n\rangle\langle n+2|\right)$$

↓ **Truncation**

$$\hat{S}^{\Lambda}(r) = e^{\frac{r}{2}\sum_{n=0}^{\Lambda}} \ell_n\left(|n+2\rangle\langle n| - |n\rangle\langle n+2|\right)$$

↓ **Trotterization**

$$\hat{S}^{\Lambda,K}(r) = \left(e^{-i\frac{r}{K}s_0^{\Lambda}} e^{-i\frac{r}{K}s_2^{\Lambda}}\right)^{K} \left(e^{-i\frac{r}{K}s_1^{\Lambda}} e^{-i\frac{r}{K}s_3^{\Lambda}}\right)^{K}$$

- Truncation results in two sources of error.

Circuit encoding: Discrete variable

$$\hat{S}(r) = e^{\frac{r}{2}([\hat{a}^\dagger)^2 - \hat{a}^2]}$$

$$= e^{\frac{r}{2}\sum_{n=0}^{\infty} \ell_n(|n+2\rangle\langle n| - |n\rangle\langle n+2|)}$$

Truncation

$$\hat{S}^{\Lambda}(r) = e^{\frac{r}{2}\sum_{n=0}^{\Lambda} \ell_n(|n+2\rangle\langle n| - |n\rangle\langle n+2|)}$$

Trotterization

$$\hat{S}^{\Lambda,K}(r) = \left(e^{-i\frac{r}{K}s_0^{\Lambda}} e^{-i\frac{r}{K}s_2^{\Lambda}}\right)^K \left(e^{-i\frac{r}{K}s_1^{\Lambda}} e^{-i\frac{r}{K}s_3^{\Lambda}}\right)^K$$

- Truncation results in two sources of error.
- The first source of error is the leakage of Fock space amplitude to outside of the truncated Hilbert space.

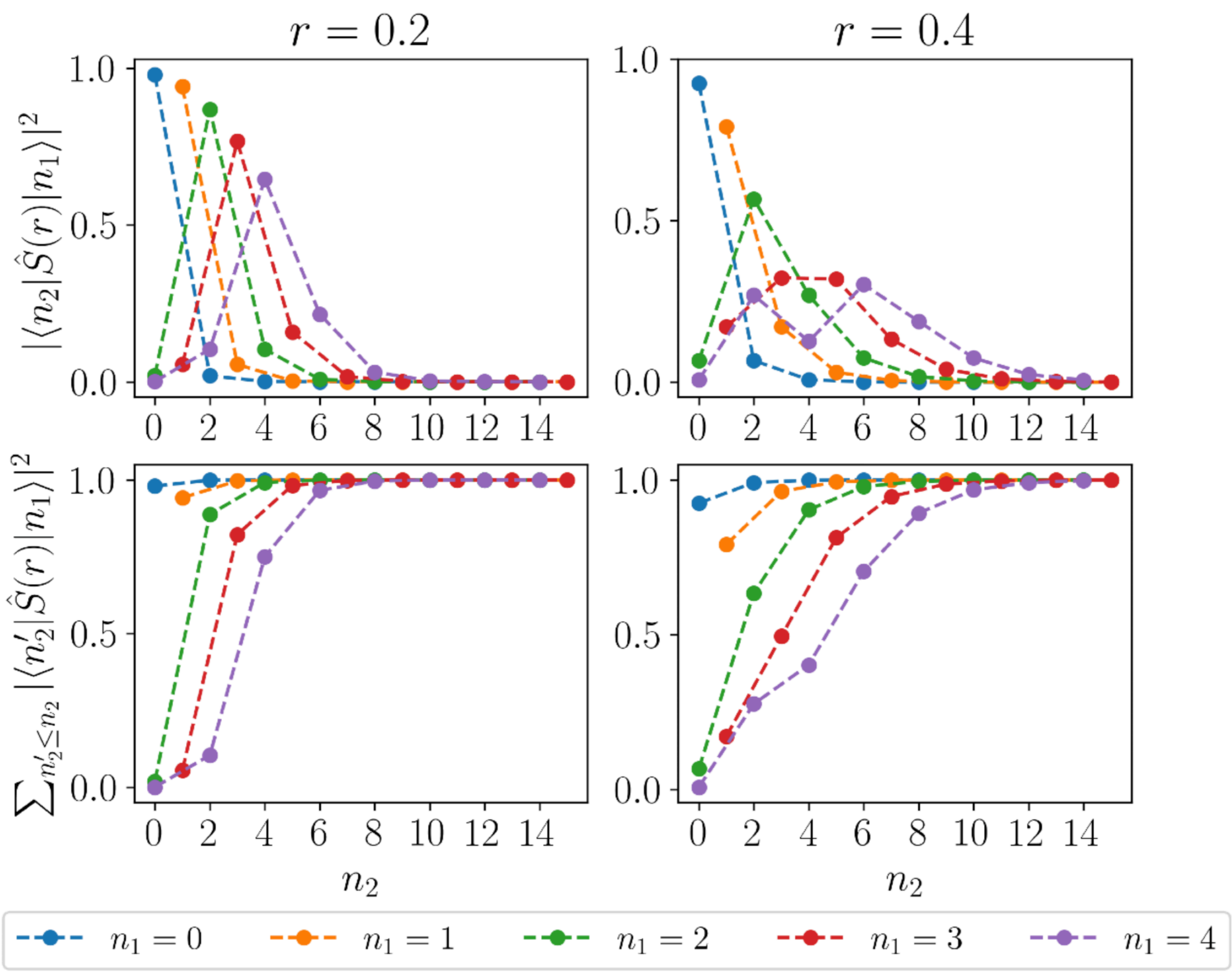

Circuit encoding: Discrete variable

$$\hat{S}(r) = e^{\frac{r}{2}([\hat{a}^\dagger)^2 - \hat{a}^2]}$$

$$= e^{\frac{r}{2}\sum_{n=0}^{\infty} \ell_n (|n+2\rangle\langle n| - |n\rangle\langle n+2|)}$$

Truncation

$$\hat{S}^{\Lambda}(r) = e^{\frac{r}{2}\sum_{n=0}^{\Lambda} \ell_n (|n+2\rangle\langle n| - |n\rangle\langle n+2|)}$$

Trotterization

$$\hat{S}^{\Lambda,K}(r) = \left(e^{-i\frac{r}{K}s_0^{\Lambda}} e^{-i\frac{r}{K}s_2^{\Lambda}}\right)^K \left(e^{-i\frac{r}{K}s_1^{\Lambda}} e^{-i\frac{r}{K}s_3^{\Lambda}}\right)^K$$

- Truncation results in two sources of error.
- The first source of error is the leakage of Fock space amplitude to outside of the truncated Hilbert space.
- The second source of error is related to the difference between relevant matrix elements of the operators $\hat{S}(r)$ and $\hat{S}^{\Lambda}(r)$.

Circuit encoding: Discrete variable

$$\langle n_2 | \hat{S}(r) | n_1 \rangle = e^{\frac{r}{2}\sum_{n=0}^{\infty} \ell_n\left(|n+2\rangle\langle n| - |n\rangle\langle n+2| \right)} = \sum_{\Delta=0}^{\infty} \frac{r^{p_0+2\Delta}}{(p_0+2\Delta)!2^{p_0+2\Delta}} \underbrace{\langle n_2| \left[\sum_{n=0}^{\infty} \ell_n \left(|n+2\rangle \langle n| - |n\rangle \langle n+2| \right) \right]^{p_0+2\Delta} |n_1\rangle}_{f(\Delta)}$$

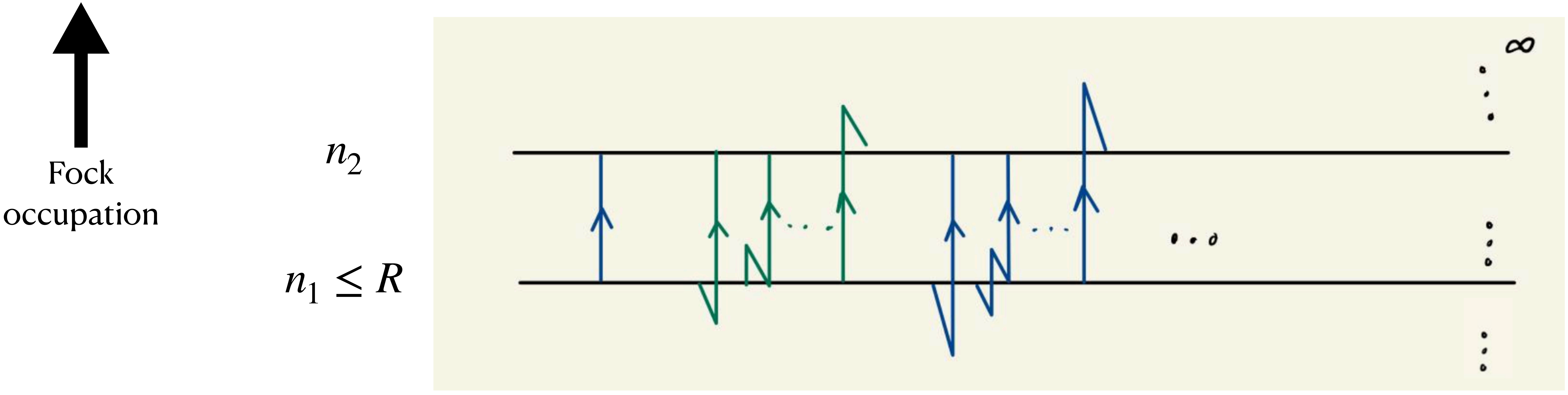

Path length $p_0 = \frac{n_2 - n_1}{2}$ $p_0 + 2$ $p_0 + 4$

Circuit encoding: Discrete variable

$$\langle n_2 | \hat{S}(r) | n_1 \rangle = e^{\frac{r}{2}\sum_{n=0}^{\infty} \ell_n\left(|n+2\rangle\langle n| - |n\rangle\langle n+2| \right)} = \sum_{\Delta=0}^{\infty} \frac{r^{p_0+2\Delta}}{(p_0+2\Delta)!2^{p_0+2\Delta}} \underbrace{\langle n_2| \left[\sum_{n=0}^{\infty} \ell_n \left(|n+2\rangle\langle n| - |n\rangle\langle n+2| \right) \right]^{p_0+2\Delta} |n_1\rangle}_{f(\Delta)}$$

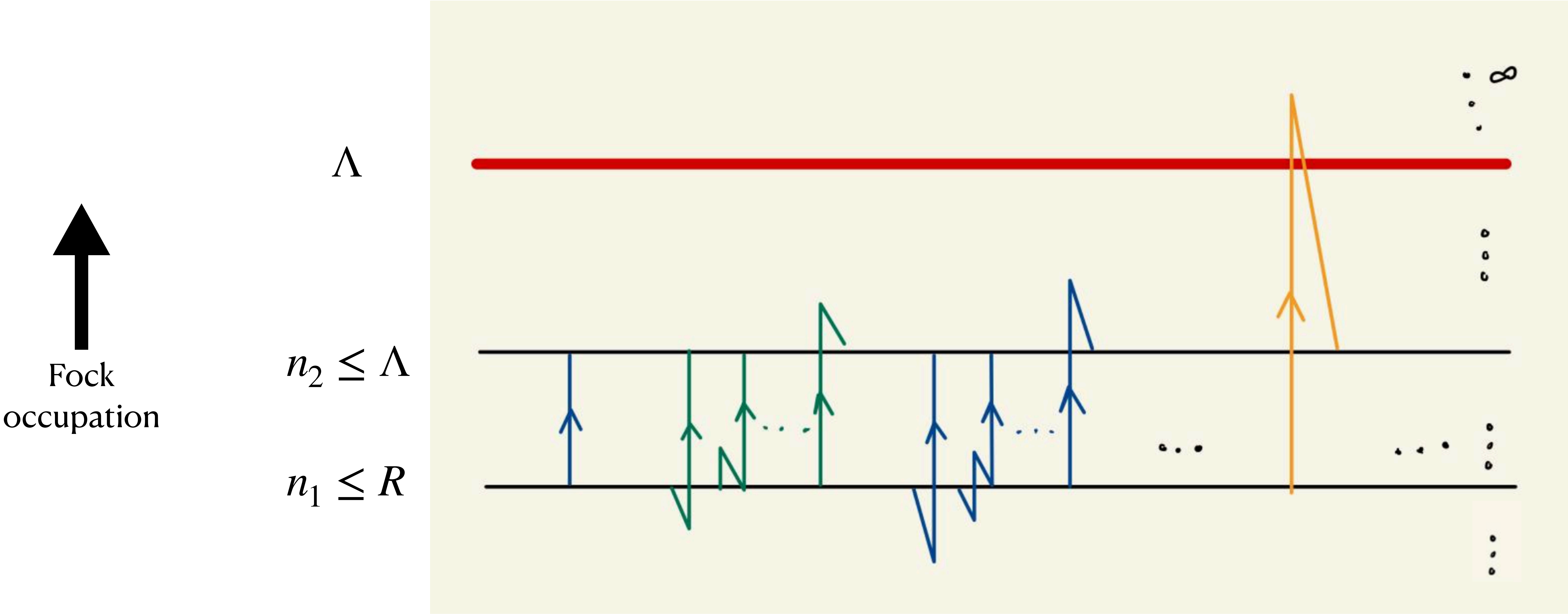

Path length $p_0 = \frac{n_2 - n_1}{2}$ $p_0 + 2$ $p_0 + 4$ $p_0 + (\Lambda + 1 - n_2)$

Circuit encoding: Discrete variable

$$\langle n_2 | \hat{S}^{\Lambda}(r) | n_1 \rangle = e^{\frac{r}{2}\sum_{n=0}^{\Lambda-2}\ell_n\left(|n+2\rangle\langle n| - |n\rangle\langle n+2|\right)} = \sum_{\Delta=0}^{\infty}{}' \frac{r^{p_0+2\Delta}}{(p_0+2\Delta)!2^{p_0+2\Delta}} \underbrace{\langle n_2| \left[\sum_{n=0}^{\infty} \ell_n \left(|n+2\rangle\langle n| - |n\rangle\langle n+2|\right)\right]^{p_0+2\Delta} |n_1\rangle}_{f(\Delta)}$$

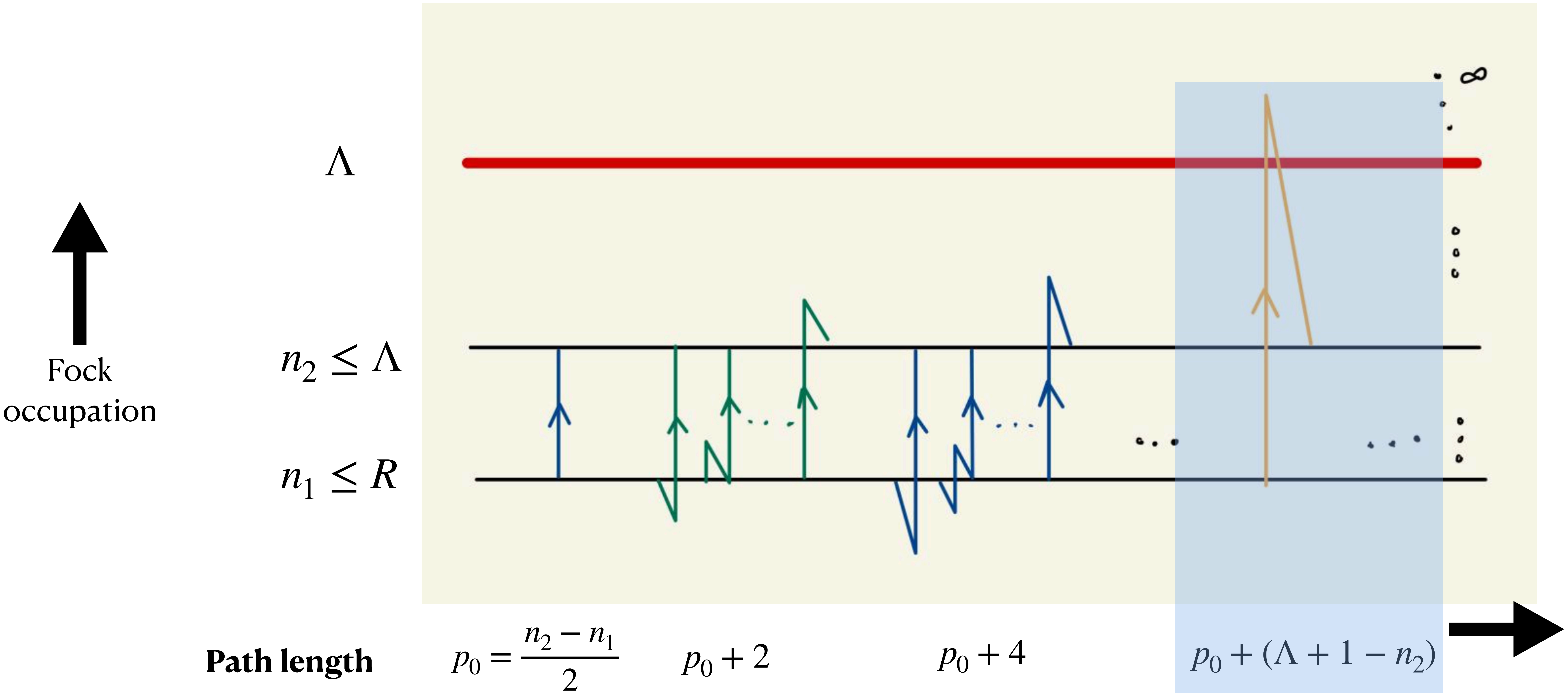

Paths at this order and beyond are discarded to compute matrix elements of the truncated squeezing operator!

Circuit encoding: Discrete variable

$$\hat{S}(r) = e^{\frac{r}{2}((\hat{a}^\dagger)^2 - \hat{a}^2)}$$

$$= e^{\frac{r}{2}\sum_{n=0}^{\infty} \ell_n(|n+2\rangle\langle n| - |n\rangle\langle n+2|)}$$

Truncation

$$\hat{S}^{\Lambda}(r) = e^{\frac{r}{2}\sum_{n=0}^{\Lambda} \ell_n(|n+2\rangle\langle n| - |n\rangle\langle n+2|)}$$

Trotterization

$$\hat{S}^{\Lambda,K}(r) = \left(e^{-i\frac{r}{K}s_0^{\Lambda}} e^{-i\frac{r}{K}s_2^{\Lambda}}\right)^K \left(e^{-i\frac{r}{K}s_1^{\Lambda}} e^{-i\frac{r}{K}s_3^{\Lambda}}\right)^K$$

- The first-order product formula results in an $O\left(\frac{Nr^2\Lambda^3}{K}\right)$ value for the spectral norm of $\hat{S}^{\Lambda}(r) - \hat{S}^{\Lambda,K}(r)$.
- This bound, however, is quite loose because it is state-independent.

Circuit encoding: Discrete variable

We now look at the values of circuit regulators Λ and K that guarantee a minimum fidelity between $|\psi\rangle_{R,Q}$ and $|\psi^{\Lambda,K}\rangle_{R,Q}$.

Optimized squeezing parameter r from energy minimization

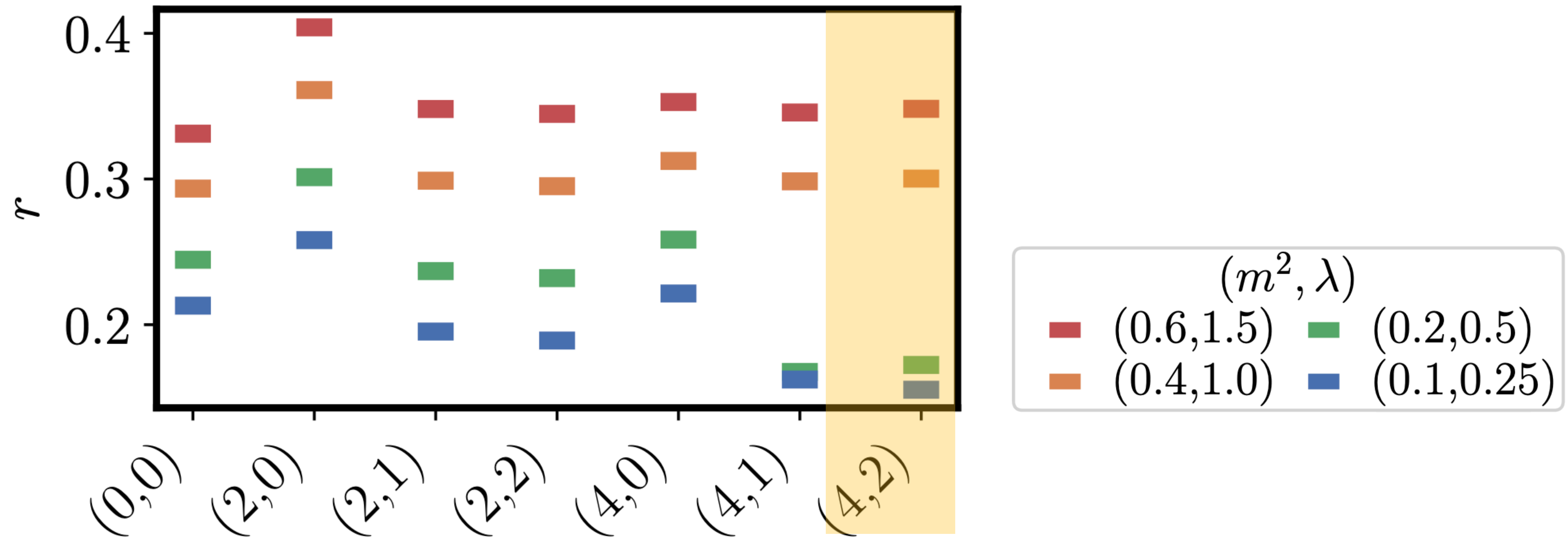

Minimum values of Λ and K that guarantee fidelity F_0 for the $(R,Q) = (4,2)$ ansatz

(m^2,λ)	r	$F_0 = 0.9$		$F_0 = 0.95$	
		Λ	K	Λ	K
(0.6,1.5)	0.348	33	2375	35	3876
(0.4,1)	0.300	27	1102	27	1569
(0.2,0.5)	0.172	15	87	15	123
(0.1,0.25)	0.155	14	59	15	100

Classically determined quantum circuits

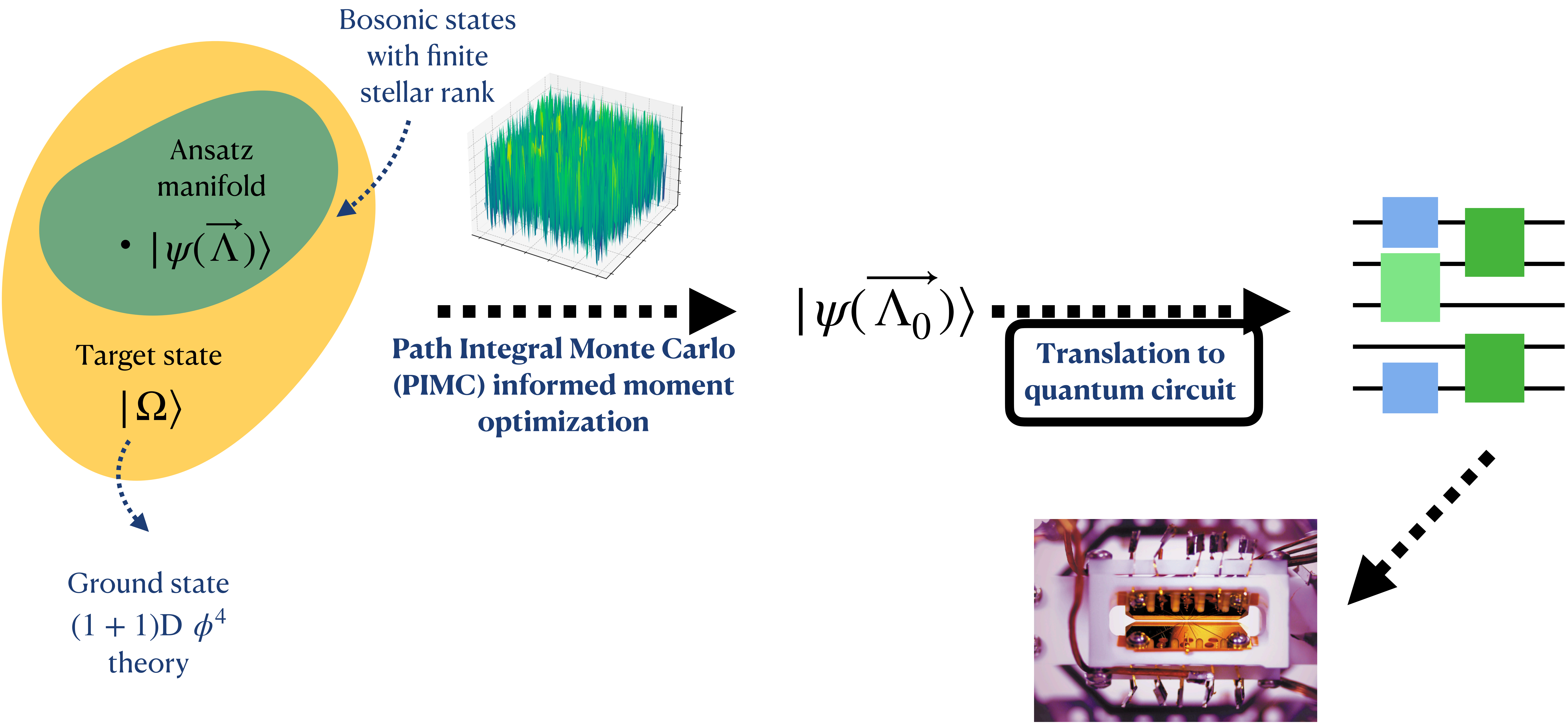

Trapped ion quantum computer from Monroe Lab (UMD, 2016)

Summary

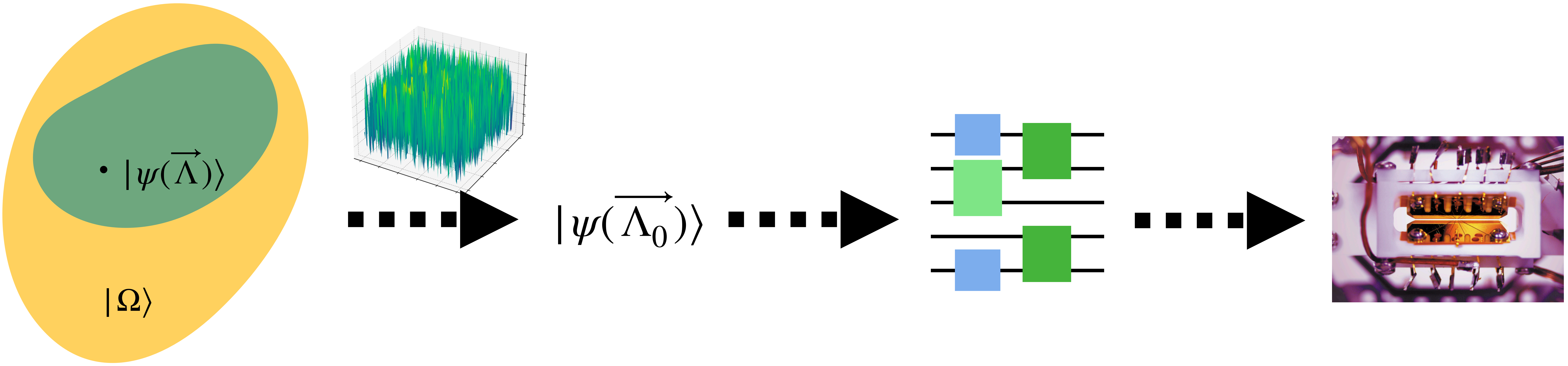

- The (R, Q) ansatz is a *classically tractable, circuit-translatable,* and *circuit-efficient* ansatz for multimode bosonic systems.
- The ansatz is optimized classically using Euclidean-Monte-Carlo-informed moment optimization. This procedure augments the familiar variational minimization of energy by penalizing deviations in selected sets of target moments.
- The optimized ansatz can thereafter be translated into a quantum circuit with polynomial complexity in system size.

Outlook

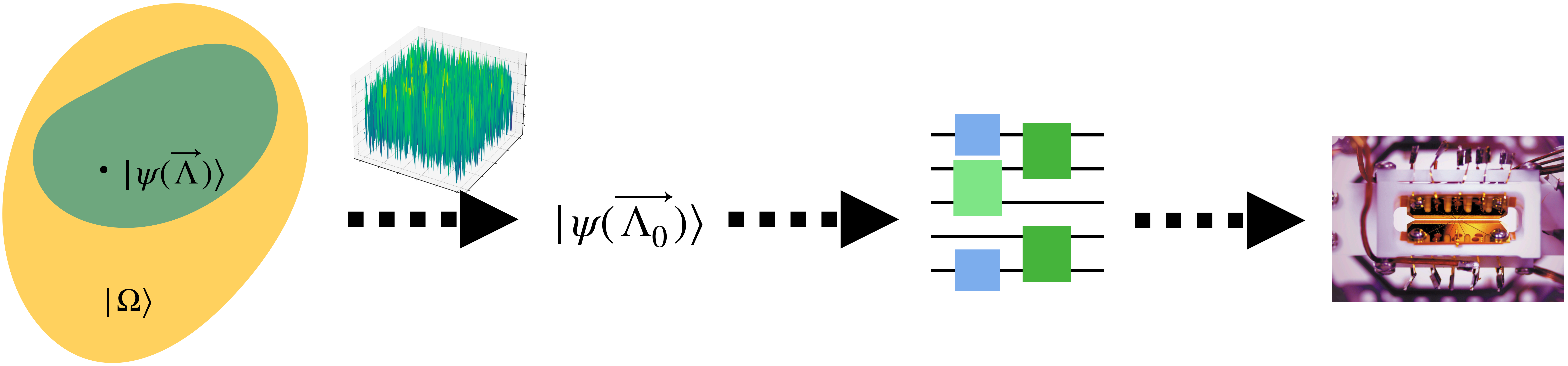

- A detailed study of the thermodynamic and continuum limits.
- Translation to bosonic quantum circuits.
- Variational quantum algorithms based on the (R, Q) ansatz.
- Study of dynamics with moment-optimized initial states.
- Extension to theories with fermions and gauge bosons.
- Implications of PIMC-induced statistical uncertainty.